THE IMPACT OF NEUTRALIZING ANTIBODY AND ADCC RESPONSES ON HIV-1 ENVELOPE EVOLUTION IN EARLY INFECTION

DIETER MIELKE

This thesis is submitted in fulfilment of the requirements for the degree of DOCTOR OF PHILOSOPHY in the Division of Medical Virology, Department of Pathology in the Faculty of Health Sciences at the University of Cape Town.

Supervisor: Professor Carolyn Williamson

Co-supervisor: Dr Colin Anthony

AUGUST 2017

For by Jesus all things were created, in heaven and on earth, visible and invisible... all things were created through him and for him. And he is before all things, and in him all things hold together.

Colossians 1:16-17

The more I study nature, the more I am amazed at the work of the Creator.

Louis Pasteur

We live on an island surrounded by a sea of ignorance. As our island of knowledge grows, so does the shore of our ignorance.

John Archibald Wheeler

Contents

ABSTRACT

The development of an effective HIV-1 vaccine remains a global priority. Neutralizing antibodies (nAbs), which block infection by cell-free virus, are likely to be an important response for vaccines to elicit. However, evidence from the RV144 vaccine trial and non-human primate vaccine studies suggest antibody-dependent cellular cytotoxicity (ADCC) responses, which target virus-infected cells, may also be protective. This thesis uses deep sequencing, together with immune assays, to characterise HIV-1 Envelope evolution associated with both nAb and ADCC responses in early infection, and investigates broadly neutralizing and non-neutralizing monoclonal antibody ADCC activity against subtype C viruses.

Recent advances in deep sequencing approaches, coupled with the primer ID method which barcodes each viral genome, enabled us to generate thousands of viral sequences to accurately track viral population dynamics in early infection. In all participants investigated, there was a significant drop in the relative frequency of wildtype (WT) virus following nAb responses. However, in three of the seven participants, when controlling for changes in viral load (VL) over time, we observed that the WT load (frequency of the WT residue x total VL) remained relatively stable despite an effective nAb response. Instead, there was an outgrowth of the escaped virus with a concomitant increase in viral loads. We found that nAbs were inefficient at blocking cell-cell transmission of early WT and escape viruses, identifying this as one mechanism by which viruses may persist despite the presence of nAbs. These results suggest that other antibody effector functions such as ADCC, which target infected cells, may be important to elicit in a protective HIV-1 vaccines.

If ADCC responses are important in controlling viral populations, one would expect to find evidence of viral escape from these responses. In all nine participants investigated, we found ADCC responses emerged prior to nAb responses, and in three individuals we observed sequence changes prior to detectable nAbs. To evaluate if these changes were due to ADCC pressure on the virus, we introduced select mutations into infectious molecular clones encoding the cognate early/acute *envelope* (Env-IMCs). In one participant, the mutation introduced conferred resistance to both nAb and ADCC responses, while in two participants, mutations were identified which resulted in resistance to ADCC but had no effect on neutralization, suggesting escape from ADCC. Longitudinal analysis in one of these participants, which targeted the CD4-binding site, revealed three distinct escape pathways, of which two conferred resistance to ADCC, and confirmed that ADCC responses can directly drive viral evolution *in vivo*.

Finally, we investigated the ADCC activity of eleven anti-HIV-1 monoclonal antibodies (mAbs), including seven broadly neutralizing antibodies (bnAbs) and four non-neutralizing antibodies (nnAbs), against a panel of nine acute subtype C Env-IMCs. We found bnAbs had low to moderate ADCC breadth (11-66%). In contrast, while the two V2 nnAbs we tested were narrow and weak, the two nnAbs targeting CD4-induced epitopes (A32 and C11) mediated the broadest (78-100%) and most potent (0.06-0.81 µg/mL) ADCC against this panel. In addition, a non-linear relationship was found between ADCC activity and strength of mAb binding to the infected cell surface (r_s = -0.5309, p=0.0001).

In conclusion, in contrast to studies which evaluated limited number of sequences, utilizing deep sequencing approaches, we found that the WT load remained relatively stable following early nAb pressure, albeit at lower relative frequency to the escape variant. Evasion of antibody responses through cell-cell transmission may contribute to the persistence of WT virus, providing further motivation for the importance of antibody effector functions that target infected cells in a protective HIV-1 vaccine. For the first time, we provide evidence of ADCC-mediated immune pressure in early infection, showing that these responses can exert selective pressure on HIV-1. However, the limited number of sequence changes relative to those observed following nAb pressure suggests that this response does not put as much selective pressure on the virus as nAbs. Lastly, the moderate breadth of bnAb ADCC activity provides evidence that there are common epitopes on free virions and on the surface of infected cells. This indicates bnAbs with potent and broad ADCC should be identified to include in antibody-based treatment and cure strategies, which aim to eliminate infected cells. Altogether, these data suggest that while eliciting nAbs should be the primary goal of HIV-1 vaccine design, ADCC-mediating antibodies may also play an important role.

This study has been presented at the following conferences/workshops:

Dieter Mielke, Colin Anthony, Nigel Garrett, Salim Abdool Karim, Carolyn Williamson. **Using NG sequencing technologies to map kinetics of early escape from neutralizing antibodies**. HIV Vaccine Trials Network Next Generation Sequencing Workshop 2016 (oral presentation).

Dieter Mielke, Colin Anthony, Nigel Garrett, Salim Abdool Karim, Carolyn Williamson. **Investigating HIV-1 Envelope Evolution in Response to Early Neutralizing Antibody Pressure Using Next Generation Sequencing**. HIV Research for Prevention 2016 (poster presentation).

Dieter Mielke, Jennifer Jones, Jie Zheng, Christina Ochsenbauer, John Kappes, Nigel Garrett, Salim Abdool Karim, Colin Anthony, Guido Ferrari, Carolyn Williamson. **ADCC-mediating antibodies target epitopes which overlap with neutralizing antibodies in early infection and can force immune escape.** Keystone HIV Vaccines 2017 (poster presentation).

List of abbreviations

^{51}Cr	Chromium-51
ARP	AIDS reagent program
ADCC	Antibody-dependent cellular cytotoxicity
ADCVI	Antibody-dependent cellular viral inhibition
AIDS	Acquired immune deficiency syndrome
ART	Antiretroviral treatment
BnAb	Broadly neutralizing antibody
Bp	Base pair
CAPRISA	Centre for AIDS research in South Africa
CCR5	Chemokine receptor type 5
CDNA	Copy DNA
CDR3	Complement determining region 3
CD4	Cluster of differentiation 4
CD4bs	CD4-binding site
CD4i	CD4-induced
CD8	Cluster of differentiation 8
CT	Cytoplasmic tail
CTL	Cytotoxic T lymphocyte
CoRBS	Co-receptor binding site
CXCR4	Chemokine receptor type 4
DEAE	Diethylaminoethyl cellulose
DMSO	Dimethyl sulphoxide
DNA	Deoxyribonucleic acid
dNTP	deoxynucleic acid triphosphate
DSL	Disulphide link
E. coli	*Escherichia coli*
EDTA	Ethylene diamine tetraacetic acid
EMBD	Electron Microscopy Data Bank
Env	HIV-1 *envelope* gene
Env	HIV-1 Envelope protein
Env-IMC	Infectious molecular clone encoding a heterogenous *envelope*
FAM	6-carboxyfluorescein

Fc	crystallisable fragment
$Fc_{\gamma}R$	Immunoglobin G crystallisable fragment receptor
FCS	Fetal calf serum
FP	Fusion protein
G	gram
Gp120	120 kDa Envelope glycoprotein subunit
Gp41	41 kDa Envelope glycoprotein subunit
H	hour
HEK	Human embryonic kidney
HIV-1	Human immunodeficiency virus type 1
HIVIG	Immunoglobin from HIV-1-infected individuals
HLA	Human leukocyte antigen
HR	Heptad repeat
IC_{50}	Inhibitor concentration resulting in a 50% reduction in infection
IFN	Interferon
IgG	Immunoglobulin G
IL	Interleukin
Kb	Kilobases
KDa	Kilodaltons
µg	Microgram
µL	Microlitre
µM	Micromolar
M	Molar
MAb	monoclonal antibody
MHC	Major histocompatibility complex
Mg	Milligram
Min	minute
ML	Millilitre
MM	Millimolar
MPER	Membrane proximal external region
NAb	Neutralizing antibody
Ng	Nanogram
NGS	Next generation sequencing
NIAID	National Institute of Allergies and Infectious Diseases

NICD	National Institute of Communicable Diseases
NnAb	Non-neutralizing antibody
NHP	Non-human primate
NIH	National institutes of health
NKC	Natural killer cell
NKR	Natural killer cell resistant
NTC	Non-template control
PBMC	Peripheral blood mononuclear cell
PBS	Phosphate-buffered saline
PDB	Protein Data Bank
PHA	Phytohemagglutinin
PNGS	Potential N-linked glycosylation site
Pol	HIV-1 *polymerase* gene
Pol	HIV-1 Polymerase protein
RFU	Relative fluorescent units
RLU	Relative light unit
RT	Reverse transcriptase
RNA	Ribonucleic acid
SGA	Single genome amplification
SHIV	HIV-1/SIV chimera
SIV	Simian Immunodeficiency Virus
SNP	Single nucleotide polymorphism
T/F	Transmitted/Founder
TAE	Tris-acetic acid EDTA (Tris acetate)
$TCID_{50}$	Tissue culture infectious dose required for 50% of maximum infection
TM	Transmembrane
Tris	2-amino-2-(hydroxymethyl)-1,2-propandial
UAB	University of Alabama
UCSF	University of California in San Francisco
UCT	University of Cape Town
USA	United States of America
VL	Viral load
WPI	Weeks post infection
WT	Wildtype

Declaration

I, Dieter Mielke, hereby declare that the work on which this thesis is based is my original work (except where acknowledgements indicate otherwise) and that neither the whole work nor any part of it has been, is being, or is to be submitted for another degree in this or any other university.

I empower the university to reproduce, for the purpose of research, either the whole or any portion of the contents in any manner whatsoever.

Signature: Signed

Date: 14 August 2017

Acknowledgements

This study would not have been possible without the help of many wonderful people. First and foremost, I would like to give thanks to my Lord, Jesus Christ, who created and sustains the universe we study.

I extend my deepest gratitude to my supervisor, Professor Carolyn Williamson. There is no doubt this study would not have been possible without her wise insight, experience, and generosity; it has been such an immense privilege and blessing to be mentored by her. I am amazed at the growth I have experienced as a scientist under her guidance since I joined her group as a naïve honours student.

I am also so grateful to my co-supervisor Dr Colin Anthony, who was always available to talk, offer important advice, insight and support, and challenge me to keep improving. My sincerest thanks also go to our lab manager, Debbie Stewart, who always accommodated me even though it often inconvenienced her, and has been a great encouragement and support to me over the years. In addition, the entire HIV Diversity group has become a family to me and I have loved the time I have spent with everyone. Special thanks in particular to Sherazaan Ismail, who has been a cherished friend since we started together in honours.

There have been many people who have contributed much to this study. I'd like to extend particular thanks to Dr Guido Ferrari at Duke University, who allowed me to come learn from his group and has taught me a lot about ADCC in particular and science in general. My thanks also go to Justin, Sherry and Whitney in his group, who helped me become proficient in the various assays. And also to the Collaboration for AIDS Vaccine Discovery who made the visit to Duke University possible, without which this study would have been much more difficult. In addition, my thanks go to Professor Christina Ochsenbauer at the University of Alabama, who willingly provided some of the Infectious Molecular Clones for this study, and important advice and insight which allowed me to make my own. Further, my thanks go again to Dr Colin Anthony, who allowed me to use deep sequencing data for two of the participants I analysed, and Drs Melissa-Rose Abrahams and Florette Treurnicht for providing some of the single genome sequences for analysis.

I am also thankful to the participants of the CAPRISA 002 Acute Infection cohort, without which this study would not have been possible; and the Desmond Tutu clinic and donors of the PBMCs (particularly PID007 who donated many cells) I used for the ADCC assays.

My sincere thanks also go to the Beit Trust, the Poliomyelitis Research Foundation and the University of Cape Town for contributing to my tuition and personal expenses, allowing me to focus completely on this study.

I am so thankful to my mother, Sheila Mielke, and late father, Jens Mielke. Without their love, care, and investment in me, I would not be where I am today. My curiosity about the mechanisms that the world works by started, and continues, from their input.

Last, but definitely not least, I cannot express how grateful I am to my incredible wife and best friend, Ru! She put up with many hours of stressful rants, odd hours of work and boring, scientific conversations. And has been a bedrock of support and love amongst it all. This belongs to both of us.

Chapter 1. Introduction and literature review

1.1 Background

Remarkable gains have been made in the last decade to manage the Human Immunodeficiency Virus-1 (HIV-1) epidemic, the causative agent of Acquired Immunodeficiency Syndrome (AIDS). This is largely due to the roll-out of anti-retroviral therapy (ART) which has resulted in a 43% decrease in AIDS-related deaths globally since 2003 (1). ART not only increases life-expectancy, but also reduces transmission of HIV-1 from treated individuals to their uninfected partners (2). The availability of effective anti-HIV-1 drugs has prompted some to doubt the necessity of an effective HIV-1 vaccine, advocating for improved access to ART and pursuing HIV-1 cure strategies instead. However, these treatment regimens are not cost-effective for developing countries, where the majority of the disease burden lies. Furthermore, individuals on long-term treatment have other risk factors associated with HIV-1 infection, such as peripheral arterial disease, cardiovascular disease and impaired renal function (3–5). In addition, despite the decrease in AIDS-related deaths, the number of new infections annually has remained relatively constant (there were approximately 1.9 million new infections in 2015), largely because treatment has not been implemented early enough and there has been insufficient coverage to impact the number of new cases (1). This is particularly true of Eastern and Southern Africa, where the greatest burden of the epidemic lies (approximately 70% of global HIV-1 infections): in South Africa alone, there were approximately 170 000 new HIV-1 infections in the 2014-2015 period (6).

Vaccines have proven to be the most effective method of controlling viral epidemics, reducing disease and death in settings where effective vaccines have been implemented (7). Consequently, the development and deployment of a safe and protective HIV-1 vaccine remains an important goal of HIV-1 research. However, the development of an effective HIV-1 vaccine has proven an unusually elusive goal: despite numerous clinical trials utilizing a number of different approaches, only one has provided any protection, a modest 31% in the RV144 trial (8). One significant challenge in the discovery of an effective vaccine has been a lack of understanding of immune correlates of risk and protection. Inadequate animal models suggest these correlates can only be identified in costly human efficacy trials (9–11).

As a result, understanding how people naturally control HIV-1 provides important insights into what a protective immune response may look like and how one may go about eliciting such a response through vaccination. Indeed, these studies have provided valuable direction in HIV-1 vaccine research, especially in the last decade. In particular, studies of humoral responses to HIV-1 suggest vaccines which elicited these immune response could, theoretically, protect

against HIV-1 infection (12). Evidence from vaccination against other viruses supports this hypothesis, as antibody responses are the correlate of protection in almost all anti-viral vaccines to date (including Smallpox, Hepatitis A and B, Human papillomavirus, Influenza and Polio, to name a few) (reviewed in (13)).

However, these viruses are all much less variable than HIV-1, which has an extraordinary global sequence variation (14), making selection of vaccine immunogens a daunting task. Further, the astonishingly high rate of virus evolution (reviewed in (15)) allows HIV-1 to rapidly evolve. Accordingly, any vaccine candidate must produce immune responses that efficiently protect against a range of diverse HIV-1 strains.

1.2 HIV: Origins, diversity and distribution

HIV can be divided into two types: HIV-1 and HIV-2, which represent two separate zoonotic transmission events (Figure 1.1). While HIV-2 is derived from Simian Immunodeficiency Virus (SIV) found in Sooty mangabeys (*Cercocebus atys*) (16, 17), HIV-1 was transmitted to humans through multiple zoonotic events from the SIV reservoir found in the Chimpanzee subspecies *Pan troglodytes troglodytes* and the Gorilla subspecies *Gorilla gorilla* (18, 19).

HIV-2 infection is immunologically distinct from HIV-1 (20), much less common (geographically restricted to West Africa) and less virulent (21, 22), although it has similar clinical presentation to HIV-1 (23). HIV-1 is comprised of four groups, each of which are thought to represent a separate zoonotic transmission event: M (main), O (outlier), N (non-M, non-O) and P (24–27). Group M, the main cause of the HIV-1 epidemic, consists of nine genetically distinct subtypes (A-J) (14), as well as 79 currently identified Circulating Recombinant Forms (http://www.hiv.lanl.gov/contents/sequence/HIV/CRFs/CRFs.html) and a number of Unique Recombinant Forms, which all produce similar clinical symptoms, but have different geographical distributions (Figure 1.2).

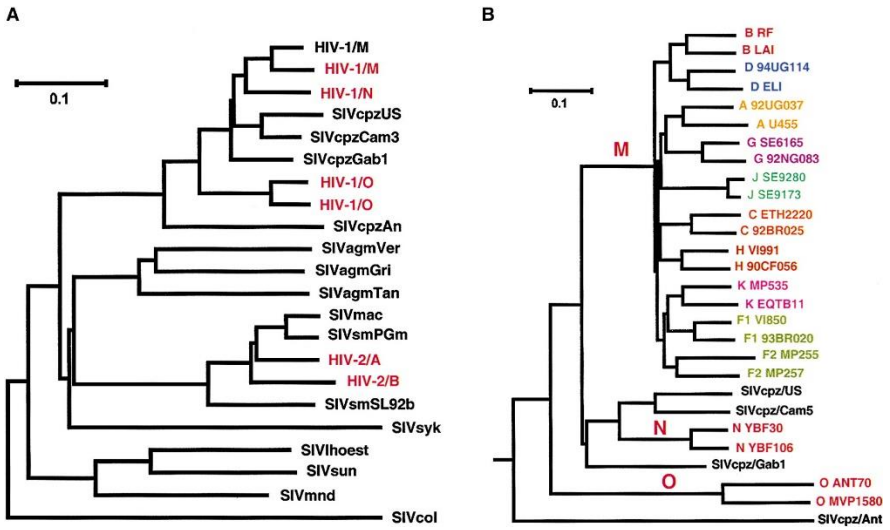

Figure 1.1. The origin of HIV. Primate lentivirus tree (derived from Pol protein sequences), showing the distinct origins of both HIV-1 and HIV-2 (in red). SIV strains have a suffix indicating their species of origin (i.e. cpz refers to chimpanzee, mac to macaque etc.) **(A)**. SIVcpz/HIV-1 tree (derived from Env protein sequences), showing the distinct origins of HIV-1 groups M, N, and O, and the numerous subtypes (A–K) within group M **(B)**. Among the chimpanzee viruses (SIVcpz, in black), Ant was isolated from the chimpanzee subspecies *Pan troglodytes schweinfurthii* and the other strains from *Pan troglodytes troglodytes*. Figure and legend reproduced from (28) with permission provided by Elsevier Publishers.

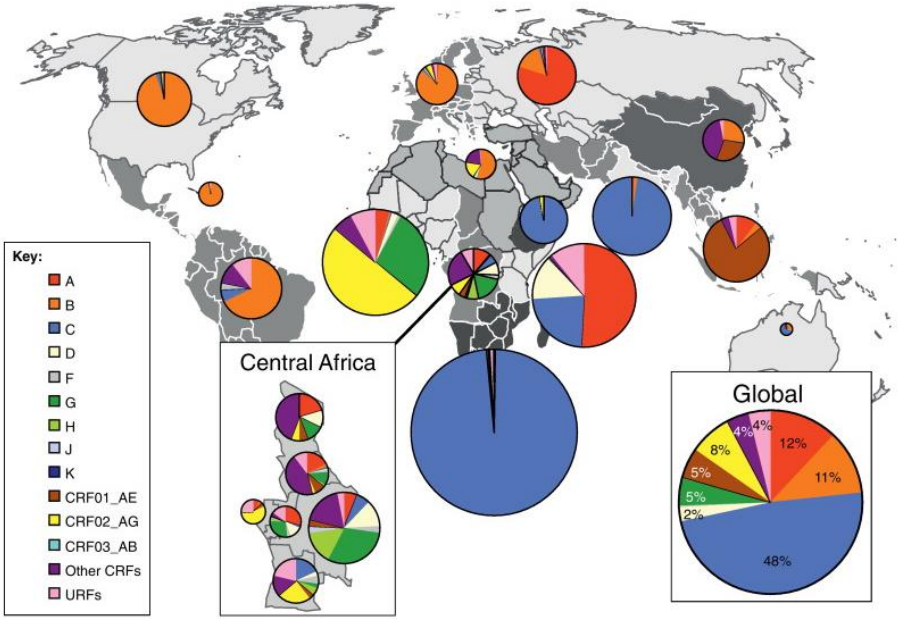

Figure 1.2 Global distribution of HIV-1 group M subtypes and recombinants. Pie charts representing the distribution of HIV-1 group M subtypes and recombinants from 2004 to 2007 in each region are superimposed on the regions. The relative surface areas of each pie chart correspond to the number of people living with HIV-1 in that region. The colours representing the different HIV-1 subtypes and recombinants are indicated in the legend on the left-hand side of the figure. The HIV-1 subtype distributions found around the world and within Central African countries are shown in the insets, as indicated. Figure and legend reproduced from (29) with permission provided by Elsevier Publishers.

Apart from the East, West and Central African epidemics (which contains considerable subtype diversity), certain subtypes are dominant in different regions: subtype A is found predominantly in Russia and Eastern Europe; Subtype B in Europe, North and South America; Subtype C in Sub-Saharan Africa, Ethiopia and India; and CRF01_AE in Southeast Asia (Figure 1.2). The burden of the HIV-1 epidemic is geographically biased (as indicated by the size of each pie chart in Figure 1.2): Eastern and Southern Africa contain ~ 70% of all HIV-1 infections (~ 19 million out of 35 million), Western and Central Africa contain ~ 6.5 million infections, while Asia and South-East Asia contain ~ 5.1 million infections (14). The substantial genetic diversity (and consequently, antigenic diversity) represents considerable challenges to attempts to design an effective global vaccine.

1.3 The HIV-1 genome

HIV-1 is a single-stranded, positive-sense RNA, enveloped virus, classified in the genus *Lentivirus* of the family *Retroviridae,* and predominantly replicates in $CD4^+$ T cells. The viral genome consists of nine genes (*gag, pol, env, tat, rev, nef, vif, vpr and vpu*) (Figure 1.3, A) which encode for 19 proteins (reviewed in (30)). *Gag, pol* and *env* encode for the structural proteins of the virion: *Gag* encodes for the Gag polyprotein which is cleaved into proteins which shape the basic interior infrastructure of the virus (matrix, capsid, nucleocapsid, spacer peptides 1 and 2 and p6 proteins), *pol* encodes for the Polymerase polyprotein which is cleaved into the virus enzymes (Reverse Transcriptase, Integrase, Protease and RNase-H) which provide the basic mechanism by which the virus replicates, and *env* encodes for the Envelope (Env) proteins which coat the surface of the virion and facilitate viral attachment (gp120) and fusion (gp41) with target cells. The HIV-1 genome also encodes two essential regulatory proteins (Tat and Rev) and four accessory proteins (Nef, Vpr, Vif and Vpu). These components, together with the structural proteins and two single-stranded, positive-sense RNA copies, usually makeup the HIV-1 viral particle (31) (Figure 1.3, B).

The error prone nature of the HIV-1 Reverse Transcriptase enzyme is largely responsible for the extensive genetic variation observed at both an individual and population level. The enzyme does not contain a proof-reading mechanism, resulting in a high rate of mutation (~ 0.2 errors per genome replicated) and extensive recombination during reverse transcription (32). This, together with remarkable replication dynamics (a single virion requires ~ 42 hours to complete the replication cycle (33), and 10^{10} - 10^{12} new virions are produced each day (34)) and strong

pressure from immune responses at an individual level, results in the abnormally high rate of evolutionary change. The corresponding genetic variation is especially evident in the HIV-1 *env* (particularly in the hypervariable regions of the gp120 (35)), which has an evolution rate of approximately 0.004 substitutions per site per year at the population level (36).

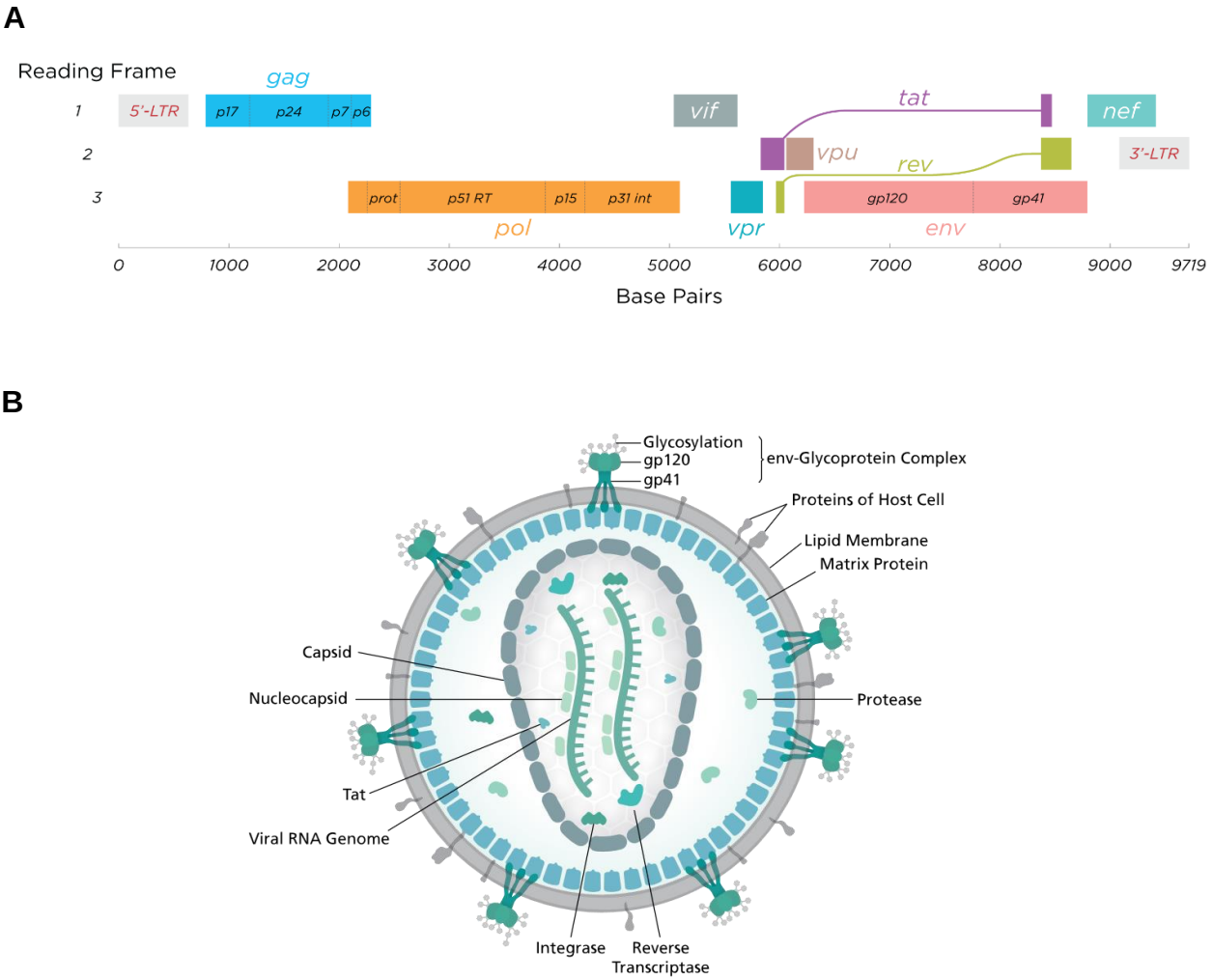

Figure 1.3 Genome and structure of HIV-1. Genomic organization of HIV-1 showing the three structural genes (*gag*, *pol* and *env*) and six regulatory genes (*tat*, *rev*, *nef*, *vpr*, *vif* and *vpu*), which are spread over three reading frames **(A)**. A representation of the structure of the HIV-1 virion **(B)**. Figure and legend reproduced from (37) under a creative commons licence**.**

1.3.2 The gp120 Envelope glycoprotein

The *env* gene encodes for the gp160 Env glycoprotein, which is located on the outer surface of the virion and is the viral component exposed to the humoral immune response. Env consists of two protein subunits: gp120 (an external protein) and gp41 (a transmembrane protein) (38) (Figure 1.4). The gp120 external protein of the Env trimer is made of up five variable regions (V1-V5) and five constant regions (C1-C5) (39, 40). Within the gp120, nine cysteine-cysteine

disulphide bonds form, four of which traditionally define the stems of the variable loops V1, V2, V3 and V4 (41).

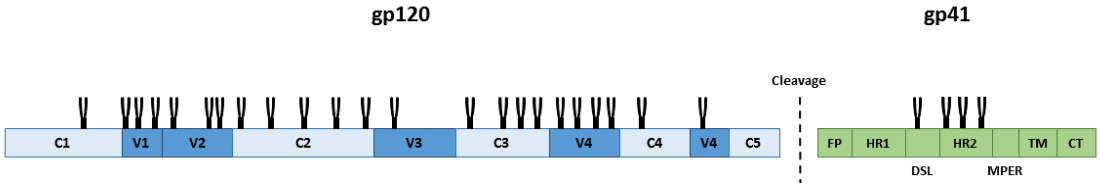

Figure 1.4 Linear schematic of the HIV-1 Envelope. The precursor gp160 is cleaved into two monomers, gp120 (blue) and gp41 (green). The gp120 subunit consists of five constant domains (C1-C5, shown in light blue) and five variable domains (V1-V5, shown in dark blue). The gp41 subunit (green) consists of the fusion peptide (FP), heptad-repeats (HR1 and HR2), a disulphide loop (DSL), the membrane-proximal external region (MPER), the transmembrane domain (TD) and the cytoplasmic tail (CT). The positions of common N-linked glycosylation sites are shown in black. Figure and legend adapted from (42) with permission provided by The American Association for the Advancement of Science.

HIV-1 binds to the CD4-receptor on the surface of target cells, which results in initiation of the cell entry process. The CD4-binding site (CD4bs) is a conserved, pocket-like structure which has been mapped to a complex, discontinuous surface of the gp120 with numerous contact residues residing within several domains (including the C2, C3, C5 and the stem of the V5) which fold into proximity in the Env tertiary structure (43). The gp120 undergoes a substantial refolding upon binding to the CD4 receptor (known as CD4-induced conformational changes), which subsequently allow the formation of the co-receptor binding surface (44–47).

Following CD4 binding, HIV-1 gp120 binds to host co-receptors CCR5 or CXCR4 to enable efficient entry into target cells. The co-receptor binding site is made up of multiple residues found around the bridging sheet, V3 and C4 (48–50). Reorganisation of trimeric gp120 following CD4 binding re-orientates the V3 loops toward the host membrane, allowing the top of the V3 loop to bind the second extracellular loop of the CCR5, positioning the Env for fusion with the target cell membrane (51).

The V3 loop is the main determinant of co-receptor tropism, facilitating binding to either the CCR5 or CXCR4 co-receptors. Transmitted viruses utilize the CCR5 receptor, with almost no exception. However, some viruses undergo a switch, enabling them to use the CXCR4 receptor during the course of infection (52). The switch between CCR5 and CXCR4 co-receptor tropism has been linked with mutations in the V3, which increase the net positive charge of the V3 allowing interaction with the negatively charged surface of CXCR4, and has been associated with faster disease progression (53, 54).

With the exception of the V3 loop, which shows relatively low length variation, the variable loops range considerably in length and largely assist in immune evasion and escape (55). In particular, the V1V2 domain varies substantially in length and glycosylation profile (56–59). This large loop, together with its extensive glycosylation, has been implicated in the occlusion of the CD4bs (60–62) and the co-receptor binding site.

The Env protein is heavily glycosylated (Figure 1.4, shown in black), with up to half of the Env's molecular weight attributed to glycans (63): a gp120 molecule has 20 – 35 N-linked glycosylation sites and a gp41 molecule has 3 – 5 N-linked glycosylation sites. The glycans incorporated onto the Env are attached by host cellular machinery in the golgi, allowing them to act as a non-immunogenic barrier to the underlying peptide structure, and consequently facilitate escape from the immune system (64). In addition to this, glycosylation has been linked with virus infectivity and virus-induced fusion (65), correct folding of the Env (66), and processing and transport in the Golgi apparatus (67).

1.3.3 The gp41 Envelope glycoprotein

While the gp120 glycoprotein facilitates binding to target cells, the gp41 glycoprotein mediates fusion of the virion and target cell by allowing the virus membrane to come into close proximity with the target cell membrane. The protein is organized into three domains: an external domain, a transmembrane domain and a cytoplasmic tail (reviewed in (55)).

The external domain incorporates the regions prominent in the fusion process: an N-terminal hydrophobic region known as the fusion peptide (FP) (68, 69), two hydrophobic regions which form α-helical coiled-coil structures referred to as heptad-repeat regions (HR1 and HR2), which are linked by a disulphide link (DSL) (70–74), and a Tryptophan-rich region referred to as the membrane-proximal external region (MPER) (75, 76) (Figure 1.4).

The FP is hidden deep within the trimer, where the gp120 and gp41 interact, but becomes exposed following binding of the gp120 to the CD4 receptor, allowing penetration of the FP into the target cell membrane and subsequent membrane destabilization (Figure 1.5). Three HR1 motifs form a core bundle in parallel and fold over a hydrophobic groove antiparallel to three HR2 domains within each trimer (Figure 1.5), forming a stable six-helix bundle which brings the viral and cell membranes in close enough proximity for fusion to occur (71). The MPER makes up the remaining 24 residues of the gp41 extracellular domain. It is a highly conserved region and is essential for both fusion and infection (75–78).

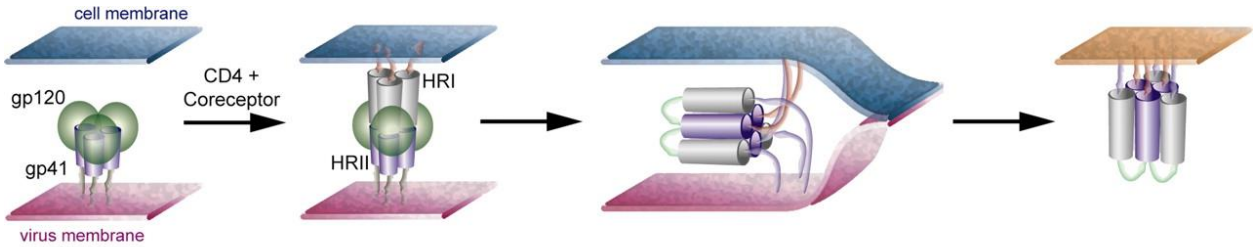

Figure 1.5 HIV-1 fusion. Binding of the gp120 subunit (green) of the trimeric Env glycoprotein to the CD4 receptor and the chemokine co-receptor (CXCR4 or CCR5) triggers a conformational change in the unmasked subunit gp41 (grey and violet), where two regions, the N-terminal HR1 (grey), and the C-terminal HR2 (violet) become separated in the so-called "hairpin intermediate," which bridges the viral and cell membranes. Collapse of the hairpin intermediate into a 6-helix bundle drives viral–cell membrane fusion. Figure and legend adapted from (79) with permission provided by The National Academy of Science.

The remaining two regions of the gp41 are the transmembrane (TM) domain and the cytoplasmic tail (CT). The TM domain is a hydrophobic region which is likely to span the viral membrane three times (80), although a structure has not yet been resolved, and is involved in the formation of fusion-competent Env protein (81). To conclude, the gp41 CT is unusually long for a TM protein (~ 150 residues). A number of studies have implicated it in a diverse range of functions, including Env incorporation into the virus (82, 83), interaction with viral matrix proteins (83–86) and targeting to vesicles (87–89).

1.3.4 HIV-1 Envelope features and states

The Env spikes on the surface of virions are comprised of three gp120 and three gp41 subunit glycoproteins, which come together to form the 'closed' heterotrimeric Env protein (Figure 1.6). The Env structure was recently resolved in crystallography and cryo-electromicroscopy studies, to a resolution of 4.7 Å and 5.8 Å respectively (42, 90). The successful crystallization of the Env trimer was a boost for the HIV-1 vaccine field, allowing accurate predictions of antibody epitopes and angles of binding. This opened opportunities for rational vaccine design of Env-based immunogens.

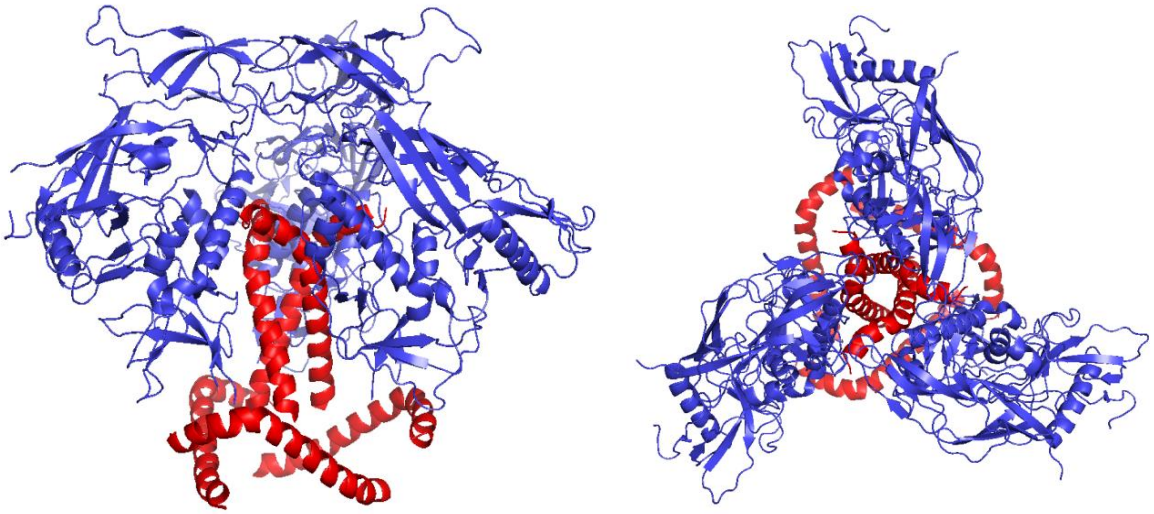

Figure 1.6 Schematic of the HIV-1 Envelope trimer. Three gp120 subunits (blue) sit on three gp41 subunits (red) (side view on the left, top view on the right). The variable loops make up the outer domain of the trimer. Figure produced using the Envelope trimer crystal structure (PDB ID: 4NCO) (91) and PyMOL 1.8 (92).

Env is found in several states on the viral membrane, making immunogen selection difficult. The highly ordered, unliganded conformation of the Env trimer is referred to as the 'closed' conformation (93). Binding of CD4 to the CD4bs induces significant conformational changes, such that the trimer adopts an 'open' configuration (where the V1V2 and V3 loops are 'unattached' and no longer shield conserved epitopes) (94). However, the trimer does spend some time in the 'open' state independent of CD4 binding. The CD4-independent equilibrium between the 'open' and 'closed' states varies from Env to Env: most Envs predominantly remain in the 'closed' state, while some Envs switch between the 'open' and 'closed' states regularly (94) (Figure 1.7).

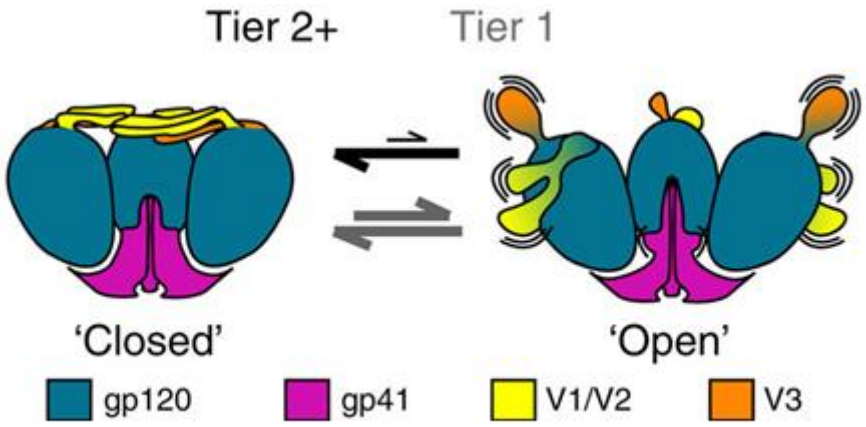

Figure 1.7 HIV-1 Envelope configurations. Env trimers exist predominantly in the closed form in which the interactions between V1/V2 from each protomer are intact and V3 is occluded. Transient sampling of open conformations disrupts the inter-protomer interactions at the trimer apex. The trimers on higher tier (more neutralization resistant) viruses are less likely to sample open conformations, thereby protecting conserved epitopes from neutralizing antibodies. Tier 1 primary and cell line-adapted isolates sample the open conformation more often or for longer periods, which renders these viruses more vulnerable to neutralization. Figure and legend adapted from (94) with permission provided by Nature Publishing Group.

These conformations have a profound effect on the ability of antibodies to neutralize the virus. Two studies have ranked several hundred Envs into tiers based on their susceptibility to neutralization, with tier 1 Envs being highly susceptible to neutralization and tier 3 Envs highly resistant to neutralization (95, 96). Tiering of the Envs has been associated with the state of equilibrium between 'open' and 'closed' Env configurations: tier 1 Envs predominantly remain in the 'open' state, while the converse is true for tier 3 Envs (94). Tier 1 viruses are not normally detected in natural infection, necessitating immune responses to the closed trimer as a requirement for an effective vaccine.

In addition to the complication this relative equilibrium between structural states signifies for vaccine design, several other HIV-1 Env features make the discovery of a successful vaccine a daunting task. These include the considerable antigenic variability, heavy glycosylation and conformational masking of receptor binding sites by variable loops (97) (previously described). Furthermore, several other Env features are important in HIV-1 vaccine design including transient exposure of epitopes (such as epitopes on the MPER) (98), the presence of non-functional Env on the viral membrane surface (99, 100), and the low density of Env surface expression, making antibody cross-linking difficult (101, 102) (Figure 1.8).

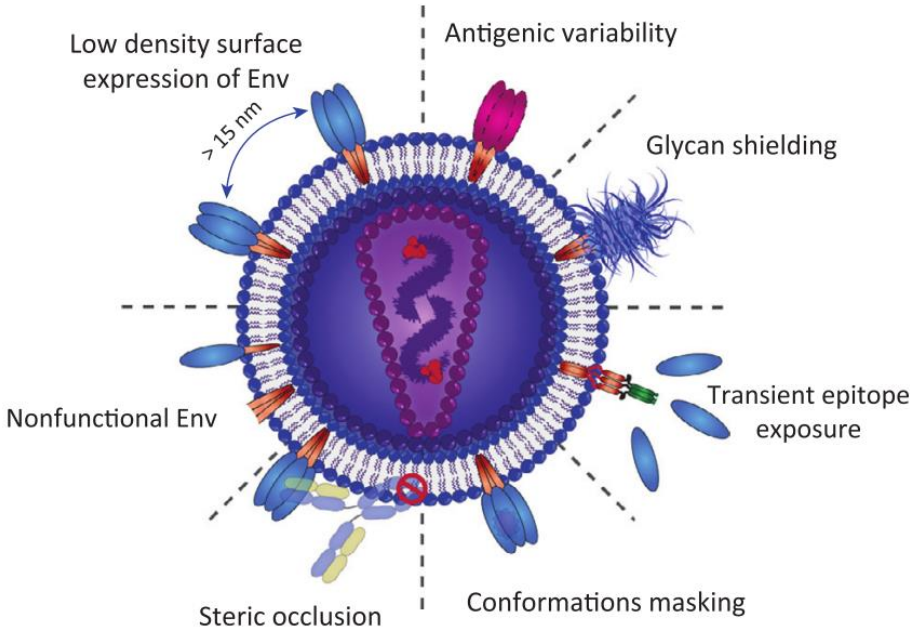

Figure 1.8 Envelope-dependent defence mechanisms of HIV-1. As well as from the Env antigenic variability, several architectural and structural features of the HIV-1 spike limit or block the access of immune effectors: (i) Many host-derived glycans cover the surface of the spike to form a 'glycan armour' protecting the virus; (ii) some epitopes are only transiently exposed, such as the 'pre-fusion state' form of gp41 and the co-receptor binding site that opens following a conformational change induced by the interaction of gp120 with a CD4 molecule (CD4i); (iii) conformational masking of the CD4bs prevents access; (iv) steric occlusion of immunoglobulins due to their large size; (v) epitopes on non-functional spikes (non-cleaved Env precursors, gp120 monomers, and gp41 trunks), which are not expressed by mature functional spikes, are a highly immunogenic decoy; and (vi) the small number of gp160 glycoproteins (~ 15 per virion), which are randomly distributed at the HIV-1 surface, likely impair the ability of the antibody to bridge two Env (bivalent antibody binding), therefore reducing avidity effects. Figure and legend reproduced from (103) with permission provided by Elsevier Publishers.

1.4 HIV-1 transmission

HIV-1 is detected in blood, as well as other bodily fluids, from infected individuals. Transmission results from exposure of an uninfected individual to virus-containing fluids from an infected individual. In Africa, the vast majority of transmission events are the result of heterosexual sex with an infected partner. Despite high viral loads in bodily fluids, approximately 80% of heterosexual infections are established from a single HIV-1 variant (termed the transmitted/founder (T/F) virus) (104, 105), suggesting the transmission event contains one or more selective genetic bottlenecks (for a comprehensive review, see (106)).

One potential bottleneck is the compartmentalization of viral populations in the genital tract, which has been shown to include both clonally amplified and diverse transient lineages (107–109). This clonal amplification, which has been identified in both male and female genital secretions, is consistent with a model by which inflammation drives HIV-1 replication from a

small collection of singly infected T cells (106). While the dominant variant in the genital compartment may have a greater chance of transmission due to their higher frequency, in one transmission pair study (with sampling between 2 and 12 weeks after the transmission event) it was found that T/F viruses were a minority variant in the genital tract of the donors (108). However, due to the timing of sampling and the transient nature of genital tract clonally-derived viruses, it is difficult to draw conclusions about the frequency of the transmitted viruses in the donors from this study.

The most stringent transmission bottleneck is thought to be in the genital tract of the recipient, where typically a single genotype initiates systemic infection (Figure 1.9). Many studies have shown that this bottleneck results in several characteristics generally found in T/F viruses. Firstly, T/F viruses are nearly always CCR5-dependent and require high surface levels of CD4 on the target cells for entry (105, 110). Secondly, there is an apparent differential in variable loop lengths, and consequently levels of glycosylation, between T/F and chronic viruses: T/F subtype A, C and D viruses contain fewer N-linked glycosylation sites (57, 110, 111), while this pattern is less obvious in subtype B viruses (57, 112, 113).

The Env density on the surface of the virion may also favour transmission of certain variants: one study, which used infectious molecular clones (IMCs), found the density of Env on the surface of the viral membrane of T/F viruses was double that found on IMCs of chronically derived viruses (114). This may increase the probability that a virus attaches to and infects a target cell in the genital mucosa (106). There is also evidence to suggest T/F viruses display enhanced binding to Dendritic cells (114). This would then allow efficient transport of T/F viruses from the epithelial surface of the genital tract, where there is a relatively high density of Dendritic cells, to the stroma or lymphoid tissue, where the virus can be presented to, and infect, $CD4^+$ T cells (115, 116).

However, the most convincing evidence of a transmission bottleneck has been recently shown by Iyer *et al*., who studied the properties of plasma and genital secretion-derived viruses from eight donor and recipient pairs (117). Here, they found that recipient viruses were approximately three-fold more infectious than donor viruses, replicated to slightly higher titers and were released from infected cells 4.2 times more efficiently. In addition, recipient viruses were significantly more resistant to type I interferons (IFN): transmitted viruses were 7.8-fold more resistant to IFN-α2 and 39-fold more resistant to IFN-β. These results indicate that the mucosal bottleneck selects for viruses which can replicate efficiently in the presence of a potent innate immune response.

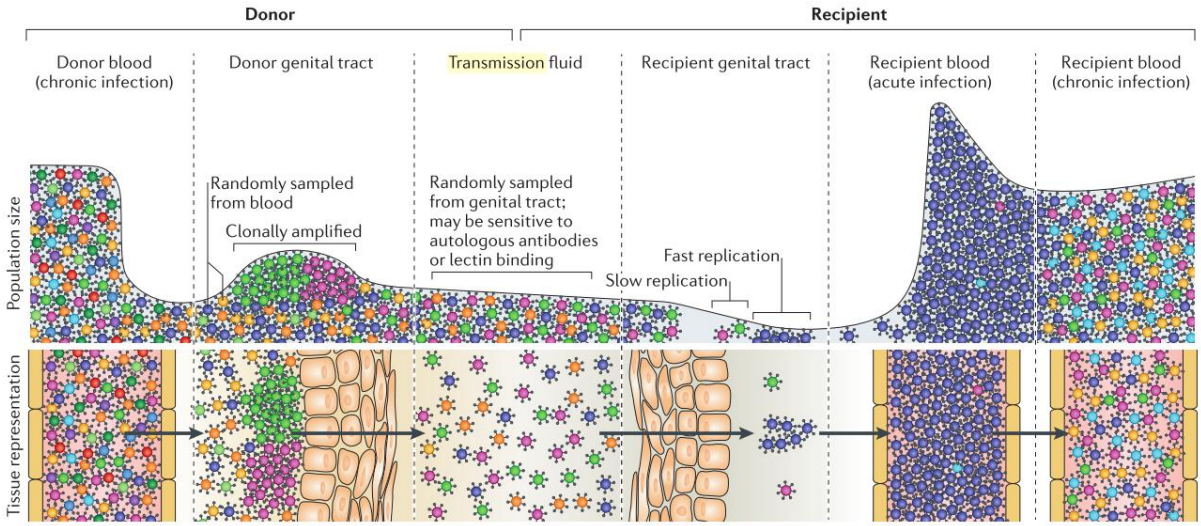

Figure 1.9 The transmitted/founder virus is shaped by multiple genetic bottlenecks. Chronically infected individuals have extremely diverse HIV-1 populations in their blood. Some viruses from the blood seed the genital tract of the donor, where the resulting viral population is less diverse than in the blood and is often dominated by a few clonally amplified variants. It is unknown whether replication in the genital tract selects for specific phenotypes. Viruses sampled from the donor genital tract are present in the transmission fluids (cervicovaginal mucus, semen or rectal secretions). The vast majority of viruses within the transmission fluid do not penetrate the genital or rectal mucosa of the recipient. Damage due to sexually transmitted infections or intercourse can increase the ability of viruses to penetrate the mucosa. Most of the viruses that can infect the recipient genital tract have a low reproductive rate (R_0 <1) owing to low densities of target cells, low viral fitness or susceptibility to host defences (such as phagocytosis or production of interferons) and will not contribute to the systemic infection. Typically, when a systemic infection is established after sexual exposure to HIV-1, the initial viral population in the recipient's blood will be genetically homogeneous because it was established from a single viral genotype (the transmitted/founder virus) that could replicate in the recipient genital tract. On progression to the chronic stages of infection, infected individuals display extremely diverse HIV-1 populations in their blood. Figure and legend adapted from (106) with permission provided by Nature Publishing Group.

1.5 Adaptive immune responses to HIV-1

1.5.1 Cytotoxic T-lymphocyte immune responses

While the RV144 trial provided some understanding of immune correlates associated with transmission risk, additional studies are still needed. Studies on the immune response to the virus in natural infection are being conducted in the hopes that this will provide valuable insight into how to design a protective vaccine (118, 119). One of the first, and most important, adaptive immune responses to HIV-1 infection is the cytotoxic T lymphocyte (CTL) response.

HIV-1-specific CTLs emerge two to three weeks after infection and play an important role in suppressing viral replication during both acute and chronic infection (120–122). In this adaptive process, viral peptides are processed and presented on Major Histocompatibility Complex (MHC) class I molecules (also known as Human Leukocyte Antigen (HLA) in

humans) on the membrane of the infected cells. T cell receptors (TCRs) expressed on the surface of CTLs then bind specifically to the MHC molecule with the viral peptide, which induces the release of perforins and proteases from the CTLs which lyse the infected cells (123).

HIV-1 has evolved several mechanisms to avoid recognition by CTLs. The first of these is non-mutational whereby the accessory protein Nef mediates a mechanism which leads to downregulation of MHC class I molecules on the surface HIV-1-infected cells, resulting in a lack of recognition by CTLs (124, 125). A second mechanism of escape involves the mutation of amino acids in viral epitopes which bind to MHC class I molecules or TCRs, resulting in loss of recognition by CTLs (126–129).

The effectiveness of the CTL response is complicated by the genetic diversity present among individuals from different populations. HLAs are grouped into subfamilies of closely related variants: HLA corresponding to MHC class I has three major genes (HLA-A, B and C) and three minor genes (HLA-E, F and G) (130). A large number of studies have shown that variation in HLA types is associated with disease progression, establishing that an individual's HLA profile determines their response to HIV-1 epitopes (131–134). Consequently, some HLA alleles are more protective, resulting in slower disease progression (135–138), such as HLA B*27:05, HLA B*57:01, HLA B*58, while other alleles, such as HLA B*35, HLA B*53 and HLA B*5802, are associated with rapid progression (139, 140).

1.5.2 Antibody-mediated immune responses

In addition to CTL immune responses, the other major adaptive immune arm against HIV-1 is the humoral response. The humoral responses have been correlated with protection in other anti-viral vaccines (141–144). This response is mediated through B cells and first becomes detectable in the form of antibody complexes, 8 to 20 days after virus is detected in the plasma (145, 146). Free antibodies, directed toward the HIV-1 gp41, are detectable in the plasma from approximately 14 days after detectable viremia. and a further 14 days are required before anti-HIV-1 gp120 antibodies (Figure 1.10 A and B) are detected in plasma (145, 146).

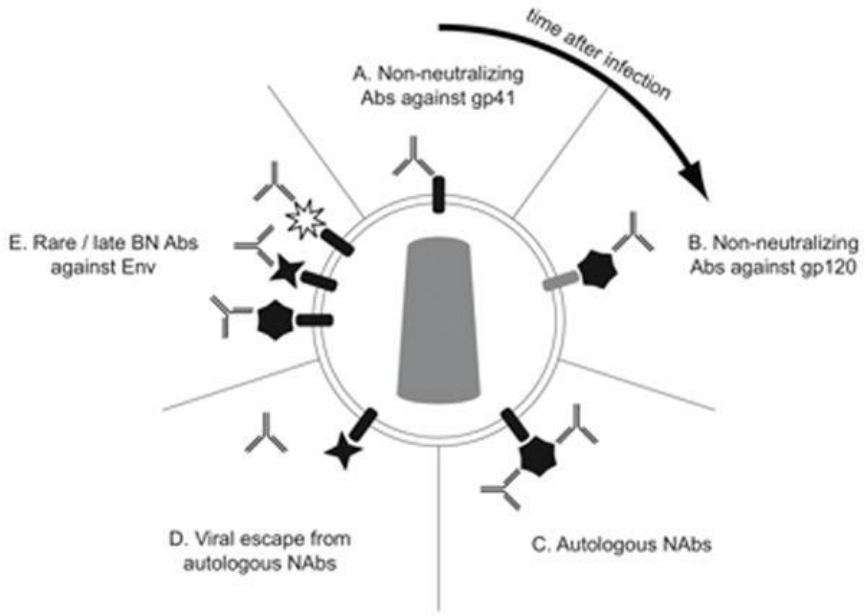

Figure 1.10 The antibody response to HIV-1. These responses occur in stages, shown here in a clockwise direction starting at the top. The initial antibody response to HIV-1 is non-neutralizing and directed at gp41 **(A)**. Soon thereafter non-neutralizing antibodies arise directed against gp120 **(B)**. After a delay of weeks to months, autologous neutralizing antibodies arise that apply selection pressure on the virus **(C)**. Viral mutation results in neutralization escape by HIV-1, represented here by a change in the shape of gp120 **(D)**. In some patients, antibodies that can neutralize a wide range of HIV-1 isolates arise, represented here by a variety of shapes of gp120 **(E)**. Figure and legend reproduced from (145) with permission from the Journal of Infectious Diseases.

These early antibodies are non-neutralizing and are elicited in all infected individuals against many different proteins (although Env elicits the strongest responses) (147–150). While these antibodies are not able to prevent cell entry, they function by binding to Env on the surface of viral particles or infected cells and elicit antibody effector functions, such as antibody-mediated virus opsonisation, resulting in complement cascade or phagocytosis (151–153) (Figure 1.11 B, C), antibody-dependent cellular cytotoxicity (ADCC) (Figure 1.11 D), antibody-dependent cell-mediated virus inhibition (ADCVI) or mucosal trapping (154, 155).

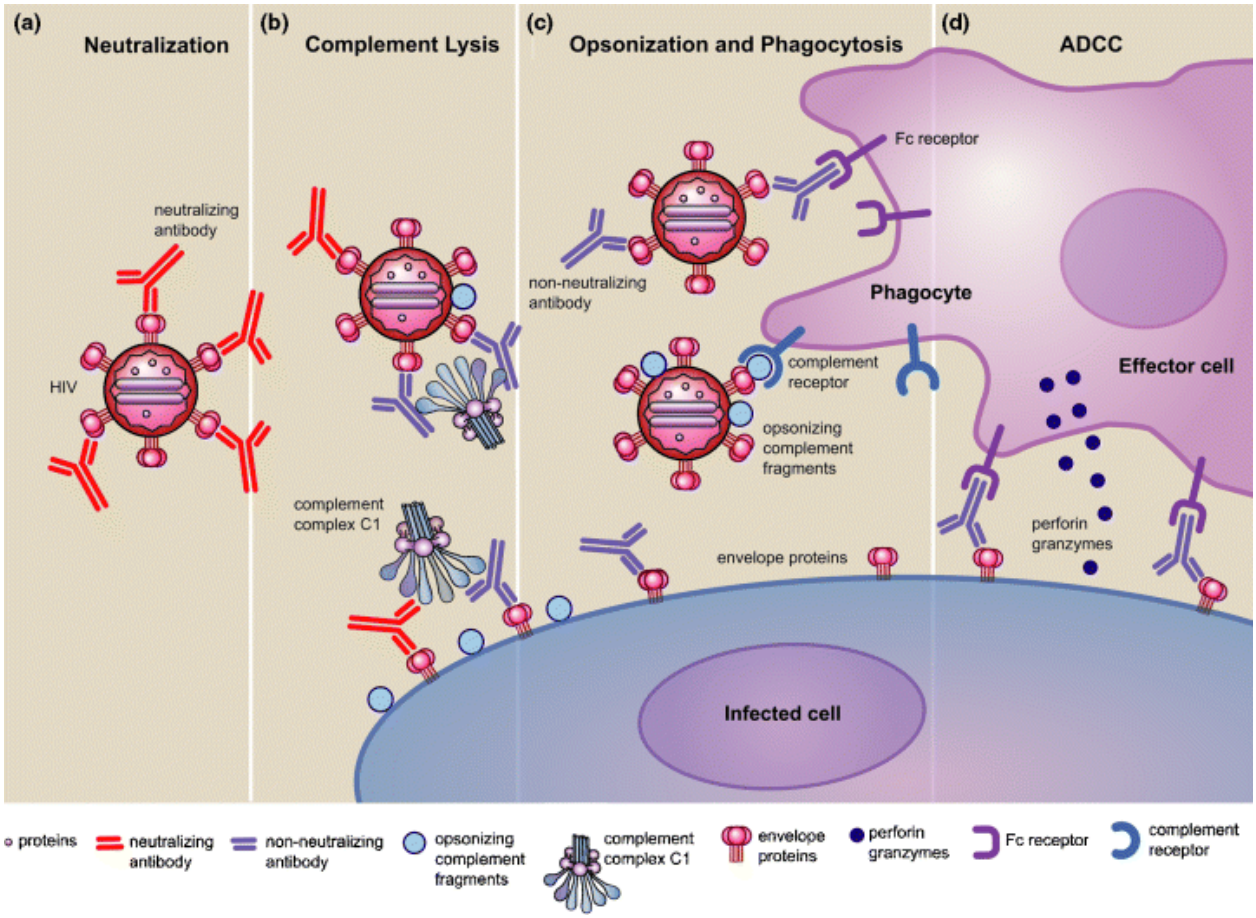

Figure 1.11 Antibody functions against HIV-1. Free virus neutralization by antibodies **(A)**, free virus and infected cell complement-mediated lysis facilitated by antibodies **(B)**, Antibody-mediated virus particle opsonisation and phagocytosis via Fc or complement receptors **(C)**, antibody-dependent cellular cytotoxicity (ADCC) against infected cells **(D)**. Neutralizing antibodies (red), non-neutralizing antibodies (blue), Fc receptor (violet), complement components (light blue), complement receptors (blue). Figure and legend reproduced from (156) with permission provided by John Wiley and Sons Publishers.

1.5.2.1 Neutralizing antibody responses

Neutralizing antibodies (nAbs) (Figure 1.10 C) prevent HIV-1 entry into target cells by binding to Env through the antigen binding fragment (Fab), coating viral particles and inhibiting binding of the virus to host cell receptors, CD4 and CCR5/CXCR4, as well as preventing fusion to the target cell membrane (Figure 1.11 A) (157).

Strain-specific nAb responses, which only target the virus which elicited them, usually appear from one to three months post-infection (146, 158–160). These responses develop after acute infection and are thought to be ineffective at controlling infection (158, 159, 161). This is likely because they often target a single specificity, predominantly in the Env variable regions (162–164). This allows the virus to rapidly escape (Figure 1.10 D) through several pathways;

including changes in N-linked glycosylation, point mutations and insertion/deletions (indels) (159, 164). Point mutations allow escape from nAbs by resulting in charge/shape changes in the epitope of the antibody (161), while N-linked glycosylation and indels (particularly in the variable loops) result in shielding of the nAb epitope (56, 165).

1.5.2.1.1 Broadly neutralizing anti-HIV-1 antibodies

A special subset of nAbs, broadly neutralizing antibodies (bnAbs), are capable of neutralizing many different virus strains, and as a result, are a highly desired outcome of an HIV-1 vaccine (157). However, most bnAbs only develop 2-4 years post infection (118, 166–168), and only in approximately 10-25% of individuals (118, 162, 169–171). Five major bnAb specificities have been discovered to date and include those targeting the CD4bs, the V1V2 loop, the V3 loop glycans, the MPER and the gp120/gp41 bridge (12) (Figure 1.12). BnAbs often have unusual features such as extensive somatic hypermutation, suggesting that affinity maturation is essential for the development of neutralization breadth (172). Further, some have unusually long complementary determining region 3's (CDR3s) (173, 174), presumably to enable the antibody to penetrate the glycan shield.

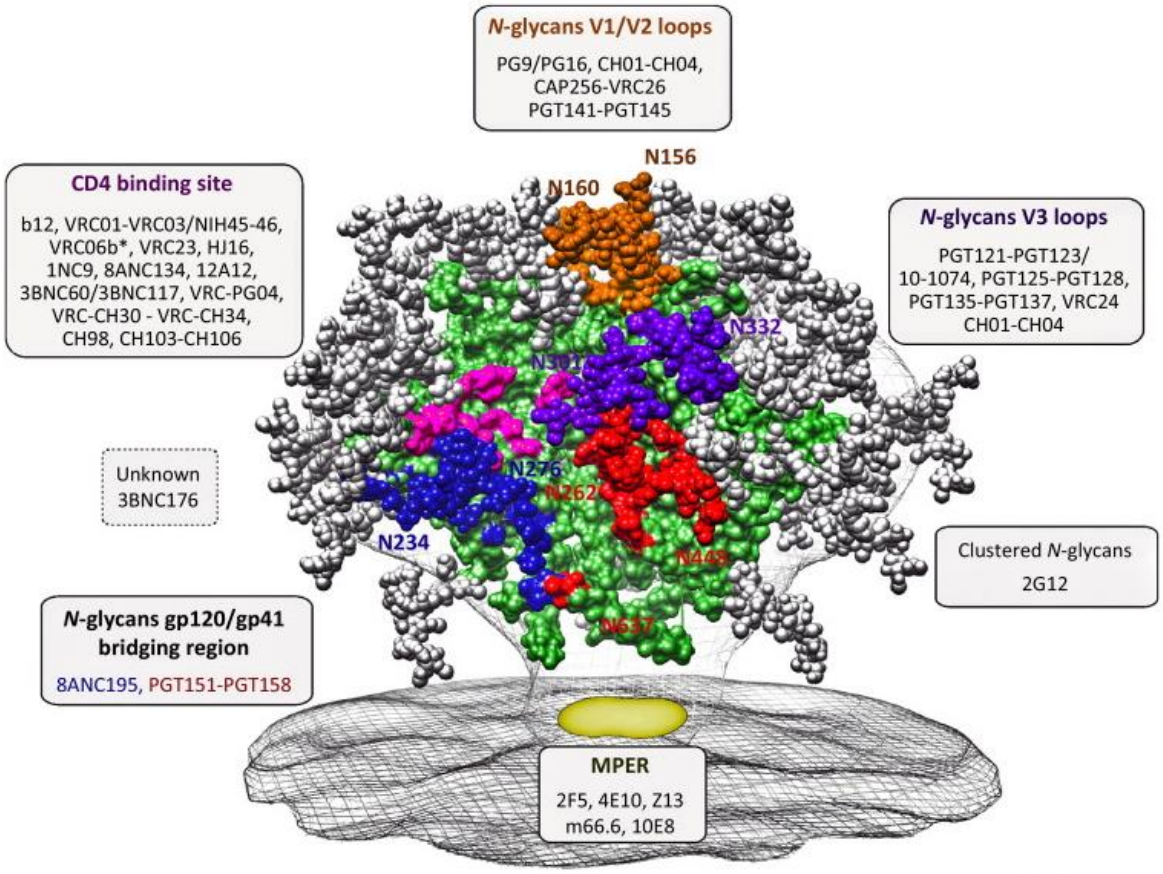

Figure 1.12 Sites of vulnerability on HIV-1 Envelope glycoprotein. The HIV-1 Env crystal structure (42) (PDB ID: 4NCO) was modelled onto the cryoelectron microscopy reconstruction of an unliganded membrane-bound HIV-1 Env trimer (175) (EMDB: 5019 and 5021). Env model that was used was fully glycosylated using predicted glycoforms (except for gp41, gp120 V2 and V4 loops, whose glycans were not modeled because of the disorder of those protein regions in the crystal structure or uncertainty in registry assignment). The figure was generated using UCSF Chimera (176). N160-dependent V1/V2 loops (orange), N332-dependent V3 loop (purple), CD4 binding-site (pink) and glycans-dependent gp120/gp41 bridging region epitopes (blue and red) are highlighted as defined by PG9 (91, 177), PGT128 (178), VRC01 (172), 8ANC195 (179) and PGT151 (180) binding. The MPER of gp41, for which only limited structural information is available in the context of the HIV-1 Env trimer, is also a site of vulnerability and is highlighted in yellow. BnAbs specifically mapped to each site of vulnerability are indicated in boxes. Figure and legend reproduced from (103) with permission provided by Elsevier Publishers.

1.5.2.2 Fc-mediated antibody effector functions

Antibodies mediate effector functions through the Fc (Fragment, crystallisable) region of the antibody. The Fc region binds to Fc receptors (FcRs) on effector cells such as Natural Killer cells (NKCs), Monocytes, Dendritic cells and Neutrophils (181) as well as other cells, and are essential for a comprehensive immune response against many pathogens (182–188). NKCs are able to mediate the killing of infected cells which display antibody-bound antigen, or mediate virus inhibition, after binding to the antibody-antigen complexes (189–191). NKC activity is

dramatically elevated during acute infection prior to the $CD8^+$ T cell response and is the dominant cytolytic effector population during acute HIV-1 infection (192–194).

Within the family of FcRs, the $Fc_\gamma Rs$ (primarily $Fc_\gamma RI$, $Fc_\gamma RIIa$ and $Fc_\gamma RIIIa$) are of particular interest. These receptors bind IgG antibodies and initiate activation of effector cells in the presence of HIV-1 (195–197). $Fc_\gamma RI$ receptors are upregulated in monocytes and mature dendritic cells in acute HIV-1 infection (198), with decreased levels of these receptors observed over the course of infection (198), possibly due to Nef which is thought to downregulate these receptors.

$Fc_\gamma Rs$ on effector cells, such as NKCs, can also bind to the Fc domain of antibodies bound to the surface of infected cells, and mediate ADCVI. This often includes secretion of antiviral factors, such as IFN-γ, as well as cytokines and chemokines by NKCs (199, 200, 328). In addition, FcRs on effector cells bound to antibody-antigen complexes on the surface of infected cells via the antibody Fc, may activate effector cells and, subsequently, result in ADCC. This involves the release of perforin, granzyme and Fas ligand by effector cells and, consequently, the death of the infected cell (200).

1.6 Antibody-dependent cellular cytotoxicity

1.6.1 ADCC and HIV-1 infection

ADCC and ADCVI responses can effectively harness the innate immune system early in acute HIV-1 infection. This may explain several recent studies which suggest ADCC plays a role in protection from HIV-1 acquisition and disease progression (8, 186). Among these, some studies have revealed that bnAbs partially protect via effector function, facilitating these functions via the Fc region. The role of antibody effector functions in protection against SHIV (an HIV-1/SIV chimera) has been implied through an Fc domain-deficient bnAb (b12) study, which showed moderately decreased protection against SHIV compared to the complete b12 antibody (201). This decreased protection may be due to less efficient neutralization of free virions, but is more likely due to decreased effector functions (202). A number of other studies have showed that removing $Fc_\gamma R$-mediated activity results in decreased protective effect of bnAbs, supporting this conclusion (203, 204). One of these studies, by Forthal *el al.*, showed that interactions between NKCs and the Fc domain results in enhanced antibody neutralization (204), suggesting nAbs function via the Fc domain, in addition to neutralization.

Fc function also plays a role in nnAb activity, which results in effector functions, such as ADCC activity, observed as early as 3 weeks post infection (205). Studies of this activity,

through *in vitro* and *in vivo* experiments, suggest that ADCC and ADCVI may play an important role in HIV-1 control (183, 206–214).

Further evidence of the importance of ADCC responses is documented in studies conducted on samples from naturally infected humans. These include mother-to-child transmission studies by Broliden *et al.* and Overbaugh *et al.*, where ADCC responses were linked with enhanced protection. These studies provide evidence that ADCC-mediating nnAbs transmitted via breast milk from the mother to infant enhanced protection of the infant from HIV-1 acquisition or, if acquisition occurred, slowed progression to disease (215, 216). In one of these studies, weak nAb activity was detected in 4 of the 19 women and was not associated with protection. ADCC responses, however, were detected in all of the women and was inversely associated with infant infection risk (216), suggesting ADCC has a role in protection against HIV-1 transmission.

Numerous other studies have observed that ADCC responses were enriched in HIV-1 non-progressors (151, 183, 186, 209, 217–220). In contrast, a lack of an ADCC/ADCVI response may lead to reduced control of HIV-1 infection (183, 208, 221). Interestingly, a study conducted by Delfraissy *et al*. noted potent ADCC activity was detected in all elite controllers in their cohort (10/10), yet was only found in 40% of viremic individuals (4/10) (186), suggesting ADCC may also have an important role in HIV-1 control.

Lastly, these findings are corroborated in a number of non-human primate (NHP) studies which showed ADCC-inducing antibodies were enriched in plasma of subjects with non-progressive disease in SIV-infected NHPs (205, 206, 212, 213). Another NHP study showed SIV viral load decline coincident with ADCVI activity. Interestingly, this containment was against phylogenetically divergent and neutralization-resistant viruses (189). The ability to contain divergent HIV-1 strains suggests that the antibodies which elicited this function targeted conserved regions of SIV and, consequently, warrant further study. In NHP vaccine studies using replicating Ad5hr-SIV prime, with an Env boost, strong systemic and mucosal antibodies which mediated ADCC activity were correlated with better control of acute viremia (206, 221).

1.6.2 ADCC in immunization studies

The RV144 Thai trial, which showed 31.2% vaccine efficacy, is the only protection achieved thus far by an HIV-1 vaccine (149). However, this efficacy did not correlate with nAb or cellular responses as predicted, but rather with nnAb responses to the V1V2 and V3 regions (8). Further, V3-specific ADCC antibodies were implicated, but not correlated, with protection from infection (222).

Evidence of the protective response offered by nnAbs is supported by several important NHP studies. A passive NHP immunization study by Moore *et al.* found that immunization of macaques with F240 nnAbs (which target an immunodominant epitope of gp41) and then vaginal challenge with SHIV protected two out of five macaques from infection, with F240 decreasing the viral load of a further two, compared to the control macaques (NS1, anti-Dengue), which all became infected (223). This finding importantly showed neutralizing activity is not necessary for protection. However, the underlying mechanism of this protection is unknown and this study suggests deeper analysis of nnAb effector mechanisms in HIV-1 immunity is required.

Vaccine studies in NHPs have shown that at least some of the protection provided by nnAbs is through ADCC and ADCVI mechanisms. Barouch *et al*. vaccinated NHPs with adenovirus/poxvirus and adenovirus/adenovirus vaccines expressing SIVsmE543 Gag, Pol and Env antigens which resulted in > 80% reduction in per-exposure probability of infection (224). This vaccine provided protection against the acquisition of the highly pathogenic, heterologous and neutralization-resistant SIVmac251 virus and correlated with both peripheral and mucosal Env-specific IgG. Further, delayed disease progression largely correlated with Env-binding antibodies and ADCC responses (224).

A similar NHP vaccine study, using SIV recombinants, elicited nnAbs with ADCC activity against SIV-infected cells. These recombinants stimulated production of nnAbs with strong ADCVI and ADCC activity (214). Moreover, production of nnAbs led to transcytosis inhibition and reduced chronic viremia (214), providing *in vivo* evidence that this mechanism of protection against acquisition and disease production is important.

Several other studies in NHPs showed vaccine candidates elicited ADCC antibody titers that did not protect from infection but did correlate with control of viral replication after mucosal challenge (201, 224), or with reduced acute viremia *in vivo*, after mucosal challenge (212).

Lastly, macaques vaccinated with *tat*/*env* replication-competent adenovirus elicited nnAb activities which had a significant impact on challenge outcome when challenged with SHIV. Acute phase protection correlated with Tat- and Env-binding antibodies, but anti-Env neutralization activity was not detected (225). Furthermore, ADCVI correlated significantly with better acute phase protection (213). Research on the epitopes which elicited these nnAbs would be beneficial: while it is known the nnAbs elicited are specifically anti-Env, knowledge

of the specific epitopes targeted could provide helpful insight into how strong ADCVI activity is elicited.

1.6.3 ADCC epitopes and escape

ADCC antibodies are generally thought to target HIV-1 proteins presented on the surface of infected cells. For this reason, the majority of epitope discovered to date are either in the gp120 (203, 226, 227) or gp41 (148). These epitopes have been comprehensively reviewed by Pollara *et al*. (228) and are summarised in Table 1.1 (reproduced from (228)).

In gp120, several epitopes have been mapped, including the CD4bs (203, 229, 230), the V2 region (231) and the V3 region (191, 203). Further to this, a number of studies have shown ADCC epitopes which are only present following the binding of CD4 to the gp120 (CD4 induced (CD4i) epitopes) (191, 229), suggesting that gp120 on the surface of cells may have another structure which exposes these epitopes or that ADCC also takes place as target cells are in the process of being infected. Studies investigating the gp41 region have described epitopes in cluster I (an immunodominant region of the gp41) (148), HR2 (148) and the MPER (148, 154).

Of particular interest is a study conducted by Ferrari *et al*. on the monoclonal antibody A32, which binds a conformational epitope including the C1 region (229). This antibody could potently induce ADCC (but not neutralize) in the presence of soluble CD4, but lacked significant neutralizing or ADCC activity in the absence of CD4, highlighting the difference in epitopes between neutralizing and ADCC-eliciting antibodies.

An important indicator of the importance of ADCC responses would be their ability to force immune escape. However, only a few studies thus far have illustrated ADCC-specific immune escape (reviewed in (232)). One such study by Chung *et al*. showed escape in the Env in chronic infection using peptides with known ADCC epitopes, and measuring NK cell activation (233). However, as only linear epitopes could be mapped using peptides, this method of screening is expected to considerably underestimate the epitopes and escape from ADCC antibodies. In order to map conformational ADCC epitopes and their escape, whole Env or infectious molecular clones need to be constructed (232).

Additionally, the complexity of humoral immune responses to the HIV-1 Env as infection progresses makes unravelling escape from ADCC difficult: as infection continues and nAb responses become detectable, escape from nAb responses, which likely overlap (at least to some degree) with ADCC responses, may confound results (228). However, this can be

overcome by demonstrating escape from ADCC responses in early HIV-1 infection, when ADCC responses are detectable but autologous nAbs have not yet developed.

Table 1.1 Defined Regions of the HIV-1 Envelope Targeted by Human anti-HIV-1 mAbs with ADCC Activity (table reproduced from (228)).

HIV-1 Envelope Glyco-protein	Envelope Region	mAb	Discontinuous or Linear Epitope	Neutralizing or Non-Neutralizing	ADCC References
gp41	**Cluster I**	246-D	Linear	Non-neutralizing	(234)
		4B3	Linear	Non-neutralizing	(234)
		98-43	Linear	Non-neutralizing	(148)
		50-69	Discontinuous	Non-neutralizing	(148)
	Cluster II (HR2)	98-6	Discontinuous	Non-neutralizing	(148)
		126-50	Discontinuous	Non-neutralizing	(148)
	Not defined	31710B	Not defined		(203)
	MPER	120-16	Linear	Non-neutralizing	(148)
		2F5	Linear	Neutralizing	(154, 234)
		4E10	Linear	Neutralizing	(234)
gp120	**CD4i C1 region (Cluster A)**	A32	Discontinuous	Non-neutralizing	(229)
	CD4i CoRBS (Cluster C)	17B	Discontinuous	Neutralizing	(229)
	CD4i	CH08	Discontinuous	Neutralizing	
	CD4i Cluster A	C11, L9-i1, N5-i5, L9-i2, N12-i3, N26-i1	Discontinuous	Non-neutralizing	(235)
	CD4i Cluster B	N12-i15	Discontinuous	Non-neutralizing	(235)
	CD4i Cluster C.1	L9-i3, N5-i1, N5-i3, N5-i4, N5-i8, N10-i1.1, N10-15.3, N12-i1, N12-i2, N12-i4, N12-i5, N12-i7, N12-i8	Discontinuous	Neutralizing	(235)
	CD4i Cluster C.2	N12-i10, N12-i17, N12-i18, N12-i19	Discontinuous	Neutralizing	(235)
	CD4i Cluster C.3	N5-i2, N5-i6, N5-i9, N5-i14, N5-i7, N5-i12, N10-i3.1, N12-i12, N12-i9, N12-i11	Discontinuous	9/10 Neutralizing	(235)

	CD4i Cluster C.4	L9-i4, N5-i10.1, N5-i13, N10-i2, N12-i14, N12-i16	Discontinuous	2/6 Neutralizing	(235)
	CD4i	N10-i4, N10-i6.1	Discontinuous	Non-neutralizing	(235)
	CD4i C1 region	CH20, CH29, CH38, CH40, CH49, CH51, CH52, CH53, CH54, CH55, CH57, CH77, CH78, CH80, CH81, CH90, CH91, CH92, CH94	Discontinuous	Non-neutralizing	(191)
	C2, C3, C4, V4 glycosylation sites	2G12	Discontinuous	Neutralizing	(236)
	C5	670-D	Discontinuous	Neutralizing	
		750-D	Not defined	Non-neutralizing	
		42F, 43F	Linear	Non-neutralizing	(226)
	CD4 binding site	15e	Discontinuous	Neutralizing	
		F105	Discontinuous	Neutralizing	
		448-D	Discontinuous	Neutralizing	
		1125H, 5145A	Discontinuous	Neutralizing	(203)
		b12	Discontinuous	Neutralizing	(230)
		VRC01	Discontinuous	Neutralizing	(229)
	V2	CH58, CH59, HG107, HG120	Linear	Neutralizing	(231)
		PG9	Discontinuous	Neutralizing	
	V3	694/98D	Linear	Neutralizing	
		4117C, 41148D	Linear	Neutralizing	(203)
		CH22, CH23	Linear	Neutralizing	(191)

1.6.4 Methods to measure ADCC activity

In comparison with the widely-recognized HIV-1 neutralizing antibody assay, there is no standard assay to detect ADCC-mediating antibodies. All the assays use antigen-coated or infected target cells, effector cells and an antibody preparation as inputs; but measure different outputs. The assays start by either coating target cells with HIV-1 peptides or proteins or infecting the target cells with replication-competent virus. Coated or infected target cells are then incubated with antibodies and effector cells, and the output is measured after a certain length of incubation.

Early studies measured radioactivity read-outs from ^{51}Cr-labelled target cells (226). While this method measured cell death due to ADCC, it was an expensive, laborious and insensitive assay. Several improved, high-throughput assays have now become available: the first, a flow cytometry-based fluorescent killing assay termed the "rapid fluorescent ADCC" (RFADCC) assay, measures the release of intracellular dyes from target cells killed by ADCC (237) after coating the target cells with peptides or proteins and then incubating the target cells with antibodies and effector cells.

Two other assays use flow cytometry-based methods to measure the loss or addition of a fluorescent dye: Stratov *et al*. (238) developed an assay that measures the increase in expression of intracellular cytokines (ICS) by NK cells, which is induced by binding of the FcγRIIIa (CD16) receptor on NK cells to antigen-bound antibodies. Further, Pollara *et al*. (239) developed a specific and high-throughput method to measure the proteolytic activity of Granzyme B after its delivery into target cells, initiated by antibody recognition of viral antigens on the target cell membrane.

The last two popular ADCC assays take advantage of *luciferase* gene expression, similar to the neutralizing antibody assay. The first, developed by Alpert *et al*. (210) uses an immortalized NK cell line and a target cell line which expresses Luciferase from a Tat-inducible promoter upon HIV-1 infection. The dose-dependent loss of Luciferase in the presence of NK cells and antibodies indicates the killing of infected target cells. Similarly, Pollara *et al*. (240) developed an assay which uses infectious molecular clones which contain the *luciferase* gene. Once target cells are infected with these viruses, the Tat-inducible *luciferase* gene is present in target cells, and the measurement is the same as the Alpert assay.

One further important factor to note is the significance of the antigen used to measure ADCC. While peptides are non-conformational and ADCC directed towards peptide-coated target cells

represent antibodies which target linear peptides, the use of proteins to coat target cells is quite different: it is thought using these gp120/140 proteins represent the virus binding to the CD4 molecule on the cell membrane and, thus, exposing CD4-inducible (CD4i) epitopes only exposed during viral entry (228). In comparison, use of infected cells is thought to expose epitopes present during both entry and viral budding from infected cells (240).

1.7 Study rationale

The RV144 vaccine trial conducted in Thailand showed modest protection from infection associated with V1V2-targeting ADCC-mediating nnAbs. This, together with several other studies, suggests ADCC responses, in combination with nAbs, may be an important response for an effective HIV-1 vaccine to elicit. Studying the relationship between the two types of antibodies will likely provide important information that aids vaccine design. While there is extensive information on nAbs, there is limited information on the role of ADCC in controlling viral populations in early infection, and how this relates to nAb responses.

One indicator of the importance of an immune response is the ability to force immune escape. Escape from nAbs and CTLs has been demonstrated in many studies and is well characterised. However, there are only a limited number of studies on the ability of ADCC responses to force immune escape in the HIV-1 Env.

This study will specifically look at HIV-1 Env evolution before, during and after the development of early nAb responses, to assess the impact of nAb and ADCC responses on Env evolution in early infection. Specifically, we would like to determine if ADCC responses exert immune pressure on the HIV-1 Env, which would suggest this is an important response. Further, the relationship between neutralizing and ADCC-mediating antibody epitopes will be assessed. This will elucidate the relationship between ADCC-mediating and neutralizing antibodies, and HIV-1 Env evolution in early subtype C infection.

The specific objectives of this project are:

1. To investigate the kinetics of early virus evolution in the HIV-1 Env in response to antibody pressure in seven subtype C-infected individuals from infection to after the detection of autologous nAbs.
2. To investigate whether Env mutations identified in early HIV-1 infection are associated with escape from ADCC responses.

3. To investigate the relationship between Env epitopes targeted by ADCC and nAb responses in early HIV-1 infection.
4. To explore the breadth of ADCC responses mediated by a panel of broadly neutralizing and non-neutralizing anti-HIV-1 monoclonal antibodies against a panel of acute/early HIV-1 subtype C viruses.

Chapter 2. Early HIV-1 neutralizing antibody pressure results in an increase in escape mutant viruses without depleting wild type viruses

ABSTRACT

The high evolution rate of HIV-1 poses one of the greatest challenges to HIV-1 vaccine development. In this chapter, we aimed to determine rates of escape from neutralizing antibodies (nAbs) following infection, and elucidate mechanisms associated with viral immune evasion.

We studied seven participants of the CAPRISA 002 acute infection cohort enrolled within 56 days of infection and followed for 6 months. Viral diversification in known nAb epitopes was quantified using a deep sequencing approach, and escape residues were confirmed using pseudovirus neutralization assays. Cell-cell transmission inhibition assays were performed as a potential mechanism by which the virus may escape nAb responses without having to mutate.

Following nAb responses, there was a significant drop in the relative frequency of wildtype (WT) virus. However, when controlling for changes in viral load (VL) over time, we observed that the WT load (frequency of the WT residue x total VL) remained relatively stable in three participants despite an effective nAb response, while the escape mutant load increased. Our data revealed that early nAbs were unable to inhibit cell-cell transmission as efficiently as free virus-cell transmission, and the incorporation of escape mutations resulted in further loss of inhibition of both free virus-cell and cell-cell transmission.

These results demonstrate that early nAb responses may not effectively clear viral populations. While changes in the viral genome is a dominant pathway to nAb escape, cell-cell transmission provides an alternative pathway. As these nAbs were less effective at inhibiting cell-cell transmission, this provides a potential mechanism whereby HIV-1 can escape early autologous nAbs. These results suggest that other antibody effector functions such as ADCC, which can target infected cells, may be important to elicit in a protective HIV-1 vaccines.

2.1 Introduction

One of the major goals of the HIV-1 vaccine field is to discover a vaccine which elicits protective nAbs. However, the high diversity of HIV-1 in the Envelope (Env), which is the target of nAbs, makes this a challenge. The diversity of HIV-1 is partially the result of rapid escape from immune responses, typically through point mutations in the nAb epitope, and lengthening of the variable loops and glycosylation changes which serve to shield nAb epitopes (56, 161, 165). This results in contemporaneous viruses that are less sensitive to autologous neutralization than earlier viruses (158, 159, 164). The consequence is that the nAb response must constantly catch-up to the escaped HIV-1, which would compromise protection from an HIV-1 vaccine.

While most studies have observed rapid and complete escape from nAbs, particularly in early infection, there have been a few exceptions. Two studies by Bar *et al*. and Moore *et al.* demonstrated persistence of the WT, nAb sensitive virus in early infection (each in one participant) (164, 241). In both studies, the WT remained detectable in all time-points tested, up to several months after the detection of nAbs, but still decreased 1-2 logs in quantity suggesting nAb pressure was still substantial. If the WT virus is persisting, the mechanism whereby it avoids nAb detection remains unclear. Further, the implication of nAb sensitive WT virus persistence is unknown.

Numerous studies have shown nAbs are less efficient at inhibiting cell-cell transmission than free virus-cell transmission, including broadly neutralizing antibodies (bnAbs), implicating cell-cell transmission as a possible mechanism whereby WT virus may avoid detection (242–248). Cell-cell transmission occurs via the formation of virological synapses (249–251), and is faster and more efficient *in vitro* than infection from cell-free virus (252–254). The efficient formation of this synapse may result in steric hindrance, preventing antibodies from accessing the synapse.

Here, we used a deep sequencing approach to quantify viral diversification in the known nAb epitope in response to early anti-HIV-1 antibody development from infection till after the detection of nAbs. Using pseudovirus neutralization assays, we then determined the kinetics of nAb escape, at a residue level. When considering changes in VL over time, we observed that following nAb responses, the WT load (frequency of the WT residue x total VL) remained relatively stable, while the escape load (frequency of the mutant x total VL) increased. Consequently, we explored cell-cell transmission as one mechanism by which the WT virus

population (viruses which contained the original, WT residue at the site of nAb escape) may be maintained. Our data revealed that nAbs were unable to inhibit cell-cell transmission as effectively as free virus-cell transmission, and the incorporation of escape mutations resulted in further loss of inhibition of both free virus-cell and cell-cell transmission.

2.2 Methods

2.2.1 Ethics statement

The CAPRISA 002 acute infection study received ethical approval from the Universities of KwaZulu-Natal (E013/04), Cape Town (025/2004), and the Witwatersrand (MM040202). All participants in this study provided written informed consent for study participation. This study further received ethical approval from the University of Cape Town (430/2014) as a sub-study of the CAPRISA acute infection study.

2.2.2 CAPRISA 002 acute infection cohort participants

The CAPRISA 002 acute infection cohort, described previously (162, 255), was established in 2004 and recruited recently HIV-1 infected women, from Durban, KwaZulu-Natal, South Africa, prospectively. HIV-1-infected participants were recruited within 3 months of a previous HIV-1 negative test. Following detection of infection, plasma samples were taken weekly for 3 weeks, fortnightly until approximately 3 months post infection, monthly until approximately 1 year post infection, and quarterly thereafter. The time of infection was estimated as the mid-point between the last HIV-1 negative sample and the first HIV-1 positive sample, or 14 days prior to the first HIV-1 positive sample if the sample was RNA-positive, seronegative. Each participant was monitored for CD4 count and viral load.

2.2.3 Cell lines

TZM-bl cells (159) were obtained from the NIH AIDS Research and Reference Reagent Program (NIH ARP, catalogue number 8129, contributed by John Kappes and Xiaoyun Wu). The 293T cell line was obtained from Dr George Shaw (University of Pennsylvania, Philadelphia, PA). All adherent cell lines were cultured at 37 °C, 5% CO_2 in DMEM containing 10% heat-inactivated Fetal Calf Serum (FCS) (Biochrom) with 50 µg/mL Gentamicin (Lonza) and disrupted at confluency by treatment with 0.25% trypsin in 1 mM EDTA (Lonza).

2.2.4 Peripheral blood mononuclear cells

Human primary peripheral blood mononuclear cells (PBMCs) were isolated by Ficoll gradient from buffy coats obtained from healthy HIV-1 seronegative donors. Buffy coats were supplied by the Western Province Blood Transfusion Services. PBMC were cultured in RPMI 1640 growth medium supplemented with gentamicin (50 U/mL), L-glutamine (2 mM) and 10% FCS (Biochrom) (subsequently referred to as R10), as well as interleukin-2 (IL-2) (30 U/mL) (Roche). The cells were stimulated by culturing in R10-IL-2 medium containing phytohemagglutinin (PHA) (2.5 μg/mL) (Sigma) for 72 h. After 72 h, the medium was removed and the cells were placed into culture with R10 growth medium containing IL-2 (30 U/mL) and used immediately.

2.2.5 Deep sequencing library preparation and data processing

RNA extraction, cDNA synthesis and subsequent amplification were carried out using the primer ID method as described previously (256, 257), with the following modifications: cDNA synthesis primers were designed to bind to the C2 (HxB2: 6907-6883), C3 (HxB2: 7343-7318) or C5 (HxB2: 7655-7632) regions of the HIV-1 *env* respectively (depending on the region to be amplified) (all primer sequences can be found in Appendix A4). First-round amplification primers were designed to bind to the C1 (HxB2: 6654-6674), C2 (HxB2: 6950-6973) or C3 (HxB2: 7114-7135) regions respectively. This allowed amplification of the C1C2, C2C3 or C3C5 regions depending on the primer set used. Raw reads were processed using a local instance of Galaxy (258–260), housed within the University of Cape Town High-Performance Computing core. Read quality was assessed using fastqc (http://www.bioinformatics.babraham.ac.uk/projects/fastqc). Short reads (<150 bp), and low-quality data, were filtered out using the Filter FASTQ (version 1.0.0) tool (258) with a minimum quality of Q35 for 3′ base trimming. Forward and reverse reads were merged using PEAR (261). A custom python script (written by Phillip Labuschagne, UCT) was used to bin all reads containing an identical Primer ID tag, to align the reads within each bin using MAFFT (262) and to produce a consensus sequence based on a majority rule. Sequences with a Primer ID that was represented in fewer than three reads were discarded, along with and those containing degenerate bases. The resulting consensus sequences were then used to generate codon aligned nucleotide and amino acid alignments using MACSE (263) and viewed using BioEdit (Version 7.1.11) (264). The Hamming distance was calculated using a custom script (adapted from a script written by Dr Colin Anthony, UCT), adjusted such that deletions of any size resulted in a score of one, and normalised to the distance of the region sequenced.

Magnitude of selection was calculated using FUBAR (265) in the HyPhy 2.2.1 software package (266).

2.2.6 Jensen-Shannon divergence

Jensen-Shannon divergence (D_{JS}) is a measure of dissimilarity between probability distributions that was introduced by Lin (267) to alleviate the limitations associated with relative entropy, and can take into account changes in distributions between two time points. D_{JS} between the two discrete probability distributions $p = (p_1, \ldots, p_n)$ and $q = (q_1, \ldots, q_n)$ is defined as follows:

$$D_{JS}(p, q) = \frac{D_{KL}(p, a) + D_{KL}(q, a)}{2}$$

where a = $(p + q)/2$ is the average of p and q, and D_{KL} (x,y) is the relative entropy between x and y. The values of D_{JS} are normalized to lie between 0 and 1.

D_{JS} can be expressed using entropy (H) with the following formula:

$$D_{JS}(p, q) = H\left(\frac{p + q}{2}\right) - \frac{H(p) + H(q)}{2}$$

D_{JS} was measured using a custom script written by Dr Colin Anthony (UCT).

2.2.7 Cloning gp160, mutagenesis and pseudovirus production

PCR amplification of HIV-1 *env* genes was done using the single-genome amplification (SGA) approach previously described (268). The second-round PCR reaction was repeated using the high-fidelity Platinum Taq DNA Polymerase (Invitrogen), together with 0.2 mM dNTPs (Invitrogen), 4 µM of Env 1A-Rx (5'- CACCGGCTTAGGCATCTCCTATAGCAGGAAGAA -3') and EnvN (5'- CTGCCAATCAGGGAAAGTAGCCTTGT -3') in a final volume of 20 µL. Amplicons were cloned into the directional vector pcDNA3.1(+) (Invitrogen) per the manufacturer's instructions. Site-directed mutagenesis was performed using the Stratagene QuickChange II kit (Stratagene). Env pseudoviruses were obtained by co-transfecting the *env* plasmid with pSG3ΔEnv (159) in 293T cells using PolyFect transfection reagent (Qiagen). Pseudovirus-containing supernatants were harvested 48 h following transfection and clarified by 0.45 µm filtration and adjusted to 10% FCS (Biochrom). The 50% tissue culture infectious dose ($TCID_{50}$) for each pseudovirus preparation was determined by infection of TZM-bl cells as previously described (162, 269).

2.2.8 Neutralization assay

Neutralization was measured, as previously described (162), by a reduction in *luciferase* gene expression after single round infection of TZM-bl cells with Env pseudo or infectious viruses. All experiments were repeated two to three times. Titers were calculated as the mean reciprocal plasma dilution which resulted in a 50% reduction (ID_{50}) of the relative light units (RLU).

2.2.9 Construction of HIV-1 infectious molecular clones and virus preparation

HIV-1 Infectious Molecular Clones encoding the *env* (Env-IMC) for early viruses CAP210 TF, CAP255 2.00.5 and CAP257 2.00.Luc, as well as mutant viruses CAP210 TF A161V and CAP210 TF V208I, were constructed as previously described in the Ochsenbauer laboratory (270) (Appendix A2). Env-IMCs for CAP239 TF and CAP239 TF L278S were constructed at UCT (D Mielke) (Appendix A2). All Env-IMCs expressed *Renilla luciferase* reporter gene under the control of the HIV-1 Tat protein, and preserved all nine viral open reading frames. Replication-competent viruses were obtained by transfecting the Env-IMC plasmid in 293T cells using PolyFect transfection reagent (Qiagen). Virus-containing supernatants were harvested 48 h following transfection, clarified by 0.45 µm filtration and adjusted to 10% FCS (Biochrom). The $TCID_{50}$ for each IMC preparation was determined by infection of TZM-bl cells as previously described (162, 269).

2.2.10 Infection of PBMCs

Stimulated healthy PBMCs from four donors were depleted of CD8+ T cells using MACS human CD8 microbeads (Miltenyi Biotec) per the manufacturer's recommendations, and pooled in a ratio of 1:1:1:1. Five million pooled, CD8-depleted PBMCs were then centrifuged, the supernatant removed and the cells resuspended in 1 mL of virus preparation. The cells were then spinoculated (1000 x g) for 2 h at 32 °C. After spinoculation, 2 mL of R10 supplemented with IL-2 (30 U/mL) (Roche) was added. Growth medium was replaced after 24 h, and infected cells were grown at 37 °C, 5% CO_2 for a further 72 h. PBMCs from the same four donors were used in each experiment and subsequent repeats.

2.2.11 Assessment of viruses used in cell-cell inhibition assays

We used the method developed by Abela *et al*. (242), which utilizes the dependence of R5-tropic viruses on polycationic supplements in cell culture medium to infect TZM-bl cells as cell-free virions, to measure the inhibition of cell-cell transmission.

To determine if viruses could be used in the cell-cell inhibition assay, viruses were tested for dependence on the polycation diethylaminoethyl-Dextran (DEAE-Dextran) to infect TZM-bl cells as free virus inoculum. Serial dilutions of free viruses were titrated over TZM-bl cells (10^4 cells per well) in culture medium in the presence or absence of DEAE-Dextran (20 µg/mL) (Sigma) for 48 h. Only viruses that resulted in at least one log reduction of infectivity over the linear range in the absence of DEAE-Dextran, when compared with infectivity in the presence of Dextran, were used in the cell-cell inhibition assay (Appendix A1, Figure A1.3). Cell-free virus input was chosen to yield infectivity corresponding to 100 000 – 125 000 RLUs (within the linear range) per well in the absence of inhibitors.

To assess the ability of virus from infected PBMCs to infect TZM-bl cells, infected PBMCs were washed three times with PBS (Lonza) and titrated on TZM-bl cells (10^4 cells per well) in culture medium in the presence and absence of DEAE-Dextran for 48 h (Appendix A1, Figure A1.4). Input of infected PBMCs for the cell-cell inhibition assay was chosen such that the resulting infection of TZM-bl cells was within the same range as the free virus infections (infectivity corresponding to 100 000 – 125 000 RLUs) and within the linear range of infection. To ensure cell-cell transmission was in the linear range of the assay, a titration of donor input cells was included in each experiment.

To ascertain that residual infectivity from free virus secreted by infected PBMCs was not interfering in the discrimination between free virus-cell and cell-cell infection in the cell-cell inhibition assay, we tested supernatants from PBMCs for infectivity of TZM-bl cells. The number of PBMCs corresponding to infectivity 100 000 – 125 000 RLUs (and calculated from the titration of infected PBMCs in the presence and absence of DEAE-Dextran, above) was added to HeLa cells (CD4/CCR5 negative) (10^4 cells per well) in culture medium to mimic the conditions of the infected PBMCs/TZM-bl infection system. Supernatant was harvested at 12 h, 24 h and 48 h and added to TZM-bl cells (10^4 cells per well) for 48 h (Appendix A1, Figure A1.5). Only viruses with residual infectivity of TZM-bl cells which resulted in < 10% above cell background at the determined input number of infected PBMCs were used in the cell-cell inhibition assay.

2.2.12 Cell-cell inhibition assay

Similar to Abela *et al.* (242), four days after the infection of PBMCs infection, previously collected plasma from CAPRISA 002 participants was serially diluted (3 x starting at 1:45). Infected PBMCs were washed three times with PBS to remove free virions and then the

appropriate number of infected PBMCs were incubated with plasma for 1 h before co-culturing with TZM-bl cells (10^4 per well) in the absence of DEAE-Dextran. 48 h post infection, cells were lysed and *luciferase* gene production was measured upon addition of Firefly Luciferase substrate (Promega). Experiments were repeated two to three times. Percentage inhibition was determined by calculating the mean inhibition at each dilution, based on data from two to three independent experiments and plotted on GraphPad Prism (v6.0).

2.3 Results

2.3.1 Defining the virus that established clinical infection

Seven participants from the CAPRISA 002 acute infection cohort, with a known target and timing of the first nAb responses to the HIV-1 Env, were selected (Table 2.1). In each case, the first nAb target was limited to one region on the Env, and varied from participant to participant (either V2, C3, C3V4, V4 or the CD4-binding site (CD4bs)), with the timing of the response ranging from 9 to 19 weeks post infection (wpi). To investigate the impact of nAbs on the early evolution of the HIV-1 Env in the region first targeted by nAbs, samples were deep sequenced using the Primer ID method (256), which allows for accurate sequencing and quantitation of viral populations. Samples from five participants were sequenced as part of this thesis, and sequences for two participants were provided by Dr Colin Anthony (UCT). An average of 8 time-points (5-10) per participant were sequenced. A consensus sequence was generated from ≥ 3 sequences with identical primer IDs by the majority rule, generating an average of 1493 consensus sequences (51-12842) per time-point.

Table 2.1. Target and timing of the initial autologous nAb responses in seven CAPRISA 002 participants.

Participant	Envelope Target	Timing (nAbs first detected/ wpi)	Reference
CAP45	C3V4	9	(164)
CAP63	V4	7	(164)
CAP88	C3	15	(164)
CAP177	C3	19	(164)
CAP210	V2	16	(164)
CAP239	CD4bs	13	Unpublished data (D Mielke)
CAP255	C3	15	(271)

To determine the multiplicity of infection, we used Poisson-Fitter on the sequences generated from the first time-point post infection (272). Sequences from six of the seven participants had a star phylogeny, suggesting single variant transmission, and one participant, CAP255, was infected with two variants at enrolment (8 wpi) (Appendix A1, Figure A1.1). Furthermore, for one of these participants with a single variant at enrolment (2 wpi), CAP177, a second variant was detected at 4 wpi (Appendix A1, Figure A1.2) (273).

Together the data suggests that in five cases, a single virus was responsible for clinical infection, and two variants for the remaining two (Appendix A1, Table A1.1).

2.3.2 Divergence observed prior to the detection of nAbs

To investigate the relationship between HIV-1 Env evolution and early nAb responses, we assessed divergence from the transmitted/founder (T/F) virus. Divergence was calculated as the average normalised Hamming distance (adjusted such that deletions were calculated as one event) from the T/F sequence. For participants with a single variant responsible for clinical infection, the T/F virus was defined as the consensus sequence from the first time-point sequenced. The two participants with multiple founders were excluded from this analysis as the presence of multiple founders and recombinants confounded the estimates of divergence.

To determine the role of nAbs on viral divergence, we measured the rate of divergence from the T/F sequence to sequences generated from the last nAb negative time-point (% normalised Hamming distance per month), and then from the last nAb negative time-point to the time-point of first detectable nAbs. In all five individuals, there was limited divergence prior to nAbs (mean: 0.012% per month) and a large increase concurrent with detection of nAbs (mean: 0.542% per month) (Table 2.1, Figure 2.1). In CAP45 C3C5, the rate of divergence prior to detectable nAbs was 0.027% per month, and increased 10-fold to 0.288% per month after nAbs. In CAP88 C2C3, the rate of divergence increased 89-fold from 0.021% per month to 1.867% per month, after nAbs were detected. In CAP63, the rate of divergence in the C3C5 increased 1.8-fold from 0.215% per month prior to detectable nAbs to 0.384% per month after nAbs were detected. In CAP210 C1C2, we observed a 4.4-fold increase in the rate of divergence from 0.040% per month prior to nAbs to 0.174% per month when nAbs were detected. Lastly, in CAP239 we investigated divergence from the consensus sequence in three regions (C1C2, C2C3 and C3C5) of the Env, as the first wave of nAbs targeted the CD4bs. No increase in the rate of divergence was detected in C1C2, but a 5.1-fold increase was detected in C2C3 (0.039%

per month to 0.198% per month) and an 11-fold increase in the rate of divergence in C3C5 (0.077% per month to 0.879% per month).

Table 2.2. Rate of divergence in the region targeted by the initial nAb response before and after the detection of nAbs.

Participant	Env Region	Last nAb negative time-point (wpi)	Rate of divergence prior to detectable nAbs (per month)	Time-point of first detectable nAbs (wpi)	Rate of divergence after detectable nAbs (per month)	Fold increase in rate of divergence
CAP45	C3C5	5	0.027	9	0.288	10
CAP63	C3C5	4	0.215	7	0.384	1.8
CAP88	C2C3	11	0.021	13	1.867	89
CAP210	C1C2	12	0.040	16	0.174	4.4
CAP239	C1C2	11	0.013	13	0.010	0.7
	C2C3		0.039		0.198	5.1
	C3C5		0.077		0.879	11

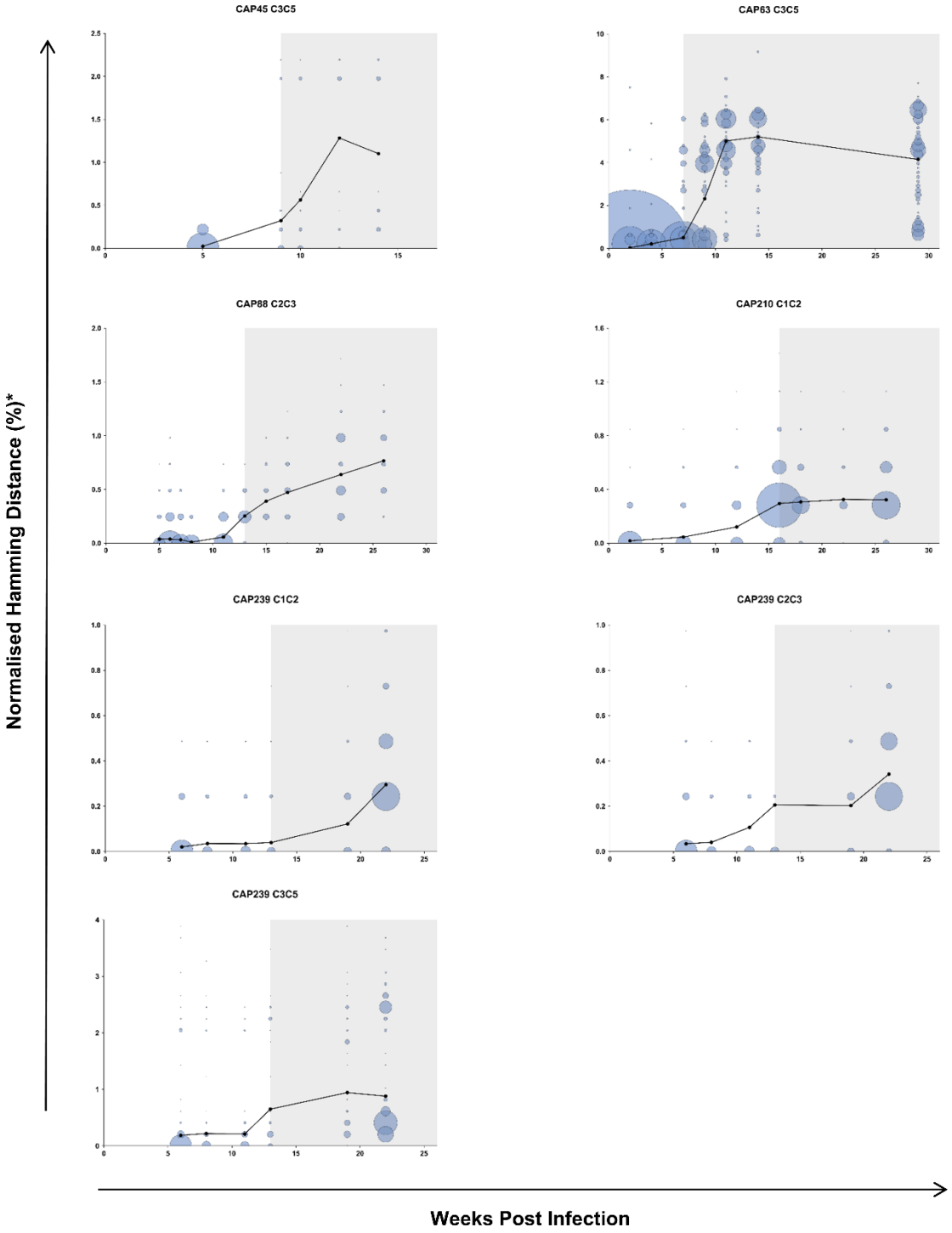

Figure 2.1. Divergence from T/F sequences in regions targeted by the initial autologous nAb responses in five individuals. Average hamming distances, normalised to the nucleotide length of each amplicon, were calculated for each time-point (black line). Bubble sizes indicate the size of the viral population, scaled by viral load, and bubble positions indicate viral populations with various degrees of divergence from the T/F sequence. The shaded region indicates the time from which the initial nAb response was first detected (IC_{50}). Hamming distances were adjusted so deletions were calculated as one event.

2.3.3 Positions exhibiting high Jensen-Shannon divergence are in the nAb epitope

In three individuals (CAP63, CAP210 and CAP239), there was evidence of divergence prior to detection of nAbs (Figure 2.1). To evaluate these changes at each amino acid position, we calculated the Jensen-Shannon divergence (D_{JS}) over time. D_{JS} was used instead of Shannon entropy as it allows the measurement of dissimilarity of probability distributions between time-points (267). Examination of these three participants revealed several sites with raised D_{JS} prior to and concurrent with the emergence of the nAb response (Figure 2.2).

We found changes occurring prior to the detection of nAb responses at 3, 4 and 2 weeks prior to detectable nAbs in CAP63, CAP210 and CAP239, respectively. In CAP63, increased D_{JS} was observed at one site in V4 (397) (Figure 2.2). The mutation (P397S), when introduced into the T/F sequence, conferred resistance to nAbs (Figure 2.3), confirming nAb escape. In CAP210, elevated D_{JS} was observed at two sites: one in the V2 of the Env (161) and the other at the start of the C2 (208) (Figure 2.2). One mutation (A161V) resulted in complete resistance to the nAb response, while the other mutation (V208I) resulted in partial resistance (Figure 2.3). In the third individual, CAP239, low D_{JS} was observed at one site (375) five weeks prior to nAb detection, due to a mutation (S375L) (Figure 2.2, white arrow). However, we could not assess escape as we were not able to produce functional pseudoviruses incorporating the mutation.

As expected, most amino acid changes observed were concurrent with or after the detection of nAbs (Figure 2.2). In CAP63, numerous variants with deletions across sites 395-410 were observed, explaining the D_{JS} observed in a wide number of contiguous sites in the region. In CAP210, there was very low D_{JS} observed at sites other than at positions 161 and 208. Further, D_{JS} was first observed in CAP239 at position 463 at the time of nAb detection, and then again at several sites across the gp120 six weeks later, including in the C1, C2 and C5 (positions 106, 278, 459 and 463.02) (Figure 2.2, blue arrows). Three of the mutations observed at these sites (K106E, L278S and K463E) were incorporated into the T/F virus and tested for neutralization sensitivity. All three mutants were resistant to the initial nAb response, with K463E and L278S becoming partially resistant to nAbs by 22 wpi, while K106E remained resistant until 29 wpi (Figure 2.3).

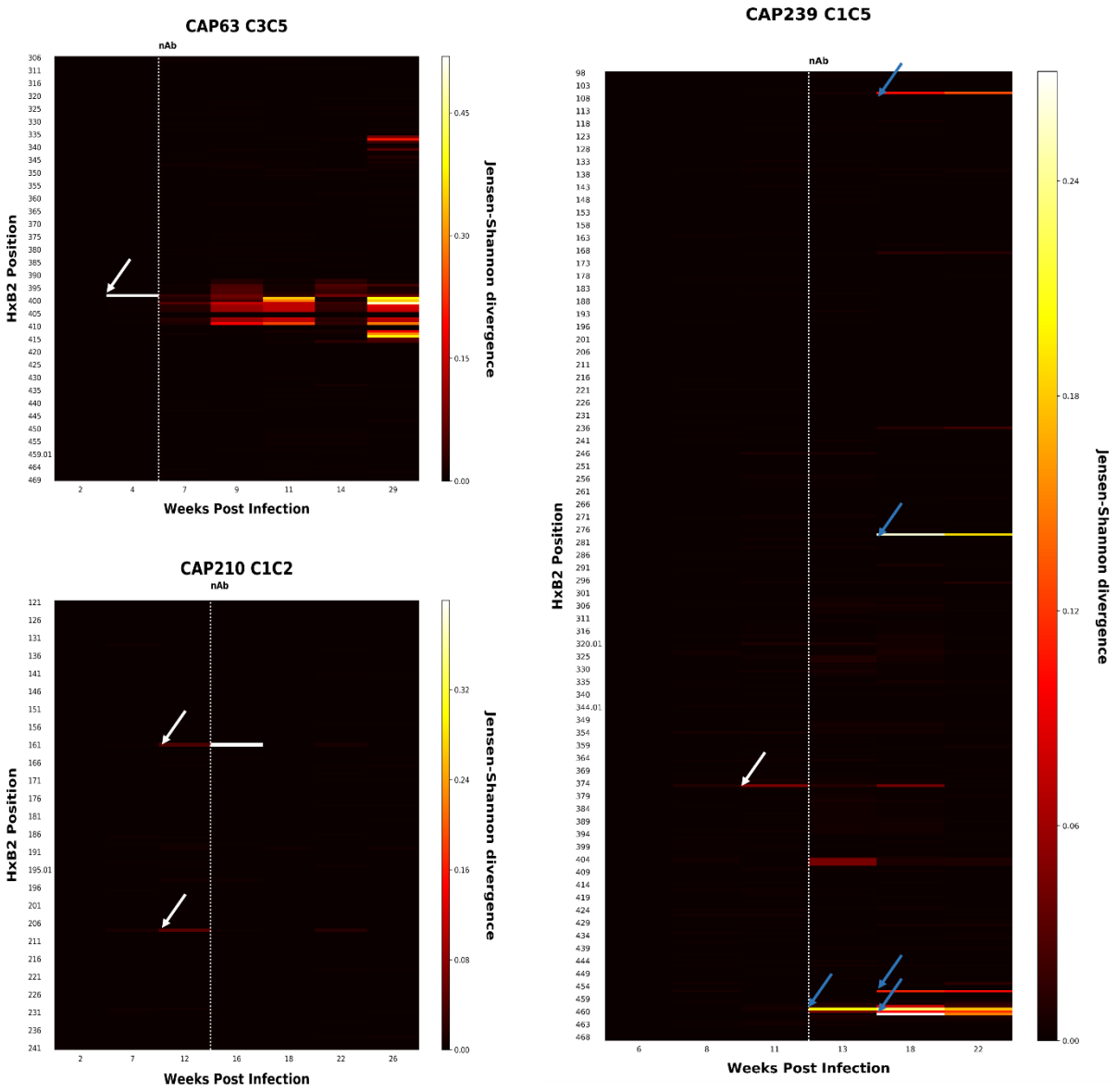

Figure 2.2. Jensen-Shannon Divergence plots of the region targeted by initial autologous nAb responses in three individuals: CAP63, CAP210 and CAP239. D_{JS} for each position at each time-point sequenced was calculated. White arrows indicate sites exhibiting high Djs prior to detectable nAbs: one site (position 397) in CAP63, two sites (161 and 208) in CAP210, and one site in CAP239 (375). Five sites (106, 278, 459, 463 and 463.02) in CAP239 were identified as a second wave of sites which diverged later (blue arrows). The white dotted line indicates the time from which the initial nAb response was first detected (IC_{50}).

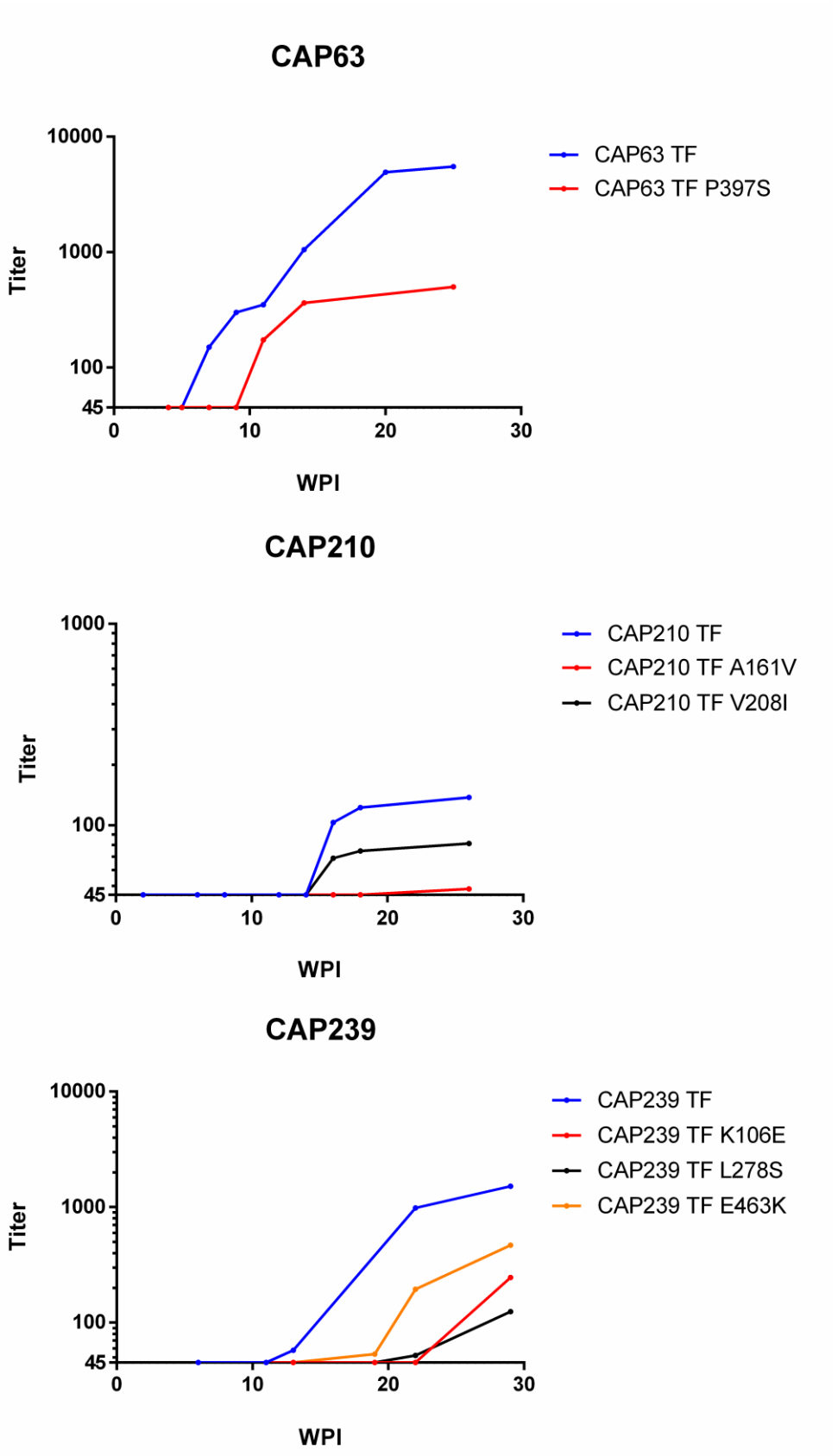

Figure 2.3. Autologous neutralization titer (ID_{50}) for T/F (blue) and escape mutants in three participants: CAP63, CAP210 and CAP239.

2.3.4 Stable presence of wildtype residues targeted by first nAbs

Having confirmed sites targeted by nAbs in early infection in three participants, we used deep sequencing to investigate the evolution of viral populations and how they adapted to nAb responses. In all three individuals, there was a significant decrease in the relative frequency of the WT residue, due to the emergence of nAb escape mutations.

In CAP63, WT frequency (P397) decreased from 99.9% at 2 wpi (prior to the detection of nAbs) to 27% at 4 wpi, and 12% at 7 wpi (the time at which nAbs became detectable), while the relative frequency of the mutant (P397S) rose proportionally (Figure 2.4A). However, there was an increase in viral load (VL) at the time nAbs were detected, which meant the change in the relative frequency of the WT residue did not translate to a decrease in the WT load (WT frequency x total VL). In fact, the WT load remained relatively stable, ranging from 75,545 copies/mL at 4 wpi (prior to detection of nAbs) to 79,101 copies/mL at 7 wpi, 86,990 copies/mL at 9 wpi and 99,695 WT copies/mL at 11 wpi (after nAbs are detected).

The relative decrease in WT virus was also observed in CAP210, where the WT (A161) frequency decreased from 99% at 7 wpi and 89% at 12 wpi (prior to the detection of nAbs) to 19% at 16 wpi (when nAbs become detectable) (Figure 2.4B). Similarly, the WT load remained relatively stable, or even increased, varying from 52,721 copies/mL at 7 wpi and 44,756 copies/mL at 12 wpi (prior to the detection of nAbs) to 94,940 copies/mL at 16 wpi (at the time nAbs become detectable).

Lastly, in CAP239 toggling at the first residue targeted by nAbs (E463) was detected, with E463 decreasing from 99% at 11 wpi (prior to the detection of nAbs) to 62% at 13 wpi (the time at which nAbs are detected), replaced by K463 (31%), G463 (3.8%) and D463 (1.7%) (Figure 2.4 C). In CAP239, due to an increase in overall VL, there was a 0.5 log increase in WT load following detection of nAbs (15,942 copies/mL at 11 wpi (before nAbs) to 34,891 copies/mL at 13 wpi). This pattern was even more evident in the second wave of escape mutants observed in CAP239, which arose 6 weeks after the detection of nAbs. In the C1, K106 decreased from 98% at 13 wpi (when nAbs are detected) to 78% at 19 wpi and 37% at 22 wpi, while E106 increased equivalently. At the same time, when considering the VL, the WT load dropped by 0.5 log (from 55,502 copies/mL at 13 wpi to 18,353 copies/mL at 19 wpi), but rose to 82,532 copies/mL at 22 wpi. This was further observed to be the case at position 278 in the C2. L278 dropped from 100% at 13 wpi to 57% at 19 wpi and 10% at 22 wpi, suggesting strong negative selection. However, the WT load decreased from 56,400 to 13,394 copies/mL between 13 and 19 wpi, and then remained relatively stable at 22,705 copies/mL at 22 wpi.

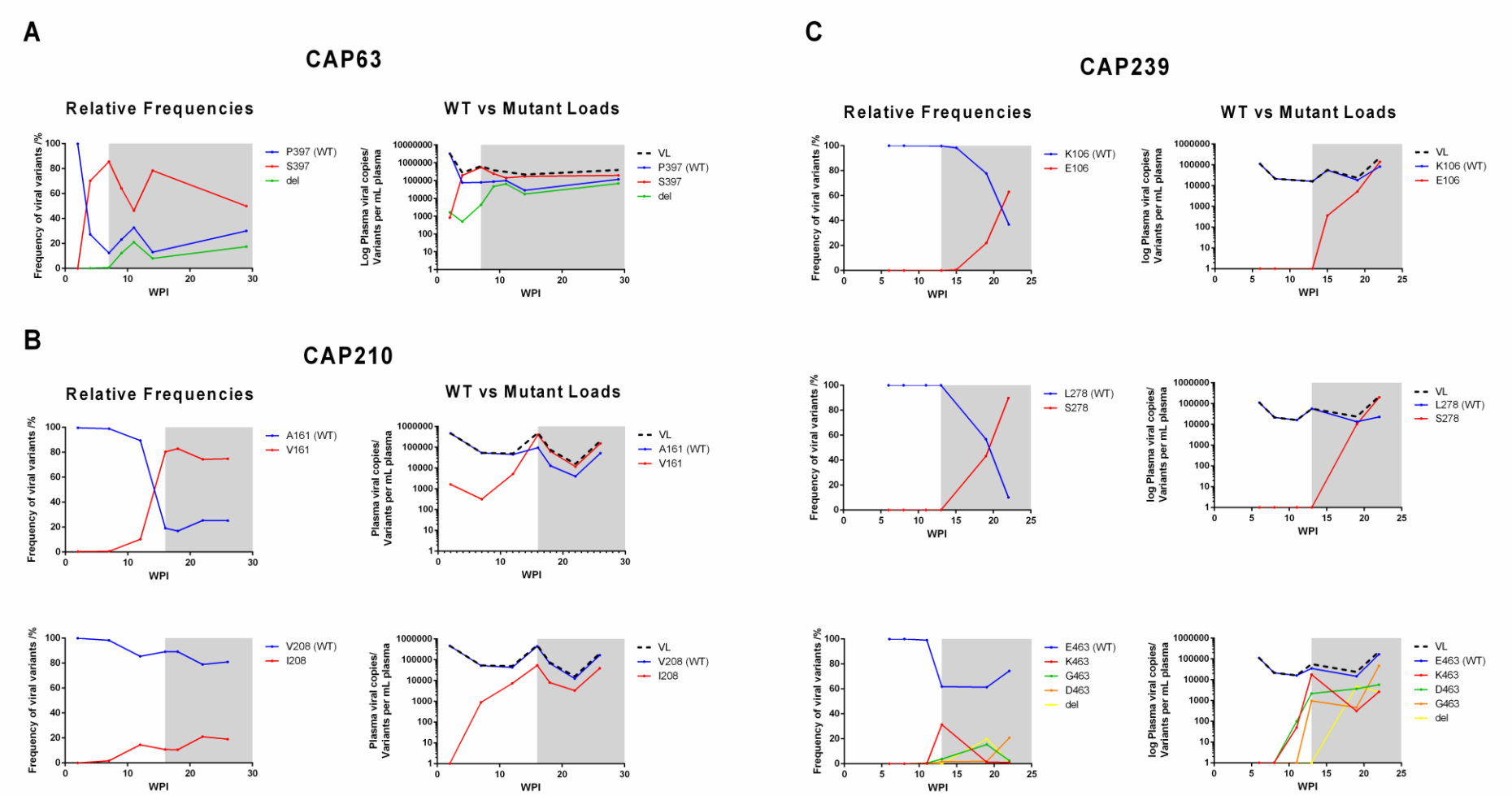

Figure 2.4. Relative frequencies and loads of wildtype and mutant residues. The relative frequencies are shown as a percentage of consensus sequences generated; and WT and mutant loads calculated as the WT or mutant relative frequency x total VL (number of viral copies/variants per mL of blood). The WT is represented by a blue line and mutant residues by red, green, orange, yellow lines. Confirmed escape mutations evaluated: P397S in V4 of the Env in CAP63 **(A)**, A161V (in V2) and V208I (in C2) of the Env in CAP210 **(B)** and K106E (in C1), L278S (in C2) and K463E/G/D/- (in C5) of the Env in CAP239 **(C)**. The shaded region indicates the time from which the initial nAb response is first detected (IC_{50}).

2.3.5 Mutant loads increased due to an increase in total viral load

An analysis of viral population dynamics at the regions first targeted by the nAb response showed that the WT load did not decrease following nAb responses. Instead, we saw a substantial increase in the mutant load (mutant frequency x total VL), due to an increase in VL in each participant at the time of nAb detection. In CAP63, the VL increased from 277,000 copies/mL to 640,000 copies/mL; and in CAP210, an increase in VL from 50,100 copies/mL to 496,000 copies/mL was observed. In CAP239, two increases were observed: an increase from 16,100 copies/mL to 56,400 copies/mL at the detection of nAbs, and an increase from 23,600 copies/mL to 224,000 copies/mL concomitant with detection of the second wave of nAb escape (Figure 2.4). In all participants, the emergence of nAbs was after acute infection, where the VL was on the decline.

This is suggestive of strong positive selection driving an increase in escape variant copies, as opposed to negative selection acting against the WT residue. To confirm this, we quantified the magnitude of selection pressure on these sites, using FUBAR (265). A value of β-α=0 was used to represent neutrality (where β denotes the rate of non-synonymous mutations and α signifies the rate of synonymous mutations) and β-α>1 as a working definition of strong positive selection pressure (as previously described by Murrell *et al.* (265)).

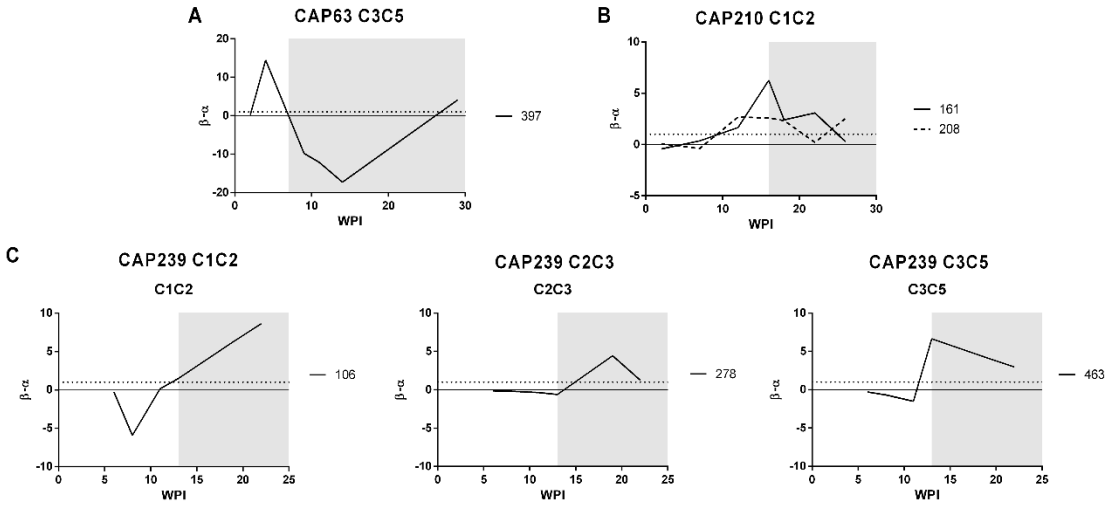

Figure 2.5. Magnitude of selection at sites in the Env regions targeted by nAbs in three participants. The magnitude of selection was calculated, using FUBAR (265), at each time-point sequenced for each site identified: 397 in the V4 of CAP63 **(A)**, 161 and 208 in the C1C2 of CAP210 **(B)** and 106, 278 and 463 in the C1C2, C2C3 and C3C5 of CAP239, respectively **(C)**. β denotes the rate of non-synonymous mutations while α signifies the rate of synonymous mutations. β-α>1 was used as a working definition of strong positive selection (dotted line). The shaded region indicates the time from which the initial nAb response is first detected (IC_{50}).

We observed strong positive selection pressure in CAP63 at position 397 at 4 wpi (β-α = 14.49), concomitant with the increased rate of divergence from the T/F sequence, increased D_{JS} at position 397 and the P397S shift (Figure 2.5 A). However, this positive selection shifted to strong negative selection soon after nAbs became detectable (β-α = -9.79 at 9 wpi, -12.15 at 11 wpi and -17.29 at 14 wpi), presumably as the nAb response developed and the virus toggled to obtain the best pathway of escape from the nAb response.

In CAP210, we also observed strong positive selection prior to the detection of nAbs at sites 161 and 208, concurrent with the increased rate of divergence from the T/F sequence and detection of increased D_{JS} (Figure 2.5 B). While selection pressure remained stable at 208, there was a considerable increase in the magnitude of positive selection at position 161 (β-α = 1.66 at 12 wpi, versus 6.27 at 16 wpi) concomitant with detection of nAbs at 16 wpi.

Finally, strong positive selection was observed in CAP239 concomitant with development of nAbs. At position 463, the first site of nAb escape in CAP239, selection pressure was close to neutral prior to detection of nAbs (β-α = -0.67 at 8 wpi, -1.51 at 11 wpi), but at 13 wpi (the time at which nAbs were detected) an elevated magnitude of positive selection was detected (β-α = 6.64) (Figure 2.5 C). The two sites which shifted later (K106E and L278S) exhibited similar results. The magnitude of positive selection increased notably between 13 wpi (β-α = 1.49 at position 106, -0.61 at position 278) and 19 wpi (β-α = 6.30 at position 106, 4.44 at position 278).

2.3.6 Neutralization sensitive viruses persist by evading plasma antibodies through cell-cell transmission

One mechanism for persistence of the WT residue is cell-cell transmission of the virus, allowing evasion from nAbs and providing a continual source of WT viruses. Accordingly, we investigated the ability of plasma antibodies to inhibit free virus-cell and cell-cell transmission. For the cell-cell inhibition assay, viruses had to be DEAE-dextran dependent, infect PBMCs to a sufficient level, and have minimal background from viruses secreted by PBMCs during the assay. Of the seven Env-IMCs encoding acute/early *envs* we had available, viruses produced from four (CAP210 TF, CAP239 TF, CAP255 2.00, CAP257 2.00) met these criteria (Appendix A1, figures A1.3-A1.5). We tested the ability of autologous plasma from these four participants from two different time-points (6 months post infection (mpi) and 2 years post infection (ypi)) to inhibit free virus-cell and cell-cell transmission.

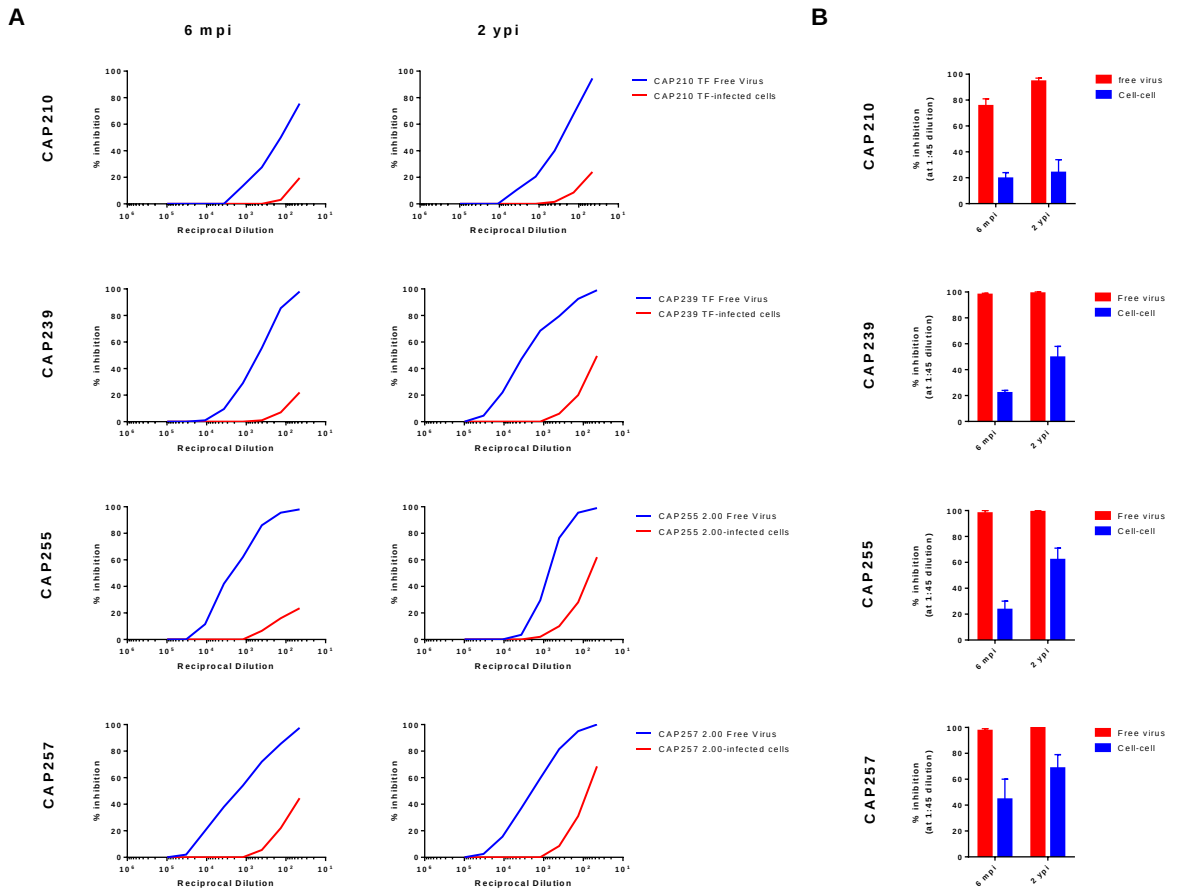

Figure 2.6. Autologous plasma inhibition of free virus-cell (red) and cell-cell transmission (blue) of acute/early viruses. Inhibition curves of free virus-cell or cell-cell transmission (CAP210 TF, CAP239 TF, CAP255 2.00, CAP257 2.00; each row representing a different virus) using autologous plasma (three-fold serial dilution starting at 1:45) from 6 mpi (left column) or 2 ypi (right column) **(A)**. The % inhibition of free virus-cell and cell-cell transmission by plasma from 6 mpi (left bars) and 2 ypi (right bars) at 1:45 dilution with standard error **(B)**.

Autologous plasma inhibition was compared by determining the % inhibition of free virus-cell transmission to cell-cell transmission at 1:45 dilution (Figure 2.6). At 6 mpi, antibodies could inhibit 100% of free virus-cell transmission in three participants (CAP239, CAP255, CAP257), and 75% of free virus-cell transmission in one participant (CAP210) (Figure 2.6 A, B). Inhibition of cell-cell transmission was substantially lower in all four participants, with maximum autologous cell-cell inhibition ranging from 21% (CAP210, CAP239, 255) to 45% (CAP257) (Figure 2.6 A, B).

We then used plasma from chronic infection (2 ypi) to establish if a more developed antibody response could better inhibit cell-cell transmission. Antibodies from plasma at this time-point

could efficiently inhibit free virus-cell transmission at 1:45 dilution (100% of free virus-cell transmission was inhibited in CAP235, CAP255, CAP257), and similar to the six month timepoint, the CAP210 virus was more resistant to neutralization, with 95% inhibited at 1:45 dilution (Figure 2.6 A, B). Chronic plasma had improved efficiency of inhibition of cell-cell transmission. However complete inhibition was not achieved, even at the lowest dilution (1:45) (inhibition of the autologous virus ranged from 24% by CAP210 plasma to 68% by CAP257) (Figure 2.6 A, B).

2.3.7 Escape mutations increase resistance of early viruses to inhibition by plasma antibodies

Having established a reduced inhibition of cell-cell transmission of the WT virus by autologous plasma antibodies, we wished to determine the effect of escape mutations on plasma inhibition of cell-cell transmission. We incorporated mutations, identified by deep sequencing, into the respective Env-IMC for two participants (A161V and V208I in CAP210; L278S in CAP239), and tested the ability of autologous plasma to inhibit free virus-cell and cell-cell transmission of the mutant viruses at a dilution of 1:45.

In CAP210, both mutations resulted in a decrease in free virus-cell transmission at 6 mpi (75% inhibition of the WT virus, in comparison with 40% inhibition of A161V and 59% inhibition of V208I) and cell-cell transmission (20% inhibition of the WT virus versus 11% inhibition of A161V and 0% inhibition of V208I) by plasma antibodies at 1:45 dilution (Figure 2.7). By 2 ypi, while there was still a decreased inhibition of the mutant viruses, plasma antibodies had developed to inhibit free virus-cell transmission to almost comparable levels (95% inhibition of the WT virus contrasted with 88% inhibition of A161V and 79% inhibition of V208I). However, inhibition of cell-cell transmission was still greatly reduced (24% inhibition of the WT virus versus 14% inhibition of A161V and 2% inhibition of V208I).

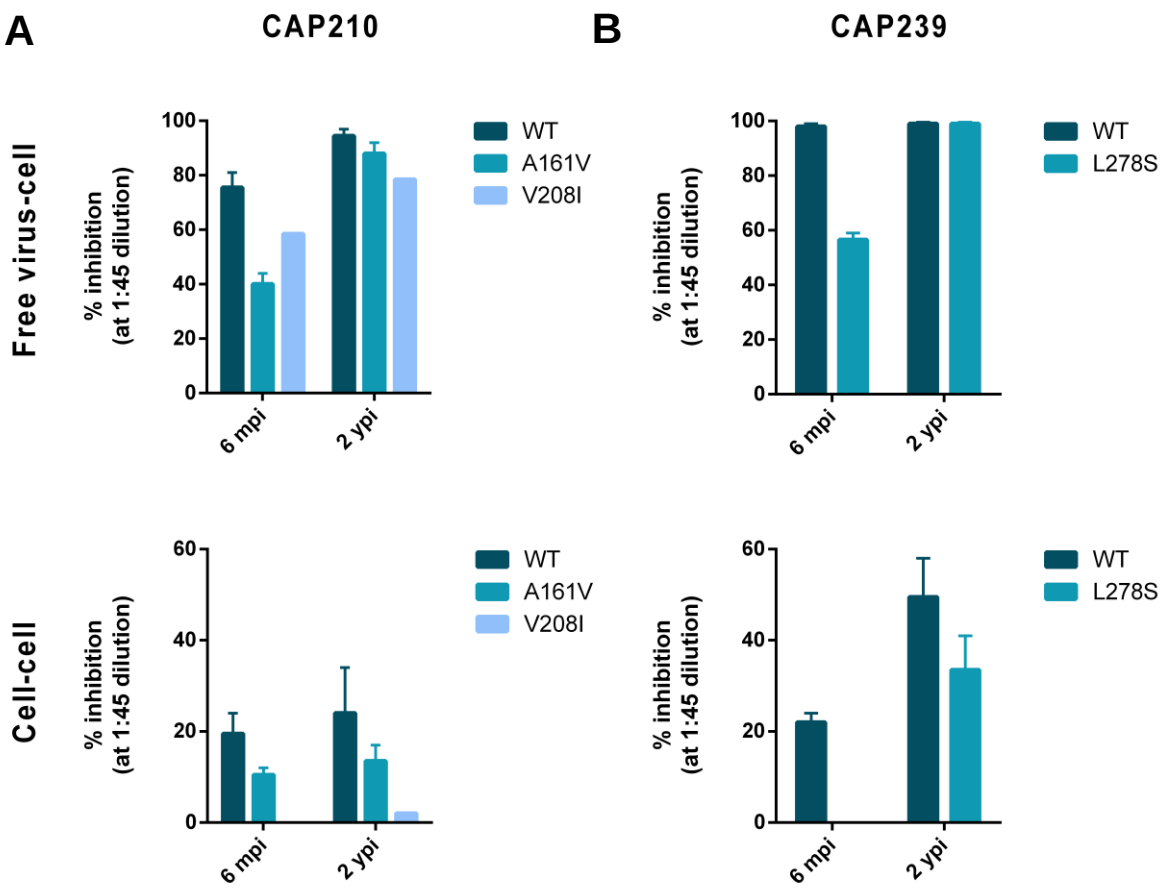

Figure 2.7. Inhibition by autologous plasma of free virus-cell and cell-cell transmission of WT and mutant viruses from CAP210 (A) and CAP239 (B). Autologous plasma was assayed against the T/F and mutant viruses for CAP210 (WT, A161V, V208I) and CAP239 (WT, L278S). Viruses were assayed against plasma from 6 mpi or 2 ypi

A similar pattern was observed in CAP239. At 6 mpi, plasma antibodies could inhibit 100% free virus-cell transmission and 22% cell-cell transmission of the WT virus, while only inhibiting 57% of free virus-cell transmission and 0% of cell-cell transmission of the L278S mutant virus (Figure 2.7). Plasma from 2 ypi could inhibit 100% free virus-cell transmission of both the WT and L278S mutant viruses at 1:45 dilution, while cell-cell transmission was reduced (50% of WT viruses were inhibited versus 34% of L278S mutant viruses).

2.4 Discussion

Using a deep sequencing approach to estimate the kinetics of total viral populations over a six-month period, we showed the WT virus persisted at a relatively stable copy number despite nAb

responses. While previous studies have reported the persistence of WT virus in the face of nAb responses (223, 241), the relative stability of this population may not have been observed using conventional Sanger sequencing (Moore *et al.*) or 454 pyrosequencing (Bar *et al.*) due to the low relative frequency of the WT virus, which could be a result of outgrowth of the escape virus associated with a concomitant increase in VL. These early nAbs, while highly effective against free viruses, were only partially effective at blocking cell-cell transmission, providing a potential mechanism whereby the WT virus may persist. These results highlight the possible limitations of antibody neutralization in a protective HIV-1 vaccine, and indicate the likely importance of antibody effector functions such as ADCC, which can target infected cells and potentially prevent cell-cell transmission.

Several studies have suggested that persistent minority variants play a role in engaging and promoting certain lineages of nAbs. Bhiman *et al.* showed that low frequency variants in the V2 effectively engaged bnAb precursors, suggesting these variants were important in promoting the CAP256-VRC26 bnAb lineage (274). In contrast, Wibmer *et al.* found a rare persistent glycan-free V5 virus lineage (< 5%) which was likely responsible for initiating a nAb with narrow breadth (257). Our study found that while the relative frequency of these viruses may have been low, the total VL remained high, thus providing a high dose, persistent exposure of the host immune system to the WT virus, which may in turn potentially enhance maturation of the immune response.

There were limited changes detected prior to the development of nAbs in the regions we sequenced. We observed no evidence of immune escape prior to the detection of nAbs in two individuals and low level of nAb escape two to four weeks prior to the detection of nAbs in the remaining three participants, consistent with a previous study by Bar *et al.*, which found evidence of very low levels of escape variants (0.2-1.1%) prior to detectable nAbs in two individuals of the CHAVI acute infection cohort (241). Their results suggest that there is very limited to no selection pressure prior to the development of nAbs in the region first targeted by these antibodies.

In comparison, development of nAbs resulted in rapid viral divergence in all five participants, with evidence of residue toggling at the sites of escape. Despite this, the WT population size remained constant when considering changes in VL in three participants; while the escape variant population size increased considerably. While it is difficult to distinguish negative (purifying) and positive (adaptive) selection pressures in a competition process, where negative selection of phenotypic

subsets may have the same outcome as positive selection of remaining subsets (275) (as is the case with residue toggling), the changes in VL allowed us to measure changes in population sizes and, thus, selection pressure. Here, the constant WT population size up to six months post infection (and between 10 and 20 weeks post the detection of nAbs) suggests there was little/no negative (purifying) selection pressure against the WT residue. This contrasts with studies by Bar *et al.* and Moore *et al*., which both observed significant decreases in the number of WT copies (a two-log decrease in the study by Bar *et al.* using 454 pyrosequencing; while a one log decrease was observed in the study by Moore *et al.* using single genome sequencing) by six months post infection (164, 241).

The WT viruses may persist following nAb responses through several mechanisms. Firstly, the high VL in early infection may result in saturation of the nAb response, where the limited nAbs produced in the early stages of infection may simply have been insufficient to neutralize all viral particles at the given VLs. Several non-human primate (NHP) passive immunization studies have shown that high levels of nAbs are required for sterile protection from high dose challenges (±25 mg/kg) (276–278). If the persistence of nAb sensitive viruses is attributable to saturation of nAbs by high VLs, the implications for vaccine development are more favourable, as exposure events in natural human transmission involve substantially lower VLs than those used in a high dose NHP model ($5 \times 10^5 – 2 \times 10^7$ copies per ejaculate (279, 280), in comparison to ~ 10^8 viral copies in a typical high-dose challenge experiment, as reported in (202)) or established acute HIV-1 infection. This is supported by Hessell *et al*., who showed that b12, a bnAb targeting the CD4bs of gp120, afforded protection to macaques at relatively low concentrations (1 mg/kg) against a low dose SHIV challenge (~30x lower than a typical high dose challenge) (202).

However, another explanation for the persistence of the WT is cell-cell transmission. Here, we found that cell-cell transmission of T/F viruses from four CAPRISA 002 participants was highly resistant to autologous sera (244). Given the reduced inhibition by autologous plasma antibodies, it is possible that cell-cell transmission allowed WT viruses in these participants to escape nAb pressure, which may have allowed nAb sensitive virions to persist despite their sensitivity. In addition, the reduced inhibition of free virus-cell and cell-cell transmission of mutant viruses, compared with WT viruses, may explain the considerable increase in the mutant population observed after the detection of nAbs. If the persistence of nAb sensitive viruses is due to cell-cell transmission, then these results highlight the importance of antibody effector functions such as

ADCC, which can target infected cells. This is supported by two recent non-human primate passive immunization studies by Hessell *et al.* and Liu *et al*., which showed bnAb-mediated protection was partially facilitated by clearing HIV-1 infection in distal tissues (281, 282).

Determining HIV-1 population dynamics provides important information to understand viral variants that may elicit bnAb responses. The limited impact of early nAbs on the overall WT viral population size suggests HIV-1 can escape nAbs via mechanisms distinct from mutations and insertion/deletions. Here, we demonstrate one mechanism (cell-cell transmission) by which WT viruses escape nAbs indirectly, notably allowing nAb sensitive viral variants to persist in the presence of autologous nAbs. Consequently, this study highlights the importance of a vaccine which elicits nAbs that mediate Fc-effector functions against infected cells to reduce cell-cell transmission.

Chapter 3. ADCC responses can drive HIV-1 Envelope evolution

ABSTRACT

Numerous studies, including the RV144 trial, suggest ADCC responses may play a role in a protective vaccine. However, there is limited evidence of viral evolution driven by ADCC pressure, which would provide strong support for their importance as an immune response. This study investigated the relationship between epitopes targeted by nAb and ADCC responses, and looked for evidence of ADCC immune escape.

To identify sites under immune pressure, longitudinal gp160 sequences, and partial gp160 deep sequence data covering the region of the nAb epitope, were generated and select mutations were introduced into the respective acute/early *env*. Infectious molecular clones encoding these *env* (Env-IMC) were subsequently used in Luciferase-based ADCC and TZM-bl nAb assays to determine the effect of each mutation on both responses.

In the CAP45 acute Env-IMC, a D462G mutation (in V5) conferred complete escape from both neutralizing and ADCC antibodies. In CAP210, two mutations (A161V in V2; V208I in C2) were evaluated. A161V had no effect on ADCC activity, but conferred complete resistance to nAbs, while V208I conferred complete resistance to the ADCC response, but only partially escaped nAbs. Lastly, in CAP239, three mutations (K97E in C1; L278S in C2; S481N in C5) were evaluated. K97E and S481N conferred complete resistance to ADCC responses, but had no effect on neutralization; while L278S conferred complete resistance to nAbs but had no effect on ADCC responses. Analysis of CAP239 gp160 sequences revealed three distinct escape pathways. Env-IMCs (n=8) from each of the pathways displayed differential resistance to nAb and ADCC responses. All Env-IMCs which incorporated S481N were resistant to ADCC, while several escape mutations were associated with nAb escape.

This study provided definitive evidence of ADCC driven immune escape and viral evolution in early infection for the first time, supporting previous studies which suggest these responses play a role in controlling infection, and highlighting their importance as a vaccine target.

3.1 Introduction

In the RV144 trial, the only vaccine to offer any protection thus far, protection against HIV-1 infection was associated with V2-directed non-neutralizing antibodies (nnAbs) with Fc-mediated effector function (31%) (8). This has raised important questions about the role of antibody effector functions, other than neutralization, in protection from HIV-1. Indeed, a number of studies have suggested that ADCC responses may be protective against, or control, HIV-1 infection (8, 201, 212, 283, 284). However, there is limited information on how these responses impact the evolution of viral populations *in vivo*, which would be an important indicator of the pressure these responses are able to exert on the virus.

Escape from nAbs in the HIV-1 Envelope (Env) has been well characterized and is observed throughout infection (159, 164). Consequently, any putative pressure exerted by effector functions after neutralization is detectable is difficult to deconvolute from neutralization-induced escape. As a result, only two studies to date have provided evidence of viral escape from ADCC responses. Chung *et al*. demonstrated escape from ADCC responses in chronic HIV-1 infection (233). This study identified mutations in the Env C1 region which escaped ADCC responses. However, this study used linear peptides, which likely missed ADCC responses targeting conformational epitope. In addition, evidence of a sieve effect which may have been due to ADCC-mediating nnAbs was detected in the RV144 trial (285). Here, vaccine efficacy against viruses matched to the vaccine protein at position 169 (K169) increased to 48%, whereas efficacy against viruses mismatched at position 181 (I181X) was 78%, suggesting V2-targeting nnAbs exerted selection pressure.

One complication in measuring ADCC is the choice of antigen/target used to measure ADCC responses. Many assays use peptides, which are non-conformational and are, therefore, likely miss the majority of ADCC responses. In comparison, the use of proteins to coat target cells is quite different: it is thought using these gp120/140 proteins represent the virus binding to the CD4 molecule on the cell membrane and, thus, exposing CD4-inducible (CD4i) epitopes only exposed during viral entry (286). The use of virus-infected cells, although technically more difficult, is thought to more accurately represent epitopes present during both viral entry and budding from infected cells (240).

Here, we used single genome sequencing, and deep sequencing over the region first targeted by nAbs, to map sites under selection in the HIV-1 *env*, from enrolment to after the detection of nAbs

in three participants of the CAPRISA 002 cohort. In two of the three individuals, putative antibody-mediated immune pressure was detectable prior to the detection of nAbs. We incorporated these mutations, or mutations which developed concurrent with the detection of nAbs, into Env-IMCs with the cognate early/acute *env*, to investigate the effect these mutations on autologous ADCC and neutralization responses. In one individual, CAP239, which targeted the CD4bs in early infection, we found evidence of ADCC-driven immune escape and *env* evolution. These data provide support for the importance of ADCC responses in early HIV-1 infection, and further motivates for their use as targets for an effective HIV-1 vaccine.

3.2 Methods

3.2.1 Ethics statement

Ethics approval was obtained as previously detailed in Chapter 2.2.1.

3.2.2 CAPRISA 002 acute infection cohort participants

Longitudinal plasma samples were obtained from the CAPRISA 002 acute infection cohort as previously detailed in Chapter 2.2.2.

3.2.3 Cell lines

TZM-bl cells and HEK293T cells were obtained and cultured as previously detailed in Chapter 2.2.3. CEM.NKR$_{CCR5}$ cells kindly were obtained through the NIH AIDS Reagent Program, Division of AIDS, NIAID (catalogue number 4376; contributed by Dr. Alexandra Trkola).

3.2.4 Peripheral blood mononuclear cells

For the ADCC assays, appropriate PMBCs were found and used as a source of effector cells (Appendix A3). PBMCs were obtained from healthy HIV-1 seronegative donors and isolated by Ficoll gradient from buffy coats. Immediately after isolation, PBMCs were counted, resuspended in 10% DMSO (Sigma), 20% FCS (Biochrom), 70% RPMI (Lonza) and cooled overnight to -80 ºC at a rate of -1 ºC/h. The next day, PBMCs were moved to liquid nitrogen storage.

3.2.5 RT-PCR amplification and sequencing

HIV-1 RNA was purified from plasma using the Qiagen Viral RNA kit (Qiagen), and reverse transcribed to cDNA using Superscript III Reverse Transcriptase (Invitrogen). Single genome amplification (SGA) or end-point dilution was carried out on plasma. Amplicons were directly sequenced using the ABI PRISM Big Dye Terminator Cycle Sequencing Ready Reaction kit (Applied Biosystems) and resolved on an ABI 3100 automated genetic analyzer. The full-length *env* sequences were assembled and edited using Sequencher v.4.0 software (Genecodes). Multiple sequence alignments were performed using Clustal X (ver. 1.83) and edited by eye with BioEdit (ver. 5.0.9).

3.2.6 Deep sequencing library preparation and data processing

Deep sequencing library preparation and data processing was carried out as previously detailed in Chapter 2.2.4.

3.2.7 Cloning gp160 and mutagenesis

Cloning and mutagenesis were performed as previously described in Chapter 2.2.6.

3.2.8 Construction of HIV-1 infectious molecular clones and virus preparation

CAP210 TF, CAP239 TF, CAP255 2.00.5, CAP257 2.00.Luc, CAP210 TF A161V, CAP210 TF V208I and CAP239 TF L278S were described in Chapter 2.2.7. In addition, Env-IMC of acute/early viruses for CAP8, CAP61, CAP228 and CAP256 were constructed in the Ochsenbauer laboratory as previously described (270). Env-IMCs of the remaining CAP239 mutant viruses (K97E and S481N), as well as CAP239 Env-IMCs representing CAP239 *envs* from 13 wpi (13-5G3, 13-9C6 and 13-9B2) and 19 wpi (19-7E4, 19-7F4, 19-7F2, 19-7B2 and 19-7C2) were constructed at UCT (D Mielke).

Virus preparation was carried out as previously described in Chapter 2.2.7.

3.2.9 Infection of CEM.NKR$_{CCR5}$ cell line with HIV-1 Env-IMC

CEM.NKR$_{CCR5}$ cells (1 x 10^6) were infected with 1 mL of virus inoculum by spinoculation at 1000 x g for 2 h at 32 ºC in the presence of DEAE-Dextran (7.5 μg/mL). The cells were subsequently resuspended at 0.3 x 10^6/mL and cultured for 72 h in R10 containing 7.5 μg/mL DEAE-Dextran. Following 72 h of infection, infected cells (1 x 10^5) were washed in PBS, dispensed in 96-well V-bottom plates, and stained with a vital dye (LIVE/DEAD Fixable Aqua Dead Cell Stain,

Invitrogen) to exclude non-viable cells from subsequent analyses. The cells were then washed twice with 250 µL per well of washing buffer (WB; PBS + 1% FCS) and incubated with Cytofix/Cytoperm (BD Bioscience) for 20 min at 4 ºC. The cells were then washed twice with 200 µL of 1% Cytoperm washing buffer (BD Biosciences). After the final wash, the anti-p24 antibody (clone KC57-RD1; Beckman Coulter) was added to the cells at a final dilution of 1:400 and the plates were incubated for 30 min at 4 ºC. The plates were washed twice with WB, and the cells were resuspended in 200 µL 1% formaldehyde-PBS. The samples were acquired within 24 h using the LSR II flow cytometer (BD Biosciences). A minimum of 10,000 total singlet events was acquired for each analysis. Gates were set to include singlet and live events. The appropriate compensation beads were used to compensate the spill over signal for the two fluorophores. Data analysis was performed using FlowJo 10.2 software (TreeStar). Uninfected CEM.NKR$_{CCR5}$ and the chronically infected A1953 cell lines were used to titer the vital dye and the anti-p24 antibody, and were used as negative and positive controls, respectively, for the described staining procedure. Downstream assays performed using the IMC-infected target cells were considered reliable if the percentage of viable p24+ target cells on assay day was ≥10%.

3.2.10 Neutralization assay

Neutralization assays were performed as previously described in Chapter 2.2.6.

3.2.11 Luciferase-based ADCC assay

The Luciferase-based ADCC assay was conducted as stated in the Duke University CFAR protocol CFAR01-A0005 and described by Pollara *et al*. (240). The day prior to the ADCC assay, PBMCs to be used in the assay were thawed in R10, counted and assessed for viability. PBMCs were resuspended in R10 supplemented with IL-15 (10 ng/mL) (Sigma) overnight.

On the day of the assay, infected CEM.NKR$_{CCR5}$ cells were counted, assessed for viability (viability had to be ≥ 45% to be used in the assay) and the concentration was adjusted to 2 x 10^5 viable cells/mL (5 x 10^3 cells/well). Stimulated PBMCs were then counted, assessed for viability, pelleted and resuspended in the infected CEM.NKR$_{CCR5}$ cells at a concentration of 6 x 10^6 PBMCs/mL (1.5 x 10^5 PBMCs/well) (effector: target cell ratio of 30:1). Plasma, mAbs or controls were serially diluted 1:5 starting at 1:50 dilution. The effector/target cell mix and antibody dilutions were plated in white opaque 96-well half-area plates (Costar), centrifuged at 300 x g for 1 min after 30 min, and then incubated for 5.5 h at 37 ºC, 5.5% CO_2. After 5.5 h, ViviRen substrate

(Promega) was diluted 1:500 in R10 and added 1:1 to the assay wells. The final readout was the luminescence intensity generated by the presence of residual intact target cells that have not been lysed by the effector population in the presence of ADCC-mediating antibodies. The percentage of specific killing was calculated using the formula

$$\% \text{ specific killing} = \frac{\text{RLU of target + effector well - RLU of test well}}{\text{RLU of target + effector well}} \text{ x } 100$$

In the analysis, the RLU of the target + effector wells represent spontaneous lysis in the absence of any source of antibody. The RSV-specific mAb, Palivizumab (MedImmune) was used as a negative control and IgG from individuals chronically infected with HIV-1 (HIVIG) (obtained through the NIH AIDS Reagent Program, Division of AIDS, NIAID, NIH: Catalogue #3957, from NABI and NHLBI) was used as a positive control. All anti-HIV-1 mAbs used in the ADCC assays had identical Fc regions with decreased fucosylation for optimized recognition of $Fc_{\gamma}RIIIa$, resulting in improved NK cell binding and ADCC (287, 288), and were kindly provided by Dr Guido Ferrari (Duke University). All experiments were repeated two to three times. The titer was calculated as the lowest mean concentration/dilution which resulted in ADCC above background activity.

3.2.12 Structural modelling and glycosylation changes

Crystal structures of the HIV-1 Env trimer and gp41 (PDB IDs: 4NCO, 4TVP, and 2B4C) were used as templates to create models from the CAP239 gp160 sequences, which was carried out using Modeller (289) and the UCSF Chimera package (176). Modelling was done in 10 replicates, and the best scoring model was chosen for further analysis. Basic mannose glycans were added at selected potential N-linked glycosylation sites using GlyProt (290).

3.3 Results

3.3.1 ADCC responses are detectable before nAbs

We previously showed that heterologous ADCC responses to gp120-coated cells were detectable in plasma prior to autologous nAb responses (Bandawe, Mielke *et al.* publication in preparation). In this study, we used early/acute Env-IMCs from nine participants of the CAPRISA 002 acute infection cohort (Appendix A2). In all nine participants, ADCC responses were detectable at the

time of enrolment (between 3 and 8 wpi), while nAbs became detectable later (between 9 and 22 wpi) (Figure 3.1 and 3.2).

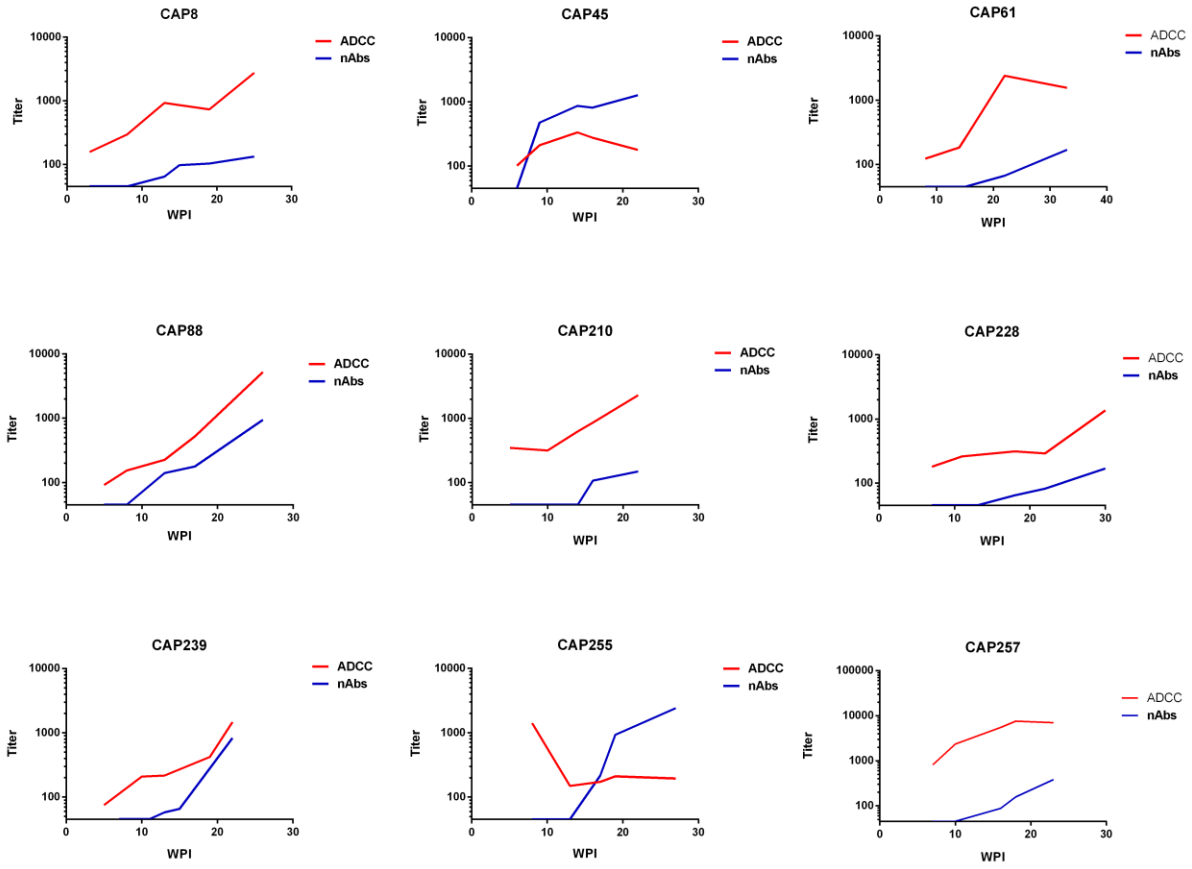

Figure 3.1 Kinetics of autologous ADCC and neutralizing antibody development. Early/Acute Env-IMCs from nine participants were used to determine kinetics of development of plasma ADCC (red lines) and nAb (blue lines) responses over the first six months of infection in nine individuals of the CAPRISA 002 acute infection cohort.

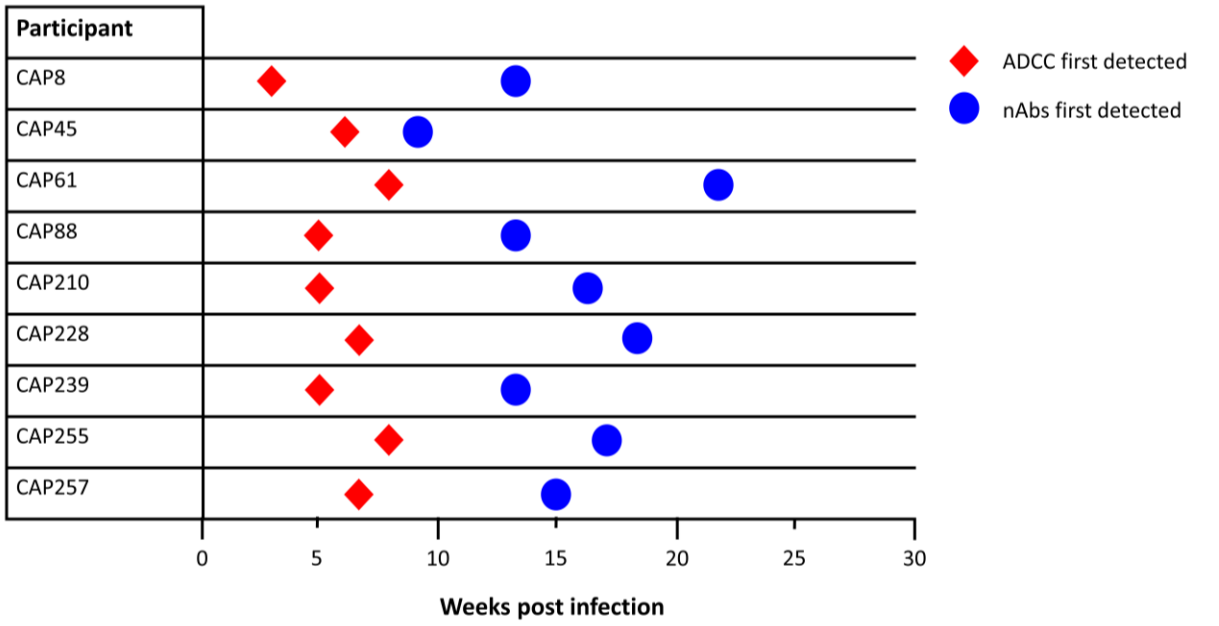

Figure 3.2 Summary of the time of first detection of ADCC and neutralizing antibody responses. The first time-point that ADCC responses (red diamonds) and nAbs (blue circles) in nine individuals of the CAPRISA 002 acute infection cohort.

In seven of the nine participants, ADCC and nAb responses to the early virus increased at approximately the same rate after nAbs were detected (Figure 3.1). However, a different pattern was observed in two participants, CAP45 and CAP255. ADCC responses in CAP45 followed a similar trajectory to nAb development until 14 wpi, after which ADCC responses decrease while nAb responses continue to increase. In CAP255, high ADCC titers (>1,000) were observed at enrolment (8 wpi), but these decreased considerably by 13 wpi (<150), the next time point tested, after which ADCC responses remained low.

3.3.2 Varied relationship between ADCC and nAb epitopes in early infection

We then investigated epitopes targeted by ADCC and nAb responses and viral escape in three participants (CAP45, CAP210 and CAP239) where we had available data on nAb kinetics and targets (164).

CAP45 nAbs targeted the C3V4 region and were detectable by 9 wpi (163, 164), but escape was conferred through mutations in the V5 region (164). In comparison, ADCC responses were detectable by 5 wpi (Figure 3.1) and have not been mapped. To identify regions under immune pressure in CAP45, we used 31 *env* sequences (previously generated by Dr Melissa-Rose Abrahams, UCT) from five time-points over 1 year of infection (Figure 3.3 A): 20 from 2 wpi; 5

from 5 wpi; 1 from 7 wpi; 3 from 12 wpi; 2 from 65 wpi. Due to very low viral loads, only three sequences were generated from 12 wpi, around the time of nAb detection, with no amplification from the 9 wpi plasma.

Sequences from 2-7 wpi were highly homogenous, with stochastic mutations consistent with Reverse Transcriptase error. However, at 12 wpi a three-residue deletion in the V5 (HxB2 positions 460-462, 460Δ3) was identified, and by 65 wpi, the viruses harbouring the deletion had disappeared, having been replaced by viruses with two mutations in the V5: K460E and D462G. To explore viral evolution in the V5 in greater detail, we generated deep sequencing from five time-points (enrolment to 14 wpi). A mean of 131 consensus sequences were generated, with a range of 52-203 consensus sequences (Figure 3.3 B). We observed the 3-residue deletion (10% of the viral population) at 9 wpi, the time of nAb detection, which increased to 23% at 10 wpi and 60% by 12 wpi, after which it decreased to 45% at 14 wpi. In addition, D462G was detected at very low levels (1.5%) at 10 wpi and increased to 11% at 12 wpi and 49% at 14 wpi. To determine the impact of these mutations on ADCC and nAb responses, we incorporated the three-residue deletion and D462G the acute CAP45 Env-IMC (CAP45 2.00). While the Env-IMC containing the deletion was not able to infect target cells at a level sufficient for the ADCC assay, the D462G virus (CAP45 2.00 D462G) conferred resistance to both ADCC (Figure 3.3 C) and nAb (Figure 3.3 D) responses.

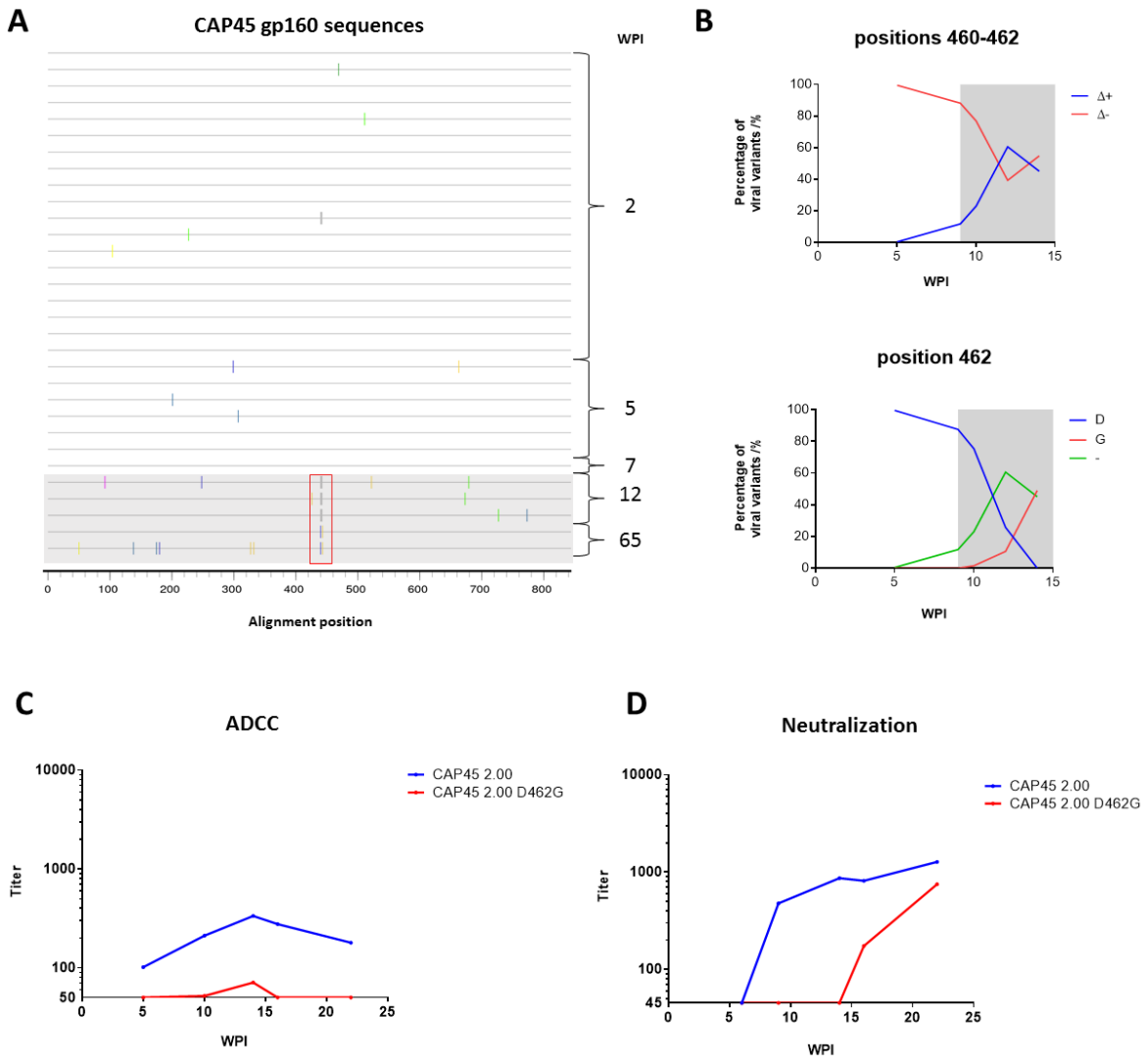

Figure 3.3 Viral evolution and development of antibody responses in CAP45. 31 single genome sequences were obtained from five time-points over 1 year of infection (nAb detection indicated with grey shading) **(A)**. Mutations were identified in a segment of the V5 (red box). Relative frequencies of sites under selection in the region were measured from deep sequencing data (nAb detection indicated with grey shading) **(B)**. One mutation, D462G was introduced into the acute virus, and ADCC **(C)** and neutralization **(D)** assays were performed to determine the effect of the mutation on each response.

In the second participant, CAP210, nAbs were detected by 16 wpi, while ADCC responses were detected at 5 wpi (Figure 3.1). We generated 39 *env* sequences (14 sequences for this thesis and 25 kindly provided by Dr Melissa-Rose Abrahams), from six time-points over six months of infection to investigate viral evolution (Figure 3.4 A): 12 from 2 wpi; 6 from 5 wpi; 7 from 10 wpi; 3 from 16 wpi; 4 from 18 wpi; and 8 from 22 wpi.

NAb responses were previously mapped to the V1V2 region (164). Here, we identified four regions under putative pressure, namely A161V in the V2, V208I in the C2, a six-residue deletion in the V4 and several sites in the cytoplasmic domain of gp41. Deep sequencing of the C1C2 region revealed that both A161V and V208I were detected several weeks before nAbs emerged (A161V was present in 10% of variants at 12 wpi, while V208I was present in 15% of variants at 12 wpi) (Figure 3.4 B). A161V became dominant, concurrent with the detection of nAbs, being present in ~ 80% of the viral population, while V208I remained a minor variant (present in 10-20% of the viral population from 16-26 wpi).

Both mutations were incorporated into the CAP210 T/F Env-IMC, and their effect on ADCC and nAb responses was investigated. CAP210 TF A161V did not have any effect on ADCC responses compared to CAP210 TF (Figure 3.4 C), but resulted in resistance to neutralization (Figure 3.4 D). In comparison, CAP210 TF V208I was completely resistant to ADCC responses, but only partially resistant to nAbs.

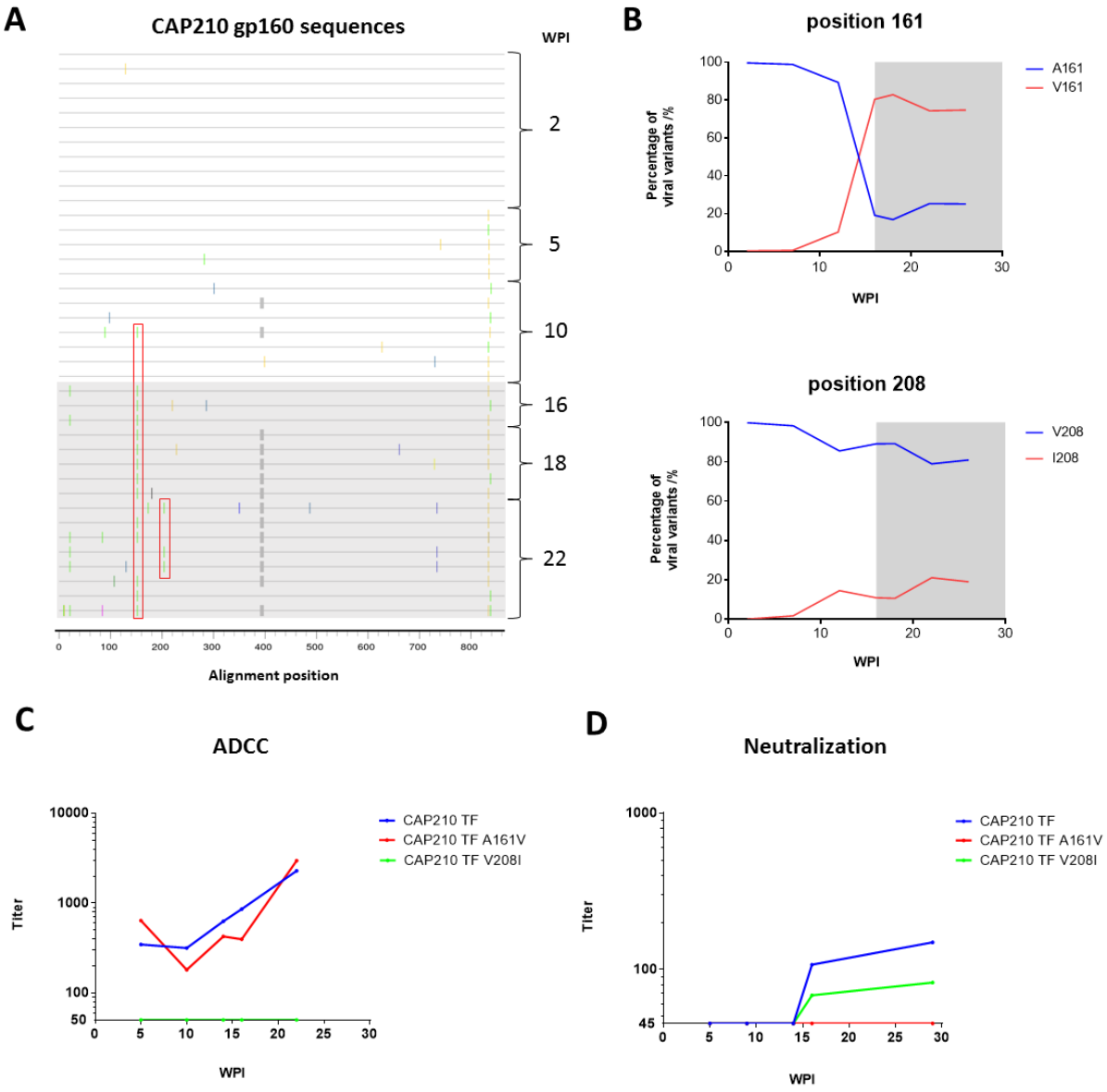

Figure 3.4 Viral evolution and development of antibody responses in CAP210. 39 single genome sequences were obtained from six time-points over six months of infection (nAbs detection indicated with grey shading) **(A)**. Mutations were identified in the V2 and beginning of the C2 (red boxes), as well as in the V4 and gp41. Relative frequencies of sites under selection in the V2 and C2 were measured from deep sequencing data (nAb detection indicated with grey shading) **(B)**. Two mutations, A161V and V208I, were introduced into the CAP210 T/F Env-IMC, and ADCC **(C)** and neutralization **(D)** assays were performed to determine the effect of both mutations on each response.

3.3.3 ADCC responses can drive immune escape in early HIV-1 infection

The last participant, CAP239, developed nAbs targeting the CD4bs, detectable by 13 wpi. In comparison, ADCC responses were detectable by 5 wpi (Figure 3.1). To investigate sites under selection, we compared 61 gp160 sequences (43 sequences generated as part of this thesis and 18 sequences kindly provided by Drs Melissa-Rose Abrahams and Florette Treurnicht) from ten time-points (2-37 wpi). Two sites were observed under putative immune pressure prior to the detection of nAbs, namely K97E and S481N. K97E was detected at in 3/22 sequences generated between 5 and 11 wpi, after which it was not detected (Figure 3.5 A), while S481N was detected in 2/22 sequences generated between 5 and 11 wpi, and then in 16/40 sequences generated between 13 and 37 wpi. Analysis of the prevalence of amino acids at position 481 using AnalyzeAlign (https://www.hiv.lanl.gov/content/sequence/ANALYZEALIGN/analyze_align.html) showed N481 was a rare mutation in subtype C sequences (present in 6.41% of sequences (85/1326)), while S481 was the dominant residue at this site (93.29% of sequences (1237/1326)). At the time nAbs were detected, two additional sites appeared under immune pressure (a three-residue deletion from position 405 to 407, and position 463). From 19 wpi, toggling was observed at four additional sites (106, 278, 456 and 463.02).

To investigate the source of immune pressure, three of these mutations (K97E, S481N and L278S, which introduced a PNGS at N276) were incorporated into the CAP239 T/F Env-IMC. K97E and S481N were introduced as putative ADCC escape sites, while L278S was introduced as a representative nAb escape mutation. While ADCC responses were detected to CAP239 T/F from the first time-point, the introduction of K97E resulted in complete resistance to ADCC responses until 10 wpi, after which antibodies which recognized the mutant were detected (Figure 3.5 B). Similarly, the introduction of S481N was associated with escape from ADCC responses until 22 wpi, at which time it became sensitive to ADCC responses. Both mutations had no effect on neutralization (Figure 3.5 C). The introduction of an L278S mutation resulted in complete resistance to nAbs until 15 wpi, after which it was still partially resistant to neutralization up to 22 wpi (Figure 3.5 C). Interestingly, introduction of an L278S mutation resulted in increased sensitivity to ADCC responses in comparison to the T/F Env virus from the first time-point (Figure 3.5 B), but sensitivity reduced to similar levels as the T/F Env virus by 19 wpi (the time at which the mutant was detectable by single genome sequencing).

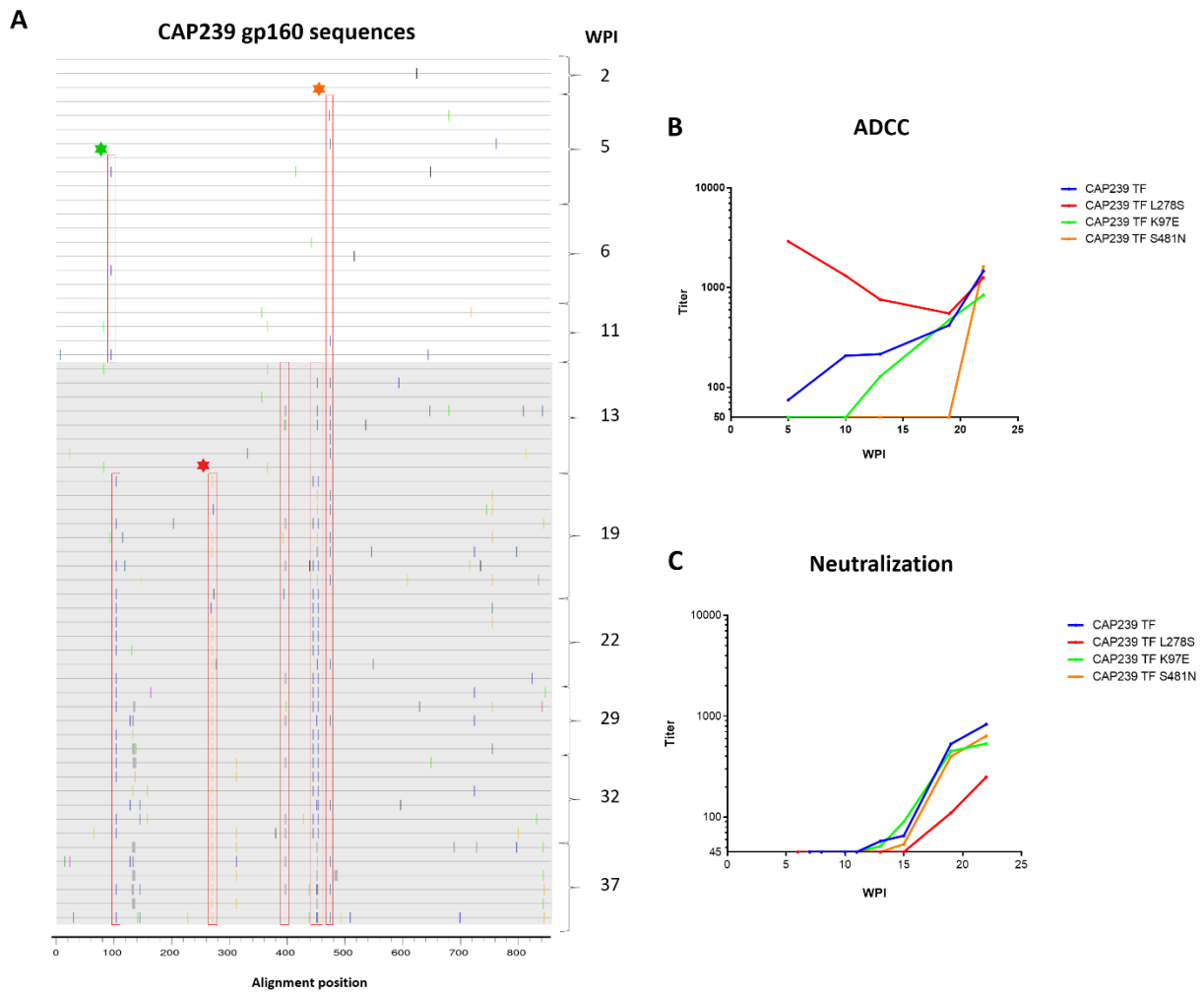

Figure 3.5 Viral evolution and development of antibody responses in CAP239. 62 single genome sequences were obtained from ten time-points over nine months of infection (nAb detection indicated with grey shading) **(A)**. Mutations were identified across the gp120 in regions in, or proximal to, the CD4bs (red boxes). Two mutations detected prior to nAb responses, K97E (green star) and S481N (orange star), as well as one mutation observed after the detection of nAbs (L278S; red star) were introduced into the T/F Env-IMC, and ADCC **(C)** and neutralization **(D)** assays were performed to determine the effect of each mutation on both responses.

3.3.4 ADCC and nAb responses drive viral evolution along distinct pathways

These results suggest that ADCC responses exerted pressure on the virus resulting in escape and that early ADCC and nAb responses targeted different epitopes. We were thus interested in how ADCC and nAb responses differentially impacted Env evolution. A maximum-likelihood phylogenetic tree of CAP239 Env sequences revealed three distinct pathways that emerged before, or at the time of, nAb detection (Figure 3.6). Pathway one (blue) was the earliest response (detectable from 5 wpi) and was characterised by escape in the C4C5 region (S481N and

E463K/G). This pathway was a dead-end evolutionary pathway as it was not detected after 22 weeks. The second pathway (purple) was characterized by mutations in loop D (L289S), the C5 (S481N) as well as deletions and toggling in the V5 (at positions 462 – 463.02) while pathway three (red) was observed from 19 wpi, and was characterized by mutations in the C1 (K106E), loop D (L278S) and C4V5 (W456R and K463.02E) regions.

To investigate how viral evolution in each of these pathways affected sensitivity to ADCC and nAb responses, we constructed Env-IMCs which incorporated the T/F *env* (black) or eight *envs* detected at 13 or 19 wpi (Figure 3.6) (list of mutations from the CAP239 T/F *env* are listed in appendix A2). Of the five Env-IMCs from pathway one, all five were resistant to ADCC (Figure 3.7 A,C) from contemporaneous plasma, while four of the five Env-IMCs were sensitive to contemporaneous nAbs (Figure 3.7 B,D). All three 13-week Env-IMCs were resistant to contemporaneous ADCC responses but sensitive to nAbs (Figure 3.6 C,D). Of the two 19-week Env-IMCs from pathway one, both Env-IMCs were completely resistant to contemporaneous ADCC responses, while one Env-IMC (CAP239 19-7F4) was 8-10 times more sensitive than the T/F Env-IMC to nAbs present at 19wpi, and the other Env (CAP239 19-7B2) was resistant to these nAb responses. The Env-IMC from pathway two (CAP239 19-7C2) was resistant to both ADCC and nAb responses present at 19 wpi. Finally, the two Env-IMCs from pathway three (CAP239 19-7E4 and CAP239 19-7F2) were as sensitive to contemporaneous ADCC responses as the T/F Env-IMC, but were resistant to nAbs.

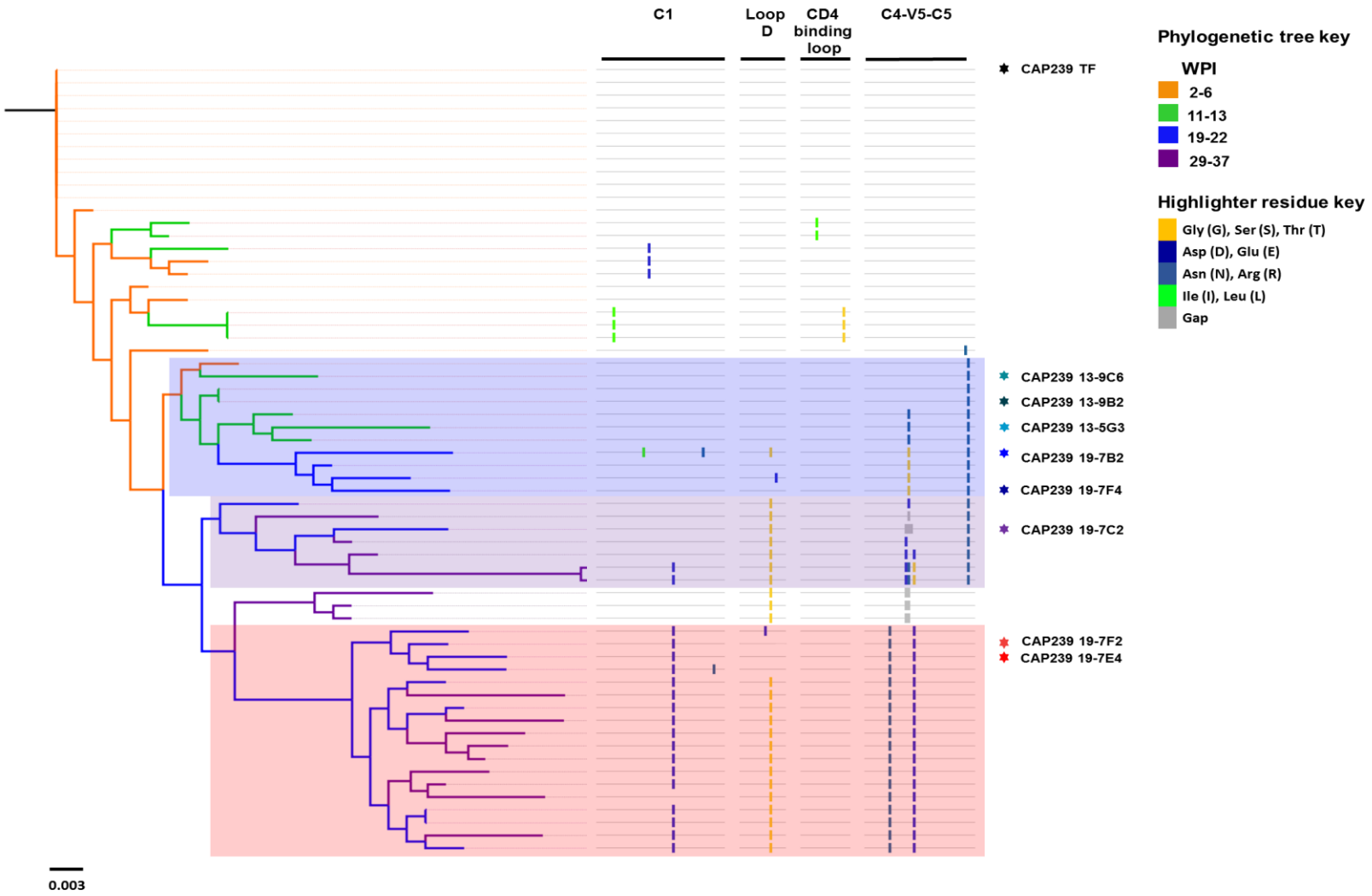

Figure 3.6 Evolution along multiple pathways in CD4bs regions of CAP239 viruses. A maximum-likelihood tree of the 62 CAP239 gp160 single genome sequences was constructed, and rooted on the T/F virus. Branches were colour-coded according to the time-point from which the sequence was sampled. Three distinct evolutionary pathways were observed at the time of, or just after, detection of nAbs. The first pathway was typified by an S481N mutation in the C5 (blue box); the second pathway was characterized by an L278S mutation in loop D, as well as S481N and a combination of deletions and toggling in the V5 (purple box); and the last pathway was characterized by K106E in the C1, L278S in loop D, as well as W456R and K464E in the V5 (red box). Env-IMCs of the T/F as well as eight representative sequences from the three pathways were constructed (identified by stars and the clone name). Three of the clones (CAP239 13-5G3, CAP239 13-9C6 and CAP239 13-9B2) represented 13 week viruses; while five viruses (CAP239 19-7F4, CAP239 19-7B2, CAP239 19-7C2, CAP239 19-7F2 and CAP239 19-7E4) represented 19 week viruses.

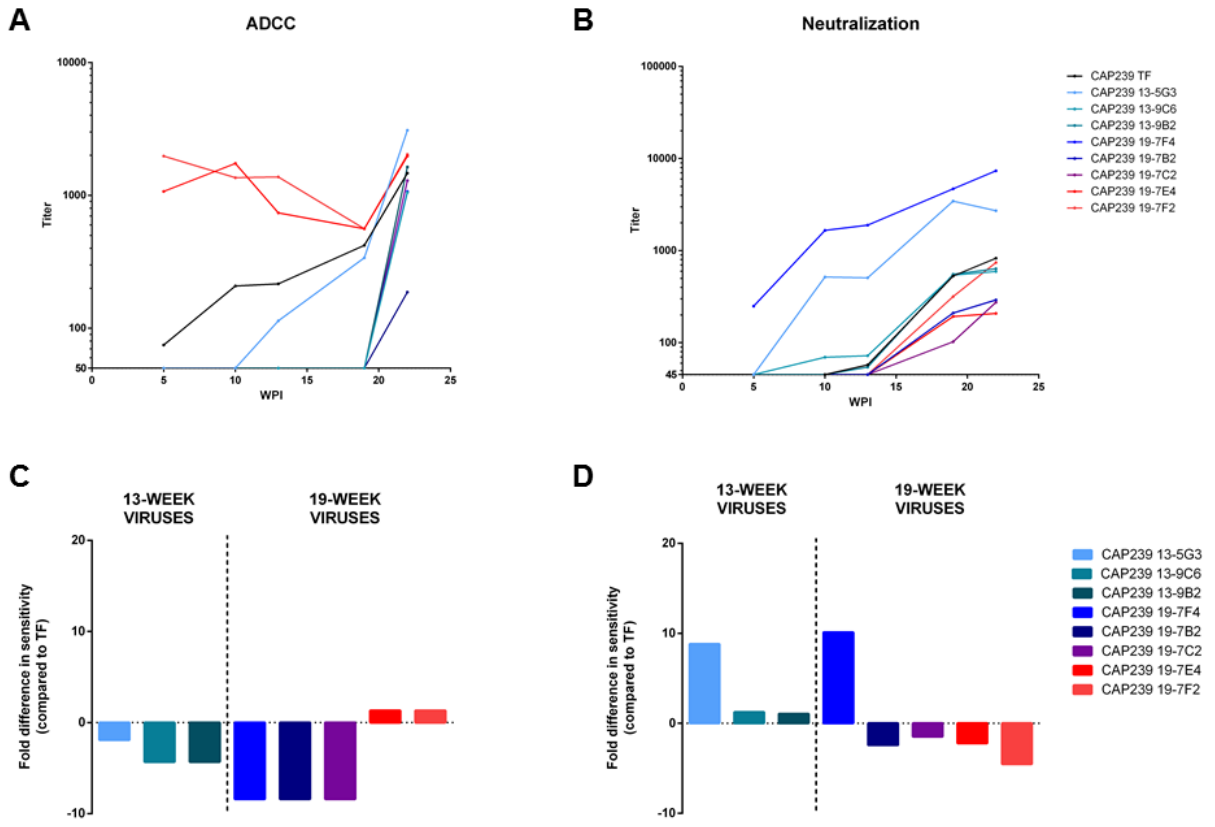

Figure 3.7 Impact of evolutionary pathways on recognition by ADCC and neutralization responses. ADCC responses against, **(A)** and neutralization of **(B)**, the CAP239 TF and eight viruses from 13 and 19 weeks post infection. The fold difference in sensitivity between each virus and CAP239 TF at the time point from which each virus was isolated and sequenced to ADCC **(C)** and neutralization **(D)** was then calculated.

The CAP239 T/F Env trimer, as well as representative Envs from each pathway, were then modelled onto the most representative trimer structure available, and one gp120 subunit was used to identify putative changes in the gp120 structure (Figure 3.8). Models of all pathways exhibited structural or charge changes in the V5: in pathway one, E462G resulted in a small helix in the V5; in pathway two, the V4 and V5 became less structured (including the loss of a β sheet in the V4), possibly due to a three-residue deletion in the V5; pathway three introduced a charge reversal in the V5 (K463.02E). In addition, a glycan was added at N276 in pathways two and three, which may have shielded the antibody epitope. Pathway three also introduced W456R in the β23 sheet, and a charge change (K106E) in the C1.

Of interest, S481N, which escaped ADCC responses and was observed in pathways one and two (resistant to ADCC), was buried within the gp120 (Figure 3.8 A, black shading).

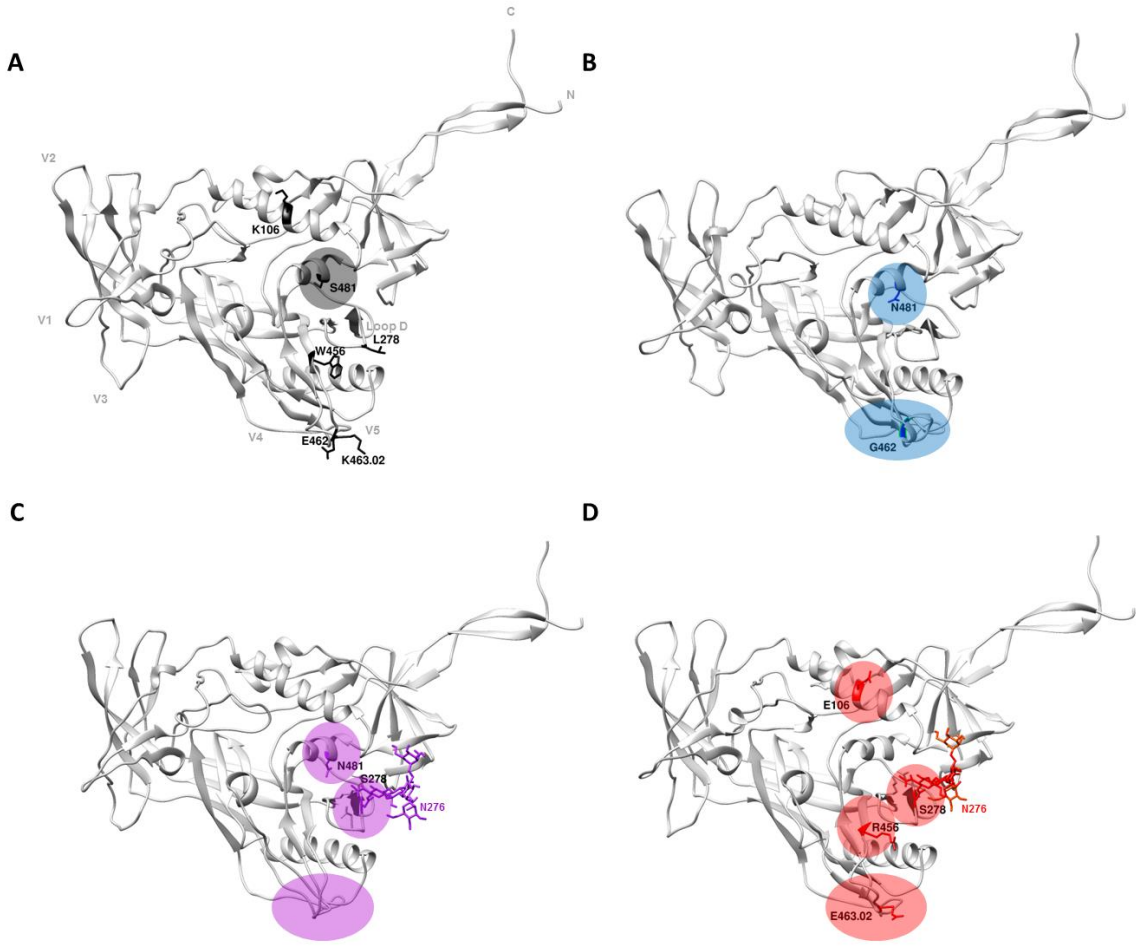

Figure 3.8 Models of the CAP239 TF gp120 and representative gp120s from each evolutionary pathway. Gp120 models of CAP239 TF and Envs from each of the three evolutionary pathways were constructed using Modeller (289) and the best scoring model was visualised using Chimera (176). Basic glycans were added at N276 in pathway two and three, which incorporated the glycan, using GlyProt (290). Structural landmarks (grey) and key residues in CAP239 viral evolution (black) are shown on CAP239 TF gp120 **(A)**. Changes characteristic to each evolutionary pathway are shown in blue (CAP239 19-7F4; pathway one) **(B)**, purple (CAP239 19-7C2; pathway two) **(C)** and red shading (CAP239 19-7H2; pathway three) **(D)**.

3.3.5 Differential neutralization and ADCC profiles of CAP239 TF by anti-HIV-1 monoclonal antibodies

The inaccessibility of S481 (ADCC sensitive), predicted by the modelling, suggested the Env structure on free virions and on the surface of infected cells may be different. To test this, we used

six bnAbs targeting diverse regions of the Env (Appendix A5) and with Fc regions optimized to bind $Fc_{\gamma}RIIIa$ (kindly provided by Dr Guido Ferrari, Duke University) to determine neutralization of the CAP239 TF Env virus and ADCC against CAP239 TF-infected cells. Of the six bnAbs we used, VRC01 and 3BNC117 (CD4bs bnAbs) were not able to neutralize CAP239 TF up to 10 μg/mL, while the other four bnAbs neutralized CAP239 TF with varying potency (Figure 3.9). In comparison, VRC01 and 3BNC117 could mediate ADCC against CAP239 TF-infected cells, while only PGT151 (which could neutralize CAP239 TF free virions) was not able to mediate ADCC against CAP239 TF-infected cells up to 10 μg/mL.

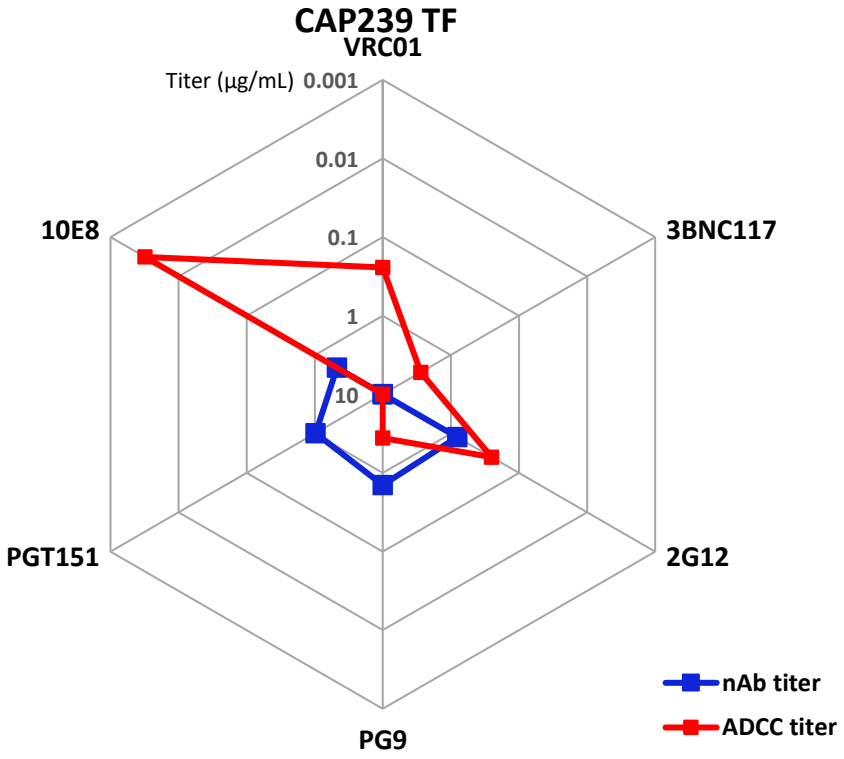

Figure 3.9 Radial plot indicating differential neutralization and ADCC profiles against CAP239 TF free virions and infected cells using six bnAbs. The neutralization (blue) and ADCC (red) profile against CAP239 TF are shown on a radial plot, with each spoke representing a bnAb. Sensitivity to each bnAb is indicated by the distance of the point between the centre (resistant) and circumference (sensitive).

3.4 Discussion

This study provided evidence of ADCC-mediated immune pressure in early infection for the first time. We found, similar to other studies (146, 189, 291), that autologous ADCC responses in nine individuals were detectable prior to nAb responses. Using single genome and deep sequencing, we

tracked the impact of early ADCC and nAb responses on viral *env* evolution in three individuals. In one individual, we identified two mutations which appeared almost two months prior to the detection of nAbs and distinct from the apparent nAb epitope. Both mutations had no effect on neutralization, but resulted in resistance to ADCC responses. Longitudinal *env* sequencing of plasma variants revealed three evolutionary pathways, which developed from infection until nine months post infection, two of which included one of the ADCC escape mutations and were resistant to ADCC responses. This suggests ADCC responses can directly impact viral evolution *in vivo*.

Many nAbs can mediate ADCC (reviewed by Pollara *et al.* (228)), indicating several Env epitopes are present on both free virions and on the surface of infected cells. Here, a nAb escape mutation in the V5 (D462G) of viruses in one participant (CAP45) resulted in resistance to ADCC, suggesting these responses overlapped or were mediated through the same antibody. However, this pattern was not observed in CAP210 where two mutations had distinctly different effects on neutralization and ADCC: one escape mutation (A161V) resulted in resistance to nAbs but had not effect on ADCC, while the other mutation (V208I) resulted in resistance to ADCC responses but had a limited effect on neutralization. This could suggest neutralization and ADCC were mediated via different antibodies, or the same antibody bound different forms of the epitope on the Env of free virions and on the surface of infected cells. The latter is possible because the relationship of Env epitopes on free virions and infected cells is likely complex and there is evidence that not all Env epitopes accessible on the surface of infected cells are present on the native trimer (100). This is further supported by the differential neutralization and ADCC profiles of bnAbs against CAP239 TF free virions and infected cells, respectively.

Several studies have suggested ADCC responses may play an important role in an effective HIV-1 vaccine, including the RV144 trial (8). However, only one other study to date has provided evidence of escape (which may provide a measure of the importance of an immune response) from ADCC responses in chronic infection (233). In that study, Chung *et al.* identified escape from ADCC responses mapped to the C1 region. Furthermore, several other studies have identified this region as a common target of ADCC-mediating antibodies (191, 229). Here, we identified one site in the C1 (K97E) of CAP239 viruses under weak selection pressure in early infection which facilitated resistance to ADCC responses but had no effect on neutralization, suggesting this region was also targeted by nnAbs in our study.

In addition, numerous ADCC-mediating nnAbs have been mapped to the C5, usually close to the gp120 C terminus (203, 226, 292). We identified ADCC escape at a single site in the C5 region (S481N) of CAP239 viruses, anterior to the epitopes previously characterized, which appeared inaccessible to antibodies in the closed trimer model. This mutation did not have any effect on neutralization, but induced resistance to ADCC. In addition, the mutation was fixed in two of the three viral evolutionary pathways identified, suggesting there was immune pressure on this site. Viruses from the first pathway were detected in sequences from 6 wpi (seven weeks prior to the detection of nAbs) and continued until 22 wpi, after which it was not detected. Earlier sequences only contained the ADCC escape mutation, but later viruses incorporated nAb escape mutations in the V5 as well, suggesting there was a dynamic adaptation process to pressure from both responses.

The two remaining pathways were observed after the detection of nAbs (from 19 wpi). Pathway two, which contained the exclusive ADCC escape mutation, was present through to 37 wpi (the last time-point sequenced) suggesting ADCC pressure continued to play a role in driving viral evolution up to this time-point. However, the third pathway incorporated mutations distinct from the first two pathways and was not resistant to ADCC responses. The continuation of this pathway, despite sensitivity to ADCC responses, suggests ADCC pressure on the viral Env was relatively weak compared to nAb pressure.

The presence of variants sensitive to contemporaneous nAbs was unexpected, but has been observed and reported previously (164, 293). In this study, while both clones which exhibited heightened sensitivity to nAbs (CAP239 13-5G3 and CAP239 19-7F4) were also resistant to ADCC responses, it does not seem likely that ADCC pressure resulted in nAb sensitive variants, as other ADCC resistant variants with similar escape mutations were not nAb sensitive. Instead, both variants contained transient mutations outside of the apparent epitope which may have resulted in increased neutralization sensitivity. CAP239 19-7F4 incorporated a glycan at N234 (A236T), which has been reported to alter susceptibility to neutralization by CD4bs antibodies (294) and may have done so here; while G600E, which added a charged side chain at a highly conserved site close to the gp41 fusion domain, was present in CAP239 13-5G3 and may have resulted in increased susceptibility to neutralization.

In summary, the ability to force immune pressure provides an indication of the importance of an immune response. We demonstrate ADCC driven immune escape and viral evolution in early infection for the first time, showing that these responses can exert selective pressure on HIV-1. Here, viruses that were ADCC resistant were selected for in the absence of nAb pressure. However, after nAbs developed the virus evolved to preferentially escape these responses, often without escaping ADCC, indicating nAbs exert stronger selective pressure on the virus. These data suggest that while eliciting nAbs should be the primary goal of HIV-1 vaccine design, ADCC-mediating antibodies may also play an important role in a protective vaccine.

Chapter 4. CD4i non-neutralizing antibodies display the greatest ADCC breadth and potency against subtype C viruses

ABSTRACT

A better understanding of the relationship between neutralization and ADCC activity of antibodies is important to guide the development of immunotherapies and antibody-based vaccines for the treatment or prevention of HIV-1 infection. Here, we assessed ADCC breadth of broadly neutralizing antibodies (bnAbs) and non-neutralizing Abs (nnAbs) against a panel of subtype C viruses.

Seven bnAbs (VRC01, 3BNC117, PG9, 697D, PGT151, 2G12 and 10E8) and four nnAbs (C11, A32, CH58 and HG107) were evaluated for ADCC activity against a panel of nine viruses with early/acute subtype C Envelopes. We found bnAb ADCC breadth ranged from 11-66%, while nnAb ADCC breadth ranged from 33-100%, of which the two CD4-induced (CD4i) nnAbs (A32 and C11) were the broadest and most potent antibodies against our virus panel. Further, our data showed anti-HIV-1 monoclonal antibodies (mAbs) which had the highest binding capacity to infected cells generally exerted the most potent ADCC responses (r_s = -0.5309, p = 0.0001).

Epitopes on free virions are likely to differ from those on the surface of infected cells. However, some bnAbs still mediated broad ADCC activity, suggesting there are some common epitopes on free virions and the surface of infected cells. The nnAbs targeting the CD4i cluster A epitopes displayed the most potent and broad ADCC activity, suggesting these antibodies may be more relevant for interventions that aim to eliminate virus infected cells.

4.1 Introduction

An HIV-1 vaccine which elicits bnAbs is a goal of the HIV vaccine field. Recently many highly potent bnAbs have been isolated and characterised, and numerous studies have shown they can protect from viral acquisition or can slow disease progression in humanized mouse and non-human primate studies (295–300). In addition, three clinical trials, which administered individual bnAbs (VRC01, 3BNC117 and 10-1074) to viremic patients, displayed a viral load reduction of up to 2.5 logs, providing definitive evidence of the clinical benefit of anti-HIV bnAbs in humans for the first time (301–303).

Many bnAbs, targeting diverse regions of the Env (including the CD4bs, V1V2 and V3 loops, and MPER), can mediate ADCC (304–307). In addition, the Fc region of bnAbs has consistently played an important role in therapeutic efficacy against SHIV and HIV-1 (201, 308, 309). Recently, the kinetics of HIV-1 suppression in infected individuals with passively administered 3BCN117 suggested Fc-mediated effector functions played a role by clearing infected cells (310). This is corroborated by two recent non-human primate studies by Hessell *et al*. and Liu *et al*., which showed bnAb-mediated protection was partially facilitated by clearing HIV-1 infection in distal tissues (281, 282).

The RV144 trial raised questions in the field about the potential protectiveness of nnAbs. These antibodies target numerous epitopes on the HIV Env (286, 311), which include the gp41 immunodominant domain, corresponding to a loop typically hidden under the gp120 trimer on mature virions (312) and different conformational CD4-induced (CD4i) epitopes revealed after Env binding to CD4 (286, 311, 313, 314). The classical examples of CD4i nnAbs are A32, which targets the C1, and 17B, which targets the co-receptor binding site (229).

HIV-1 subtype C accounts for almost half of the global epidemic (29), and consequently is a major focus of vaccine efforts. Here, we assessed ADCC breadth using eleven anti-HIV-1 mAbs, including seven bnAbs and four nnAbs, and a panel of nine viruses with acute/early subtype C *envelopes*. We found bnAbs had low to moderate ADCC breadth against subtype C viruses. However, the classical CD4i nnAbs, A32 and C11, exhibited broad and potent ADCC. We then explored the relationship between ADCC activity and binding to the surface of infected cells using the same eleven mAbs. Our data showed mAbs which bound infected cells the strongest generally mediated the most potent ADCC responses.

4.2 Methods

4.2.1 Ethics statement

Ethics approval was obtained as detailed in Chapter 2.2.1.

4.2.2 Cell lines

TZM-bl cells and HEK293T cells were obtained and cultured as previously detailed in Chapter 2.2.3. CEM.NKR$_{CCR5}$ cells were obtained and cultured as described in Chapter 3.2.3.

4.2.3 Peripheral blood mononuclear cells

PBMCs were obtained and maintained as previously described in Chapter 3.2.4.

4.2.4 Construction of HIV-1 infectious molecular clones and virus preparation

Env-IMCs were constructed as described in Chapter 3.2.8 and virus preparation was carried out as described in Chapter 2.2.7.

4.2.5 Infection of CEM.NKR$_{CCR5}$ cells with HIV-1 IMCs

CEM.NKR$_{CCR5}$ cell infection was carried out as previously described in Chapter 3.2.9.

4.2.6 Luciferase-based ADCC assay

The Luciferase-based ADCC assay was performed as previously described in Chapter 3.2.12. All anti-HIV-1 mAbs used in the ADCC assays had identical Fc regions with decreased fucosylation for optimized recognition of Fc$_\gamma$RIIIa, resulting in improved NK cell binding and ADCC (287, 288), and were kindly provided by Dr Guido Ferrari (Duke University).

4.2.7 Indirect cell-surface staining

Infected CEM.NKR$_{CCR5}$ cells were obtained as previously described (Chapter 3.2.5). Cells incubated in the absence of virus (mock infected) were used as a negative infection control. Following infection, infected and mock infected cells (2 x 10^5/well) were washed in PBS, dispensed into 96-well V-bottom plates and incubated with 5 μg/mL mAb for 2 h at 37 ºC. Subsequently, cells were washed twice with 250 μL/well of WB and stained with vital dye (Live/Dead Fixable Aqua Dead Cell Stain, Invitrogen) to exclude nonviable cells from subsequent analysis. Cells were then washed with WB, resuspended in 100 μL/well Cytofix/Cytoperm (BD Biosciences) and incubated in the dark for 20 min at 4 ºC. Following the incubation period, cells

were washed in 1% Cytoperm wash solution (BD Biosciences) and co-incubated with anti-p24 antibody (clone KC57-RD1; Beckman Coulter) to a final dilution of 1:400 and a secondary FITC-conjugated antibody (goat anti-human IgG(H+L)-FITC, 172-1006; KPL) to a final dilution of 1:100, and the plates were incubated in the dark for 25 min at 4 ºC. Cells were washed three times with 1% Cytoperm wash solution (BD Biosciences) and resuspended in 150 μL PBS-1% paraformaldehyde. The samples were acquired within 24 h using an LSR II flow cytometer (BD Biosciences). A minimum of 10,000 total events was acquired for each analysis. Gates were set to include singlet and live events. The appropriate compensation beads were used to compensate the spill over signal for the three fluorophores. Data analysis was performed using FlowJo 10.2 software (TreeStar). The median fluorescent intensity (MFI) of surface binding for each anti-HIV-1 antibody was calculated by first subtracting the background florescence, calculated as the MFI of virus-infected cells stained with the secondary antibody in the absence of anti-HIV-1 antibodies, and then subtracting the MFI for each anti-HIV-1 mAb stained on the surface of mock (uninfected) cells.

4.2.8 Sequence alignment and analysis

Multiple sequence alignments were performed using Mega (v7.0.21) (315) and edited by eye with BioEdit (ver. 5.0.9) (264). Maximum-likelihood trees were generated using FastTree (v2.1) (316) and visualized using FigTree (v1.4.3).

4.2.9 Statistical and graphical analysis

Statistical analysis and generation of graphs were completed using Prism (v6.01) (Graphpad).

4.3 Results

4.3.1 The subtype C Env-IMC panel is broadly representative of acute subtype C *envelopes*

To explore the breadth of anti-HIV-1 antibody responses against subtype C viruses, we used a panel Env-IMCs (n=11) with HIV-1 subtype C acute/early *envs* constructed by the Ochsenbauer group (UAB) (n=10), and Williamson group (D Mielke, UCT) (n=1) (described in Appendix A2). To determine if this panel represented acute subtype C *envs*, we compared the panel viruses to 69 acute subtype C *env* sequences generated by Abrahams *et al.* (104) (Figure 4.1). *Envs* from the

panel (shown in blue) were distributed evenly around the tree, indicating that this panel was broadly representative of acute subtype C sequences.

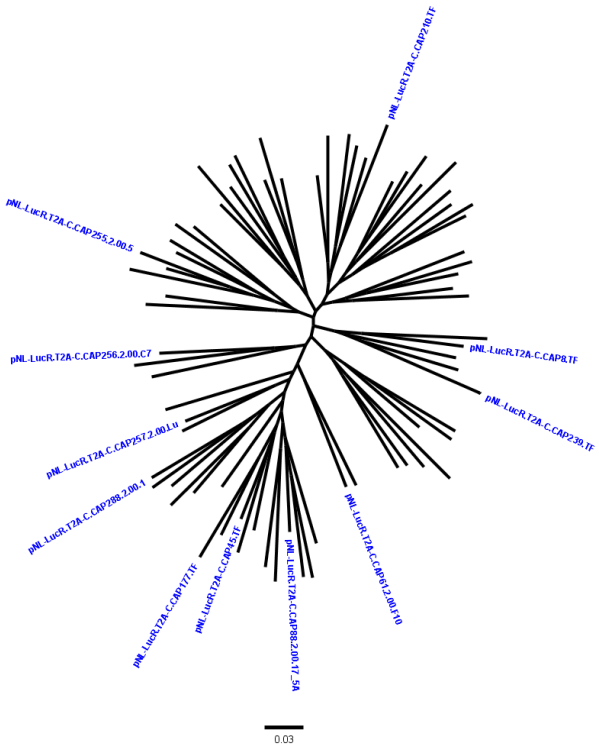

Figure 4.1 Maximum-likelihood phylogenetic tree illustrating the representativeness of the acute/early subtype C Env-IMC panel. The ectodomain of Env-IMC *env* sequences were aligned with the ectodomain of *envs* from the dataset, as all Env-IMCs contained the rev response element and endodomain of NL4-3. A maximum-likelihood tree was then constructed and ENV-IMC *envs* (represented by blue labels) were visualized in an unrooted tree of 69 acute subtype C *env* sequences (104). Scale bar = 0.03 substitutions per site.

4.3.2 CD4i non-neutralizing antibodies display the greatest ADCC breadth and potency against subtype C viruses

To determine the breadth and potency of ADCC responses against an acute/early subtype C Env-IMC panel (n=9), we used a selection of eleven anti-HIV-1 mAbs, including seven bnAbs targeting the CD4bs (VRC01, 3BNC117), V2 (PG9, 697D), V3 glycan (2G12), gp120/41 interface (PGT151) and MPER (10E8) and four nnAbs targeting the CD4i epitopes (A32, C11) and V2 (CH58, HG107) (Appendix A5) (Table 4.1, Figure 4.1). Two Env-IMCs (CAP177 TF and CAP256 2.00, Appendix A2) were removed from the virus panel as they did not meet the infection criteria for the ADCC assay (Appendix A6, Table A6.1).

Of the seven bnAbs, the CD4bs bnAbs had the broadest ADCC activity, with VRC01 recognizing 66% (6/9) of the panel; while 3BNC117 recognized 56% (5/9) (Table 4.1, Figure 4.2). The bnAbs recognising the MPER (10E8) and V2 (PG9) had slightly lower ADCC breadth, both recognising 56% (5/9) of the panel viruses, while the gp120/41 interface antibody (PGT 151) ADCC breadth was only 33% (3/9). Lastly 697D (V2) and 2G12 (V3 glycans) had very narrow breadth, only recognizing 11% (1/9) of the panel.

10E8 mediated the most potent ADCC against the panel (defined as the lowest dilution of mAb that mediated ADCC activity above background) followed by VRC01, which was over two times more potent than 3BNC117 (Table 4.1, Figure 4.2). Of the seven bnAbs, 2G12 and 697D mediated ADCC with the lowest potency.

Of the four nnAbs we tested, the two CD4i nnAbs (C11 and A32) had the greatest ADCC breadth, with C11 recognizing 100% (9/9) of the panel and A32 recognizing 78% (7/9) of the panel. In contrast, the two V2-targeting nnAbs (CH58 and HG107) exhibited lower breadth (33% (3/9) and 44% (4/9), respectively). In addition, C11 and A32 were the most potent mAbs (0.14 µg/mL and 0.06 µg/mL, respectively), with A32 (the most potent nnAb tested) over 13 times more potent than 10E8, the most potent bnAb tested (Table 4.1, Figure 4.2). As with the breadth, CH58 and HG107 showed low potency.

Table 4.1. ADCC breadth and potency of eleven anti-HIV-1 mAbs.

bnAb	Neutralizing/non-neutralizing	Epitope	ADCC breadth	ADCC potency (geometric mean titer)/ µg/mL
VRC01	Neutralizing	CD4bs	66% (6/9)	1.85
3BNC117		CD4bs	56% (5/9)	4.09
PG9		V2	56% (5/9)	3.66
697D		V2	11% (1/9)	5.95
PGT151		Gp120/41 interface	33% (3/9)	4.48
2G12		V3 glycans	11% (1/9)	6.64
10E8		MPER	56% (5/9)	0.81
C11	Non-neutralizing	CD4i	100% (9/9)	0.14
A32		CD4i	78% (7/9)	0.06
CH58		V2	33% (3/9)	7.35
HG107		V2	44% (4/9)	3.64

Figure 4.2. Radial plots representing ADCC breadth and potency profiles of seven bnAbs and four nnAbs. Each plot shows the ADCC profile of a bnAb (red)/nnAb (blue) against nine viruses (spokes). Antibody ADCC potency increases as the distance from the centre of the plot increases.

4.3.3 Viruses exhibit differential susceptibility to ADCC

To investigate if viruses displayed differential susceptibility to ADCC, as has been shown for neutralization sensitivity, we ranked the nine viruses according to the ADCC geometric mean titer (GMT) against each virus (Figure 4.3). Of the nine viruses, CAP255 ranked the most resistant to ADCC (recognized by five of the eleven mAbs, but with titers <1 μg/mL for all of them) while CAP239 was the most sensitive to ADCC mediated by the 11 mAbs, being recognized by eight of eleven mAbs at low titers. In general, there seemed to be a hierarchy of resistance/sensitivity to ADCC, suggesting there may be some intrinsic Env characteristics that confer resistance/sensitivity to ADCC.

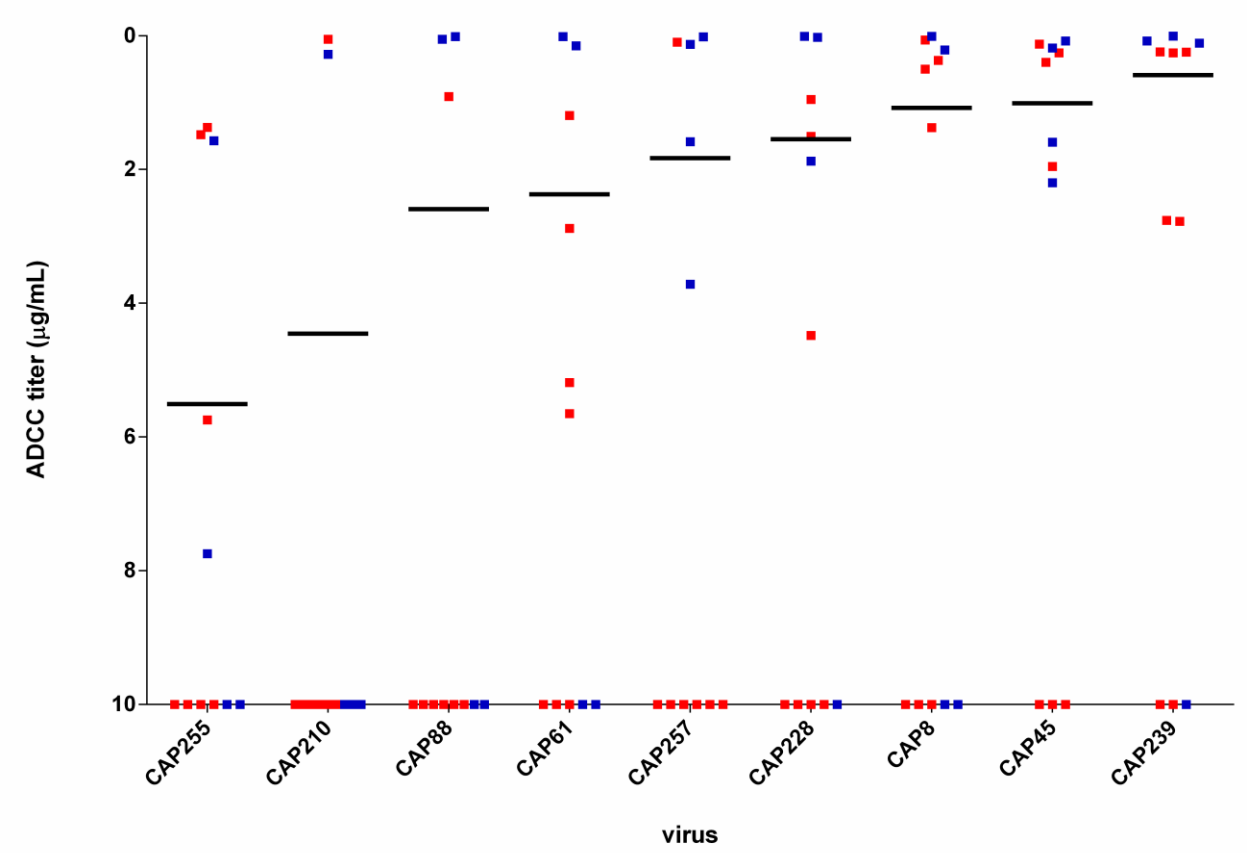

Figure 4.3. Susceptibility of subtype C viruses to ADCC by 11 anti-HIV-1 mAbs. Viruses were ranked by susceptibility to ADCC from 11 mAbs (7 bnAbs and 4 nnAbs). BnAbs are shown by red dots and nnAbs are shown by blue dots. The geometric mean titer of ADCC against each virus is indicated by the black line.

4.3.4 The most potent ADCC-mediating mAbs efficiently bind to the surface of infected cells

ADCC effector function requires anti-HIV-1 antibodies to bind to viral antigens on the surface of infected cells. To investigate the relationship between ADCC and binding to Env on infected cells, we used the same 11 anti-HIV-1 mAbs against the acute/early subtype C *env* virus panel.

The median fluorescent intensity (MFI) of a FITC-conjugated secondary antibody which bound to IgG antibody was used to quantify anti-HIV-1 antibody binding to infected cells. No linear relationship between mAb ADCC titer and surface binding was found when ADCC titers above the maximum threshold of 10 μg/mL were included (n=94) ($r = 0.1537$, $p=<0.0001$), and did not change when data points above the ADCC titer threshold were removed (as these antibodies may have still bound to antigen, but only mediated ADCC at higher concentrations tested) (n=46) ($r = 0.1443$, $p=0.0092$).

Each mAb was then ranked by ADCC GMT against the nine viruses, and the corresponding mean MFI for each mAb was calculated (Figure 4.4). NnAbs A32, C11 and bnAb 10E8, which ranked the highest by ADCC GMT (0.0603 μg/mL, 0.1463 μg/mL and 0.8132 μg/mL, respectively), also bound Env on the surface of infected cells most efficiently (mean MFI = 2516, 1736 and 730). In contrast, nnAb CH58, which ranked the lowest by ADCC GMT (7.3570 μg/mL), had the lowest binding to the surface of infected cells (mean MFI = 7.25). When testing for a non-linear relationship (by rank), the Spearman's rho indicated there was a non-linear inverse relationship between ADCC titer and surface staining MFI ($r_s = -0.4402$, $p < 0.0001$), which increased when data points with ADCC titer ≥ 10 μg/mL were removed ($r_s = -0.5309$, $p = 0.0001$).

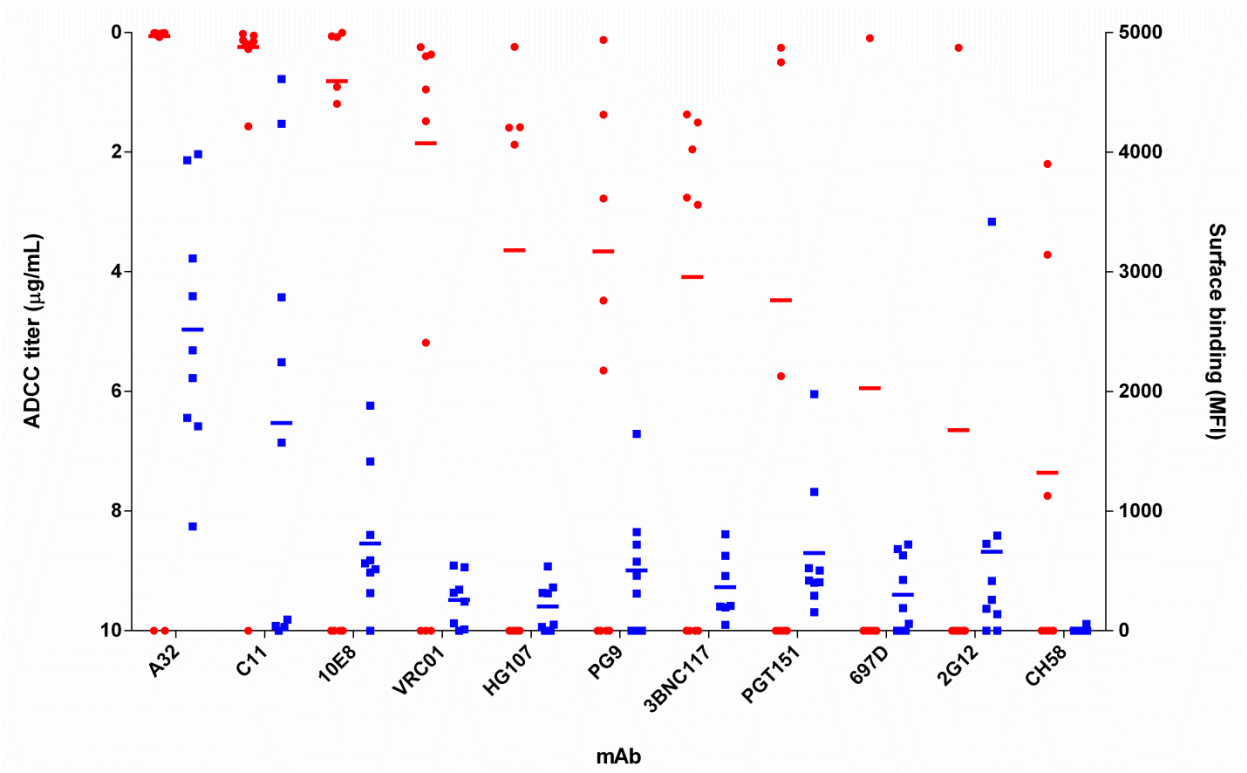

Figure 4.4 ADCC activity and surface binding of 11 anti-HIV-1 mAbs. The ADCC titer (red) and MFI (blue) were plotted for each mAb against nine viruses. MAbs were ranked by ADCC GMT (red lines) and the mean MFI (blue lines) for each mAb was also plotted.

4.1 Discussion

There is increasing evidence that Fc$_\gamma$R-dependent functions are important for optimal antibody anti-HIV-1 activity (201, 202, 308, 309). Consequently, a better understanding of Fc effector functions of neutralizing and non-neutralizing antibodies is important to guide the development of immunotherapies and antibody-based vaccines for the treatment and prevention of HIV-1 infection. Here, we explored the breadth of ADCC activity mediated by seven bnAbs and four nnAbs targeting diverse regions of the Env against nine early/acute subtype C viruses. In general, the breadth of ADCC exerted by bnAbs was low to moderate, with the CD4bs bnAbs (and in particular, VRC01) exhibiting the highest breadth against our panel. Instead, the two CD4i nnAbs we used (A32 and C11) mediated the broadest and most potent ADCC. In addition, as expected, the level of ADCC activity was predicted by the ability of a mAb to bind Env on the surface of infected cells.

Epitopes on the Env trimer of virions are not necessarily accessible on the surface of infected cells. Acharya *et al*. showed the importance of antibody orientation for Fc_{γ}-receptor interaction, highlighting the impact fine differences in the epitope footprint, or angles of approach, may have on ADCC activity (317). It is possible this played a role in the levels of ADCC activity exhibited by the bnAbs used in this study. In particular, this may explain the profile exhibited by PGT151, which binds the gp120-gp41 interface on the Env trimer. This bnAb has a high reported neutralization breadth against subtype C viruses (73%) (318), and bound to Env on the surface of infected cells with relatively high affinity, yet poorly mediated ADCC.

In contrast to nAb epitopes, many nnAb epitopes are not accessible on the closed Env trimer. These include the targets of A32 and C11, which bind CD4i epitopes of the gp120 inner domain (61, 229, 319–321). Previously, Bruel *et al*. reported nnAbs had low ADCC breadth against a panel of eight T/F HIV-1 strains (322). However, these nnAbs did not include the prototypic CD4i antibodies A32 and C11. In this study, similar to Bruel *et al*., we found the two V2 nnAbs we used (CH58 and HG107) were relatively narrow and weak at eliciting ADCC. However, A32 and C11 were the most broad and potent mediators of ADCC, in agreement with previous studies (191, 229). Furthermore, both nnAbs bound infected cells efficiency. Together, this suggests the A32 and C11 epitopes are conserved in subtype C viruses. Interestingly, von Bredow *et al.* reported resistance of NL4-3-infected cells to A32-mediated ADCC, possibly due to down-modulation of CD4 on the surface of infected cells (305). However, our subtype C Env-IMC panel utilized an NL4-3 backbone. Consequently, it seems more likely the NL4-3 Env did not contain the A32 epitope.

Understanding the breadth of ADCC responses by anti-HIV-1 antibodies is important to understand if bnAbs elicited by a vaccine will also be able to target infected cells. The breadth of ADCC activity mediated by some bnAbs implies there are some common epitopes on free virions and the surface of infected cells, suggesting these bnAbs would be able to clear early infected tissues. In addition, nnAbs targeting the CD4i epitopes displayed potent and broad ADCC activity, suggesting these antibodies may be worth exploring as additional vaccine targets.

Chapter 5. Conclusions

Almost thirty-five years after HIV-1 was discovered, a protective vaccine remains elusive. However, many studies have provided valuable insight into what might constitute a protective immune response. Passive immunization studies have indicated neutralizing antibodies (nAbs) have the potential to provide sterilizing protection. In addition, the RV144 vaccine trial, among other studies, indicated antibody Fc effector functions, such as ADCC, may play an important role in an effective vaccine. In this study, we wished to understand the impact of both responses on early HIV-1 Envelope evolution to further inform vaccine design.

Recent advances in deep sequencing approaches, coupled with the primer ID method which barcodes each viral genome, enabled us to generate thousands of viral sequences over time and accurately track viral population dynamics. In three of the seven individuals we investigated, we found that the absolute population of nAb sensitive viruses remained relatively stable, despite detectable nAbs. The decrease in frequency of this population relative to the escape variant was attributable to an outgrowth of the escaped virus which resulted in an increase in the overall viral load. For vaccine studies, it will be important to further understand the mechanism by which the virus persists despite antibody responses, and if this phenomenon occurs in chronic infection, in the presence of a broader antibody response. In addition, we found that early nAbs do not effectively inhibit cell-cell transmission, providing further evidence for the significance of antibody effector functions such as ADCC in a vaccine, which can target infected cells and potentially prevent cell-cell transmission.

If ADCC responses are important in controlling viral populations, we expected to find evidence of viral escape from these responses. In nine participants, we found that ADCC responses emerged before nAbs, enabling us to define ADCC-mediated pressure. To explore this, we evaluated three participants in detail. In all three participants, we observed limited evolution after ADCC responses were detected but prior to nAbs. In contrast, once nAbs developed, there was a marked divergence in the nAb epitope. In one individual, nAb and ADCC responses targeted the same epitope, suggesting they may have been mediated via the same antibody. However, the relationship between these responses in the other two participants was more complex. In one participant, we found ADCC-driven immune escape and viral evolution in early infection, providing evidence of their importance as an immune response. However, soon after nAbs developed, these viruses

evolved to preferentially escape nAbs, often without escaping ADCC, indicating nAbs exerted significantly stronger selection pressure on the virus.

Lastly, several ongoing clinical trials are assessing the protectiveness of broadly neutralizing antibodies (bnAbs) by passive immunization, and there is evidence their protective efficacy is enhanced by Fc function. Here, we used a panel of anti-HIV-1 mAbs and a panel of viruses with early/acute subtype C Envs to explore the ADCC breadth of broadly neutralizing and non-neutralizing antibodies against infected cells. We found bnAbs had low to moderate (11-66%) ADCC breadth. However, their potency was generally low (ranging from 0.81 µg/mL for 10E8 - 6.64 µg/mL for 2G12). In contrast, while the V2 nnAbs were narrow (33-44%) and not potent (3.64-7.35 µg/mL), two of the CD4i nnAbs (A32 and C11) exhibited higher breadth (78-100%) and were highly potent (0.06-0.14 µg/mL) (A32 was 13.5 times more potent that the most potent bnAb, 10E8). Larger panels of infectious molecular clones need to be constructed, such as those developed for characterising nAbs, to fully understand the relationship between neutralization and ADCC.

In conclusion, this study was the first to show a stable persistence of nAb sensitive viruses in early natural infection, highlighting the need to further understand how these viruses persist as this poses a potential challenge for vaccine responses. In addition, we provide further motivation for including antibody effector functions, such as ADCC, in an HIV-1 vaccine. To our knowledge this study was the first to provide evidence of ADCC-driven immune escape in early infection, showing that these responses can exert selective pressure on HIV-1, albeit less than nAbs. The moderate ADCC breadth of some bnAbs indicates there are common epitopes on free virions and on the surface of infected cells, and evaluating further anti-HIV-1 antibodies against subtype C viruses will provide further information as to which bnAbs/nnAbs or combinations may be suitable for prevention and treatment programmes. A vaccine should elicit both bnAb and ADCC responses, and ideally bnAbs used in passive immunization strategies should target a common neutralization/ADCC epitope, such that it was able to potently neutralize free virions and kill infected cells. Altogether, this study provided important considerations for design of a protective HIV-1 vaccine.

Appendices

Appendix A1. Supplementary figures for chapter two

Table A1.1. Sequence characteristics of seven CAPRISA 002 participants based on results from Poisson-fitter (272)**.**

Participant	Sequence convolution
CAP45	Follows a star-phylogeny
CAP63	Follows a star-phylogeny
CAP88	Follows a star-phylogeny
CAP177	Non-homogenous
CAP210	Follows a star-phylogeny
CAP239	Follows a star-phylogeny
CAP255	Non-homogenous

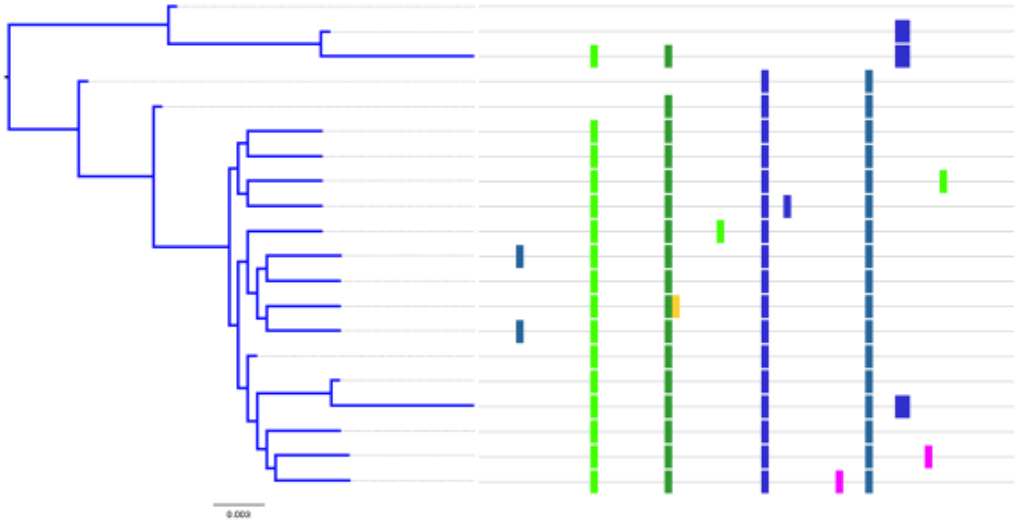

Figure A1.1. Phylogenetic tree and highlighter plot of the C2C3 of CAP255 variants from the enrolment sample. A phylogenetic tree (left) and highlighter plot (right) of the C2C3 region were constructed using the twenty most common haplotypes of CAP255 sequences isolated from the enrolment sample (8 wpi). Two distinct variants were detected: three haplotypes represented the first variant (top three haplotypes) while one haplotype represented the second variant (fourth haplotype). The remainder of the haplotypes detected represented recombination of the two variants.

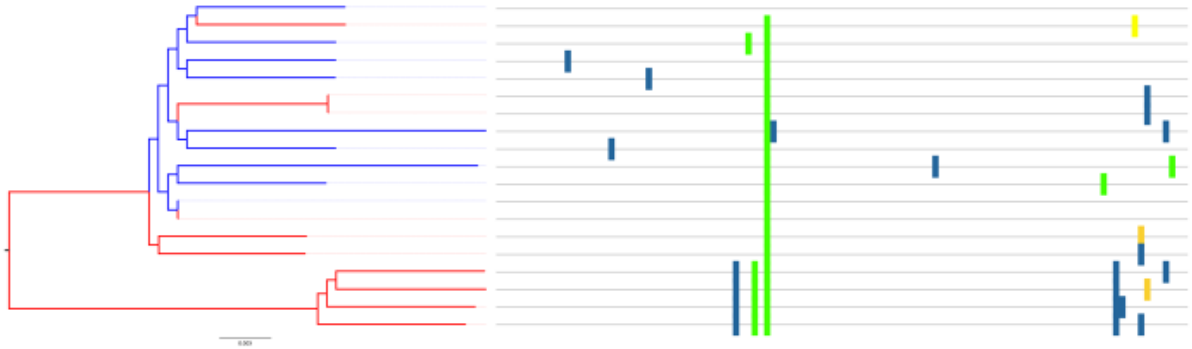

Figure A1.2. Phylogenetic tree and highlighter plot of the C2C3 of CAP177 variants from the enrolment and second samples. A phylogenetic tree (left) of the C2C3 region using the ten most common enrolment haplotypes (blue; 2 wpi) and ten most common haplotypes detected at the second sampling time (red; 4 wpi), and a highlighter plot (right) were constructed using CAP177 sequences isolated. One variant was detected at 2 wpi, but by 4 wpi a second variant (last four haplotypes) was detected.

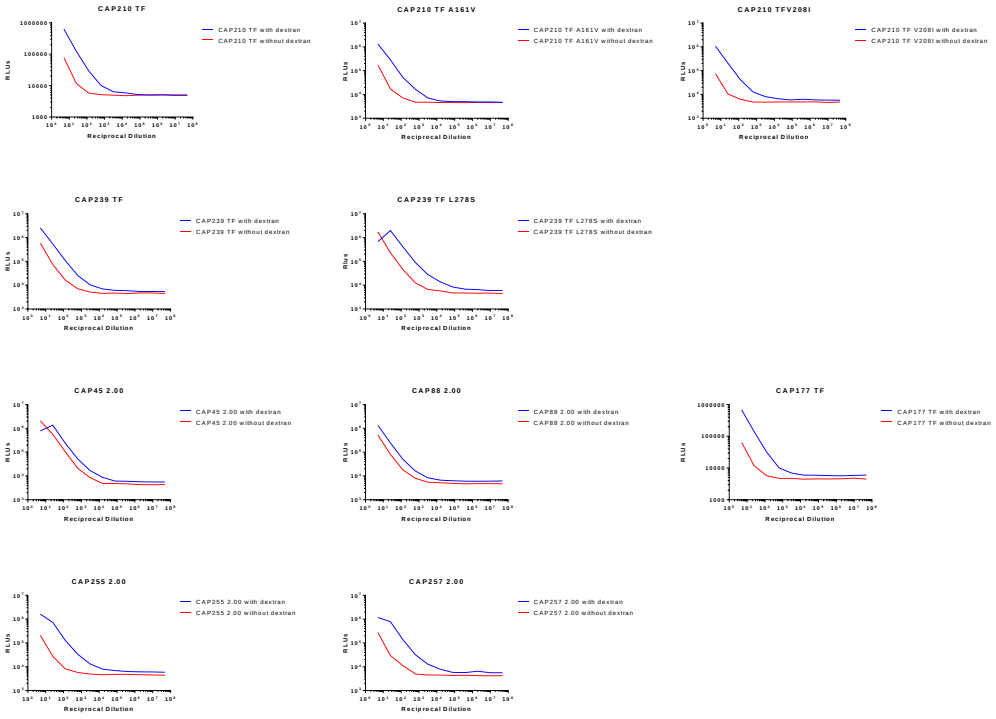

Figure A1.3. DEAE-Dextran dependence of ten cell-free early/acute or mutant viruses. The DEAE-dextran dependence of ten viruses (seven acute/early viruses and three mutant viruses) was determined by titrating the virus on TZM-bl cells in the presence and absence of DEAE-Dextran. Eight viruses were determined to be Dextran dependent, while two (CAP45 2.00 and CAP88 2.00) were Dextran independent.

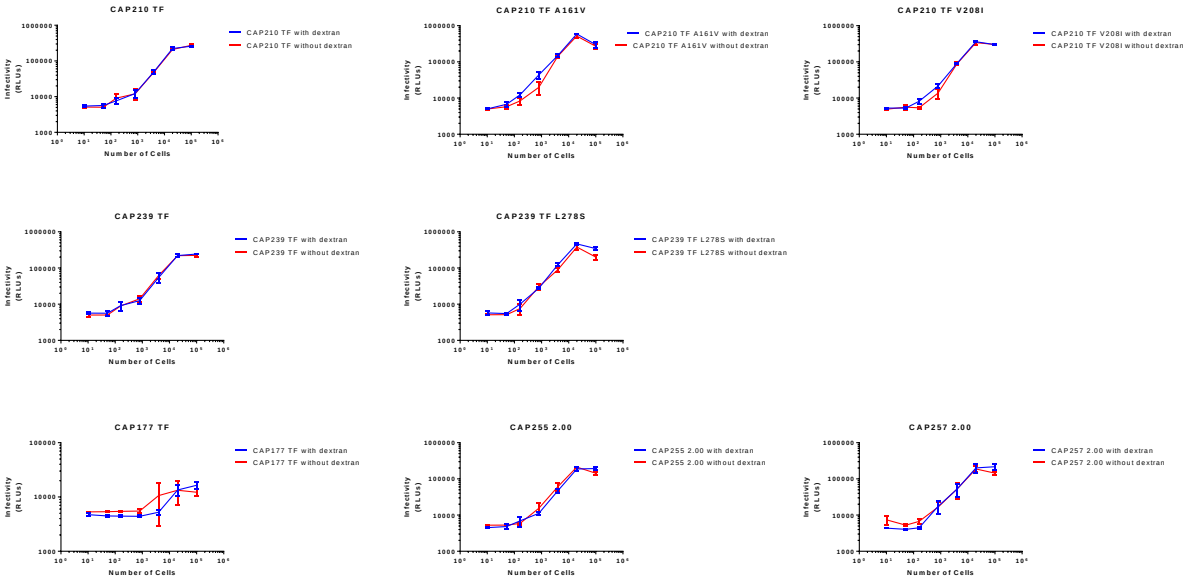

Figure A1.4. Titration of PBMCs infected with eight early/acute or mutant viruses. PMBCs from eight viruses (five acute/early viruses and three mutant viruses) were titrated on TZM-bl cells in the presence and absence of DEAE-Dextran. All eight cell-associated viruses were Dextran independent. However, one virus (CAP177 TF) did not infect PBMCs at levels required for the cell-cell inhibition assay.

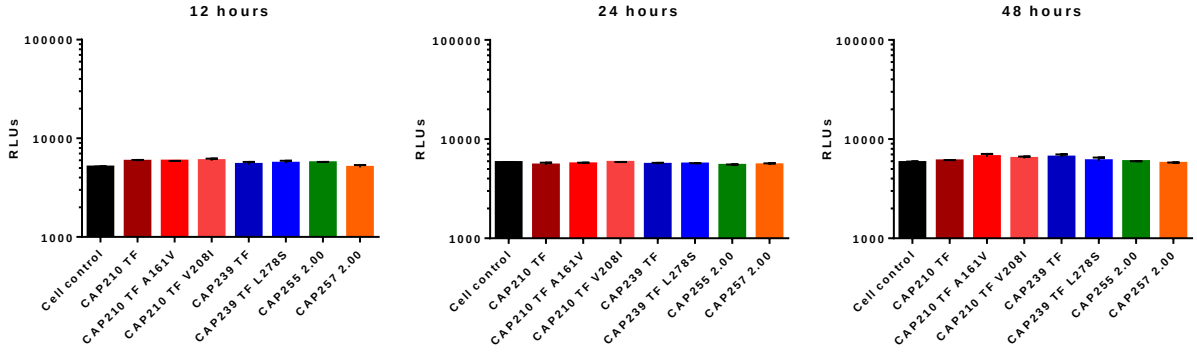

Figure A1.5. Determining the background signal from viruses secreted from infected PBMCs. Supernatant from infected PBMCs was collected at 12 hours, 24 hours and 48 hours and titrated on TZM-bl cells to measure the background signal from cell-free viruses secreted from infected PBMCs. Secreted virus signal did not increase more than 10% over the cell control, indicating this did not account for significant levels of signal.

Appendix A2. List of infectious molecular clones

IMC Identifier	IMC name	WPI *env* sequence was isolated	Amino acid mutations from T/F Env	Constructed by
CAP8 TF	pNL-LucR.T2A-C.CAP8.TF.ecto	3	-	Ochsenbauer lab
CAP45 TF	pNL-LucR.T2A-C.CAP45.TF.ecto	5	-	Ochsenbauer lab
CAP45 TF D462G	pNL-LucR.T2A-C.CAP45.TF.D462G.ecto	-	D462G	Ochsenbauer lab
CAP45 TF 460Δ3	pNL-LucR.T2A-C.CAP45.TF. 460Δ3.ecto	-	460Δ3	Ochsenbauer lab
CAP61 2.00	pNL-LucR.T2A-C.CAP61.2.00.F10(J).ecto	8	-	Ochsenbauer lab
CAP88 2.00	pNL-LucR.T2A-C.CAP88.2.00.17_5A.ecto	5	-	Ochsenbauer lab
CAP177 TF	pNL-LucR.T2A-C.CAP177.TF.ecto	4	-	Ochsenbauer lab
CAP210 TF	pNL-LucR.T2A-C.CAP210.TF.ecto	2	-	Ochsenbauer lab
CAP210 TF A161V	pNL-LucR.T2A-C.CAP210.TF.A161V.ecto	-	A161V	Ochsenbauer lab
CAP210 TF V208I	pNL-LucR.T2A-C.CAP210.TF.V208I.ecto	-	V208I	Ochsenbauer lab
CAP228 2.00	pNL-LucR.T2A-C.CAP228.2.00.18.ecto	7	-	Ochsenbauer lab
CAP239 TF	pNL-LucR.T2A-C.CAP239.TF.ecto	5	-	D Mielke
CAP239 TF K97E	pNL-LucR.T2A-C.CAP239.TF.K97E.ecto	-	K97E	D Mielke
CAP239 TF L278S	pNL-LucR.T2A-C.CAP239.TF.L278S.ecto	-	L278S	D Mielke
CAP239 TF S481N	pNL-LucR.T2A-C.CAP239.TF.S481N.ecto	-	S481N	D Mielke
CAP239 13-5G3	pNL-LucR.T2A-C.CAP239.13-5G3.ecto	13	E462K, S481N, G600E	D Mielke
CAP239 13-9B2	pNL-LucR.T2A-C.CAP239.13-9B2.ecto	13	S481N	D Mielke
CAP239 13-9C6	pNL-LucR.T2A-C.CAP239.13-9C6.ecto	13	K171E, A221T, E340K, S481N	D Mielke
CAP239 19-7B2	pNL-LucR.T2A-C.CAP239.19-7B2.ecto	19	M95L, K117N, L278S, N397S, E462G, S481N	D Mielke
CAP239 19-7C2	pNL-LucR.T2A-C.CAP239.19-7C2.ecto	19	L278S, 462Δ3, S481N	D Mielke
CAP239 19-7E4	pNL-LucR.T2A-C.CAP239.19-7E4.ecto	19	K106E, D211N, W456R, K463.02E	D Mielke
CAP239 19-7F2	pNL-LucR.T2A-C.CAP239.19-7F2.ecto	19	K106E, V208I, W456R, K463.02E, I675N	D Mielke
CAP239 19-7F4	pNL-LucR.T2A-C.CAP239.19-7F4.ecto	19	A236T, S481N, S553N	D Mielke
CAP255 2.00	pNL-LucR.T2A-C.CAP255.2.00.5.ecto	8	-	Ochsenbauer lab
CAP256 2.00	pNL-LucR.T2A-C.CAP256.2.00.C7.ecto	6	-	Ochsenbauer lab
CAP257 2.00	pNL-LucR.T2A-C.CAP257.2.00.Lucifer.ecto	7	-	Ochsenbauer lab

Appendix A3. Obtaining an appropriate source of effector cells for the luciferase-based ADCC assay

1. Introduction

A good source of effector cells is fundamental to a successful ADCC assay. Consequently, to establish the Luciferase-based ADCC assay at the University of Cape Town (UCT), an effective and constant source of appropriate effector cells was needed. The single nucleotide polymorphism (SNP) at position 158 of the $Fc_{\gamma}RIIIa$ has been identified as an important SNP for antibody Fc binding to $Fc_{\gamma}RIIIa$ (reviewed by Mellor *et al.* (323)), the major receptor involved in NK cell-mediated ADCC. While a homogenous phenylalanine (158F/F) binds IgG1 strongly by allowing more flexibility of the $Fc_{\gamma}RIIIa$ receptor binding to the Fc region of antibodies, homogenous valine (158V/V) binds IgG1 weakly (324, 325). Currently, the Luciferase-based ADCC assay used in the Ferrari laboratory, from which this assay was learnt and established at UCT, uses 158F/V heterogenous PBMCs as the source of effector cells (Dr. Guido Ferrari, personal communication).

2. Method

2.1. Ethics statement

This sub-study received ethical approval from the University of Cape Town (914/2015). All participants in this study provided written informed consent for study participation.

2.2. Study participants

Fifteen participants were recruited for this study from within UCT with permission from the Department of Student Affairs and the Department of Human Resources, UCT. Participants were screened for HIV infection status, and 5 mL of blood was drawn to isolate PBMCs and screen PBMCs for genotype and functionality in the ADCC assay.

One participant was chosen as a source of effector cells based on the above screening. 450 mL of blood was drawn once every 4 months, as per NIH guidelines.

2.3. Screening donors for FcγRIIIa 158F/V single nucleotide polymorphism

Genomic DNA was extracted from donor PBMCs (1×10^6) using the Qiaprep DNA miniprep kit (Qiagen) as per manufacturer's recommendations. PCR clean water was added to 5 ng of genomic

DNA and 1.25 µL of 20x Taqman genotyping probe mix (Assay ID C__25815666_10, SNP ID rs396991, Thermofisher Scientific) which contained VIC dye linked to the 5' end of the Allele 1 probe and 6FAM dye linked to the 5' end of the Allele 2 probe, to a volume of 12.5 µL as per manufacturer's recommendations. This was added to 12.5 µL of 2x Taqman Genotyping Master Mix (Thermofisher) to a total volume of 25 µL per reaction. A non-template control (NTC), as well as 158F/F, 158V/V and 158F/V template controls (kindly provided by Dr Ria Lassauniere, NICD, Johannesburg), were used as controls for allele detection. The PCR conditions were used as per manufacturer's recommendations using a CFX96 Real-Time PCR Detection System (Biorad) and allelic discrimination analysis was carried out using CFX Manager Software (v3.1).

2.4. Screening donor PBMCs for ADCC activity

$CEM.NKR_{CCR5}$ cells were infected with CAP239 TF as described in Chapter 3.2.9. The luciferase-based ADCC assay was then performed as described in Chapter 3.2.11, using the A32 mAb and purified IgG from HIV-1 infected individuals (HIVIG) as sources of antibodies and PBMCs isolated from each donor as a source of effector cells.

2.5. Storage of PBMCs

Isolated PBMCs were stored in liquid nitrogen at 20 x 10^6 cells/mL in RPMI supplemented with 20% FCS (Biochrom) and 10% DMSO (Sigma).

3. Results

3.1. Three donors had the 158F/V genotype

Thirteen donors were recruited as potential donors of effector cells. 5 mL of blood was drawn from each participant and PBMCs were isolated from the blood. In 6 of the 13 participants, an insufficient number of PBMCs was isolated for genotype and ADCC analysis. Consequently, PBMCs from the remaining 7 participants were used for further analysis. Genomic DNA from these participants was extracted from the PBMCs and genotyped for the 158F/V polymorphism. Of the seven participants, three donors (donor 5, donor 7 and donor 13) had the 158F/V polymorphism (green) (Figure A3.1).

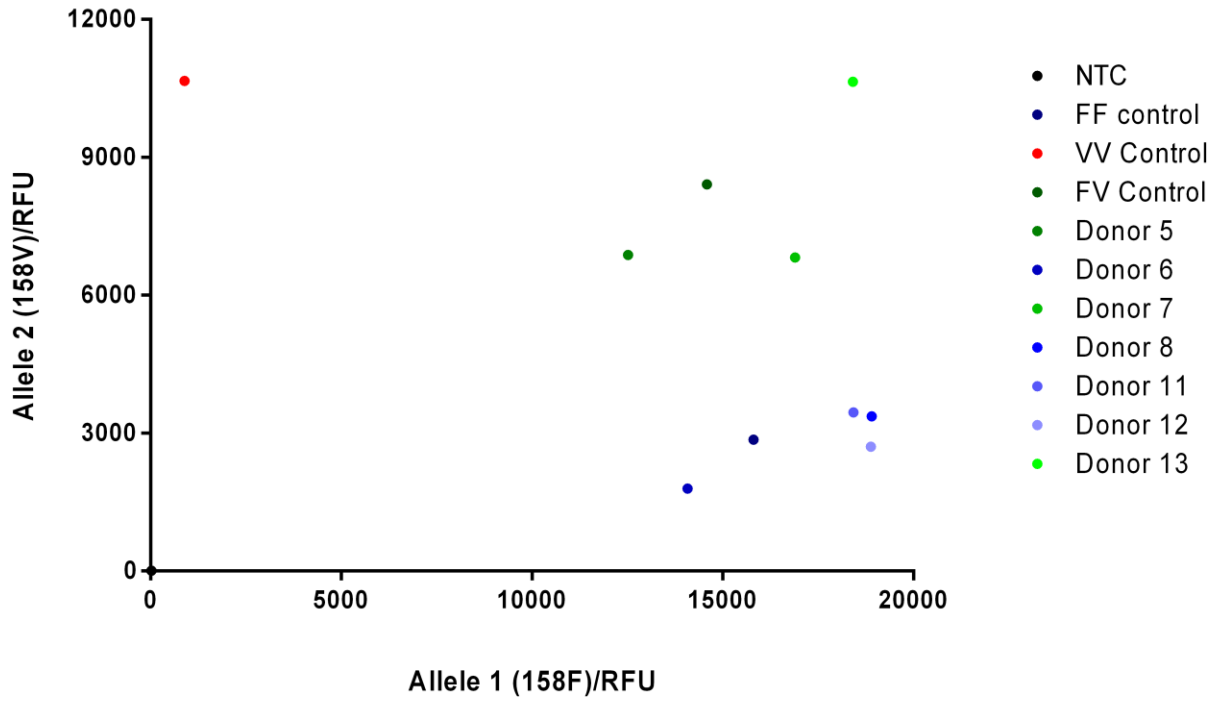

Figure A3.1. Scatter plot indicating the genotype of seven PBMC donors and four controls. The relative fluorescent units (RFU) for each probe binding to donor genomic DNA was determined. A NTC and controls for each of the genotypes (158FF, 158VV and 158FV) were used to determine the genotype of each participant.

3.2. Donor 7 had the highest ADCC activity using A32 and HIVIG against CAP239 TF-infected cells

Having determined the genotype of the seven donors, we used PBMCs from each donor as a source of effector cells in ADCC assays, with the mAb A32 and HIVIG as a source of antibodies and CAP239 TF-infected cells as a source of target cells. Of the seven donors, donor 7 had the highest ADCC activity (Figure A3.2). As donor 7 had the correct genotype as well (158F/V), PBMCs from this donor were isolated and used in all subsequent ADCC assays.

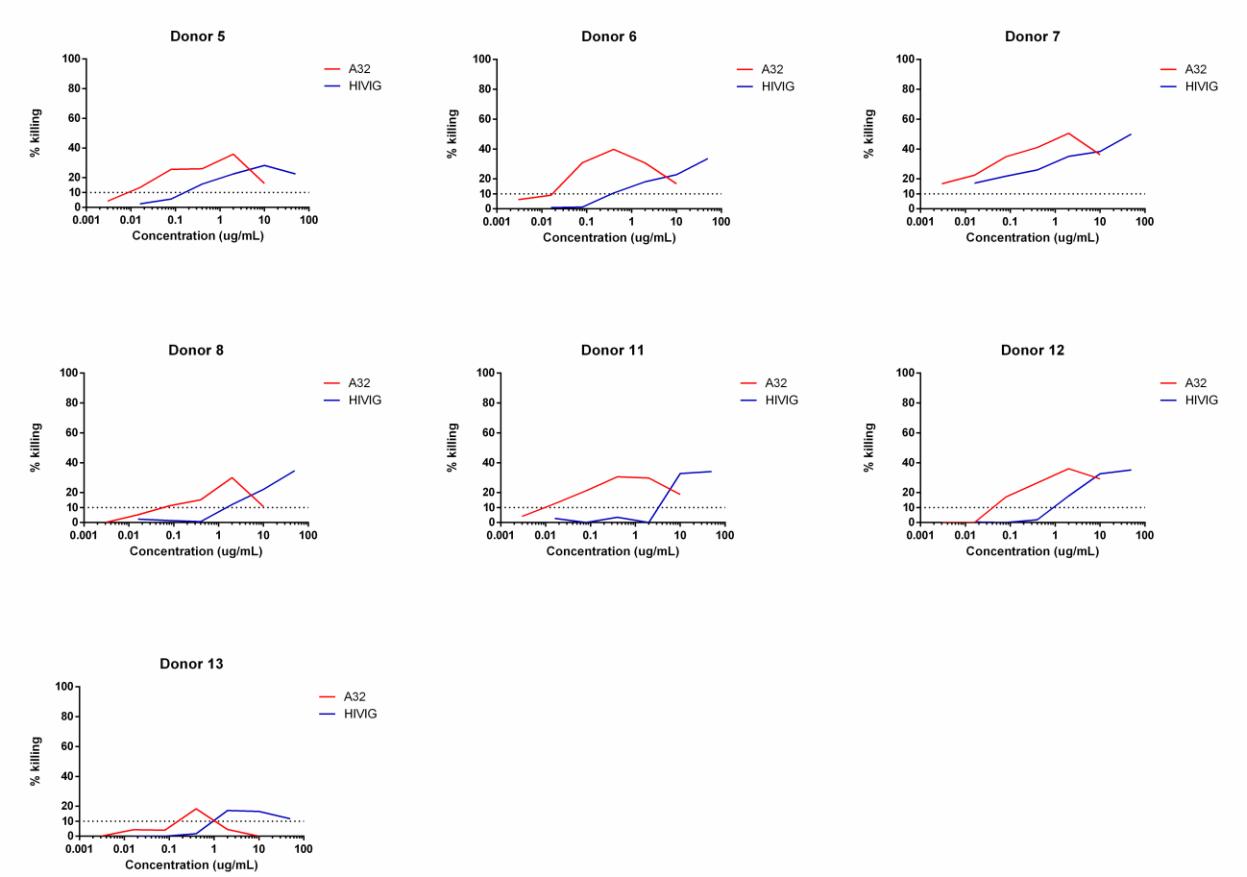

Figure A3.2. ADCC activity against CAP239 TF using A32 and HIVIG and PBMCs from seven donors as a source of effector cells. The % specific killing of target cells using donor PBMCs as effector cells is shown over serial dilutions of A32 (red) and HIVIG (blue).

Appendix A4. List of primers used

Table A4.1. Deep sequencing primers

Primer name	Primer description	Direction	Hxb2 position	Sequence (5'-3')
cDNA_C2	cDNA primer		6907-6883	GCCTTGCCACACGCTCAGNNNNNNNNNN ATTCCATGTGTACATTGTACTGTRCTGAC
cDNA_C3	cDNA primer		7343-7318	GCCTTGCCACACGCTCAGNNNNNNNNNN GTTGTAAYTTCTAGRTCCCCTCCTG
cDNA_C5	cDNA primer		7655-7632	GCCTTGCCACACGCTCAGGCNNNNNNNNN GTCCYTCATATYTCCTCCTYCAGG
C1C2_fwd	First round forward	Forward	6654-6674	TCGTCGGCAGCGTCAGATGTGTATAAGAGA CAGNNNNTATGGGATSAAAGYCTMAARCCATGTG
C2C3_fwd	First round forward	Forward	6950-6973	TCGTCGGCAGCGTCAGATGTGTATAAGAGAC AGNNNNAATGTCAGYACAGTACAATGTAC ACATGG
C3C5_fwd	First round forward	Forward	7144-7135	TCGTCGGCAGCGTCAGATGTGTATAAGAGA CAGCRAGACCCRAYAATAATACAAG
Universal_ rev	First round reverse	Reverse		GTCTCGTGGGCTCGGAGATGTGTATAAGA GACAGNNNNGCCTTGCCACACGCTCAG

Table A4.2. Cloning primers

Primer name	Primer description	Direction	Hxb2 position	Sequence (5'-3')
EnvA-1RX	Cloning primer	Forward	5957-5982	CCACGGCTTAGGCATTTCCTATGGCAGGAAGAA
EnvN	Cloning primer	Reverse	83-60	TTGCCAATCAAGGAAGTAGCCTTGTGT

Table A4.3. Single genome amplification primers

Primer name	Primer description	Direction	Hxb2 position	Sequence (5'-3')
OFM19	Envelope nested PCR outer primers	Forward	4903-4923	GCACTCAAGGCAAGCTTTATTGAGGCTTA
VIF1		Reverse	544-519	GGGTTTATTACAGGGACAGCAGAG
EnvA	Envelope nested PCR inner primers	Forward	5957-5982	GGCTTAGGCATTTCCTATGGCAGGAAGAA
EnvN		Reverse	83-60	TTGCCAATCAAGGAAGTAGCCTTGTGT

Table A4.4. HIV-1 subtype C *envelope* sequencing primers

Primer name	Hxb2 position	Sequence (5'-3')
EF00	6201-6228	GGGAAAGAGCAGAAGACAGTGGCAATGA
FOR14	6556-6582	TATGGGACCAAAGCCTAAAGCCATGTG
FOR16	7350-7375	TTTAATTGTGGAGGAGAATTTTTCTA
EF170	7799-7816	AGCAGGAAGCACTATGGG
EF200	8092-8118	GGGATAACATGACCTGGATGCAGTGGG
EF260	8520-8544	TTCAGCTACCACCGATTGAGAGACT
EF175	6401-6378	TTTAGCATCTGATGCACAGAATAG
REV15	7015-6990	CTGCCATTTAACAGCAGTTGAGTTGA
EF115	7374-7397	AGAAAAATTCTCCTCTACAATTAA
EF55	7940-7914	GCCCCAGACCGTGAGTTGCAACATATG
EF15	8445-8466	TGCTCTCCACCTTCTTCTTC
REV19	8820-8797	ACTTTTTGACCACTTGCCACCCAT

Table A4.5. Mutagenesis primers

Primer name	Sequence (5'-3')
CAP45_460Δ3_f	CTCAAGTATCACAGGACTCCTATTGACACGTGATGGAGGGAGGAATGACACAGAG
CAP45_460Δ3_r	CCTCCTCCAGGTCTGAATATCTCTGTGTCATTCCTCCCTCCATCACGTGTCAATAGGAG
CAP45_D462G_f	GGAGGGAAAACAGGCAGGAATGACACAGAGATATTCAG
CAP45_D462G_r	CTGAATATCTCTGTGTCATTCCTGCCTGTTTTCCCTCC
CAP210_A161V_f	GATACTATGAAAATTTGTTCTTTCAATGTAACCACAGAACTAAGAGATAAG
CAP210_A161V_r	CTTATCTCTTAGTTCTGTGGTTACATTGAAAGAACAAATTTTCATAGTATC
CAP210_V208I_f	GCACAAGCCTGTCCAAAGATCTCTTTTGACCCAATTCC
CAP210_V208I_r	GGAATTGGGTCAAAAGAGATCTTTGGACAGGCTTGTGC
CAP239_K97E_f	GGGAAATGTAACAGAGAAATTTAACATGTGGGAAAATGACATGGTGG
CAP239_K97E_r	CCACCATGTCATTTTCCCACATGTTAAATTTCTCTFTTACATTTCCC
CAP239_K106E_f	GACATGGTGGACCAGATGCATGAAGATATAATCAGTTTATGGG
CAP239_K106E_r	CCCATAAACTGATTATATCTTCATGCATCTGGTCCACCATGTC
CAP239_L78S_f	GATCTCAAAATATATCAGACAATACCAAAACAATAATAGTACATCTCAAGG
CAP239_L278S_r	CCTTGAGATGTACTATTATTGTTTTGGTATTGTCTGATATATTTTGAGATC
CAP239_E463K_f	GACATGGGATGGTGGAGACAGTAAGAAGAATAAGACAAGGCATAATGAGAC
CAP239_E463K_r	GTCTCATTATGCCTTGTCTTATTCTTCTTACTGTCTCCACCATCCCATGTC
CAP239_S481N_f	GGAGATATGAGAGATAATTGGAGAAATGAATTATATAAATATAAAGTGG
CAP239_S481N_r	CCACTTTATATTTATATAATTCATTTCTCCAATTATCTCTCATATCACC

Appendix A5. List of monoclonal antibodies used

mAb name	Target	Neutralizing/Non-neutralizing	Reference (for ADCC activity)
VRC01	CD4-binding site	Neutralizing	(229, 306)
3BNC117	CD4-binding site		(306, 309)
2G12	C2,C3,C4,V4 glycans		(229, 236)
PG9	V2		(326)
697D	V2		(231)
PGT151	Gp120-gp41 interface		(327)
10E8	MPER		(306)
C11	CD4i cluster A (C1 region)	Non-neutralizing	(235)
A32	CD4i cluster A (C1)		(229)
HG107	V2		(231)
CH58	V2		(231)

Appendix A6. Infection analysis

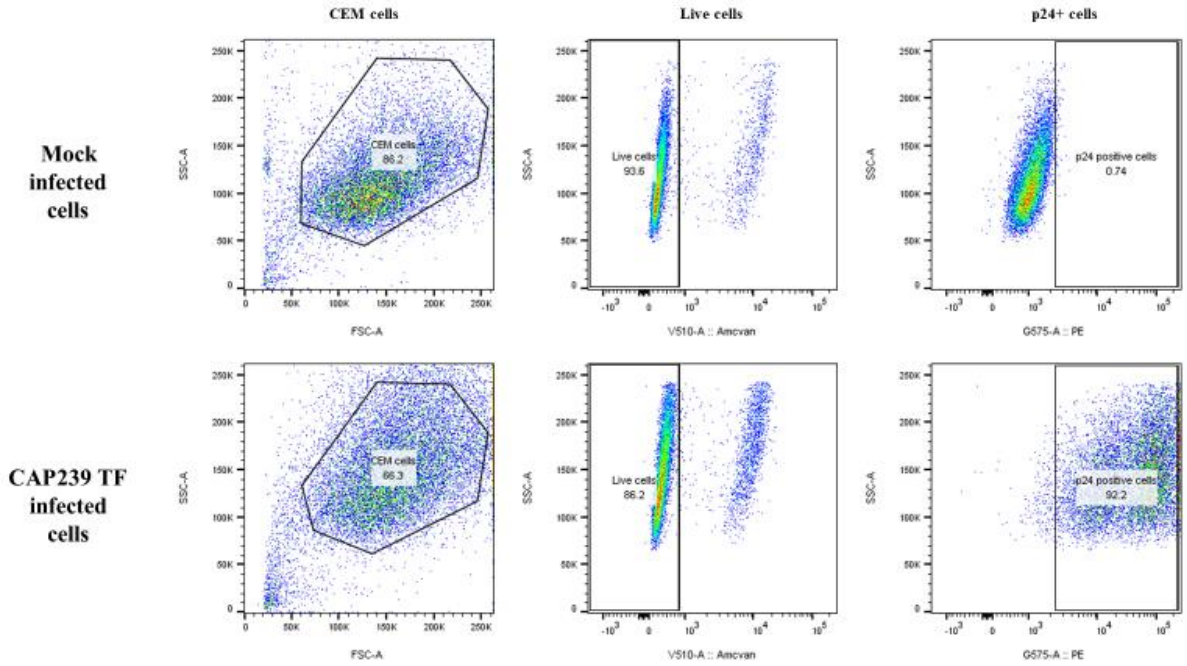

Figure A6.1. Example of p24 staining analysis using mock- and CAP239 TF-infected cells. Mock (top) and CAP239 TF-infected cells (bottom) were stained with live/dead aqua (middle). Live cells were gated for and % p24 staining was measured in viable cells (right).

Table A6.1. Relative light units of target cells and p24 staining of viruses used in this study.

Virus name	Average RLUs of 5000 target cells	Average % p24 cells
CAP8 TF	541345	72.3
CAP45 TF	44936	88.3
CAP45 TF D462G	65457	35.4
CAP45 TF 460Δ3*	8494	3.79
CAP61 2.00	27949	15.9
CAP88 2.00	116711	42.6
CAP177 TF*	4732	2.19
CAP210 TF	124261	38.2
CAP210 TF A161V	43826	30.4
CAP210 TF V208I	21613	12.4
CAP228 2.00	1099962	26.4
CAP239 TF	125016	93.2
CAP239 TF K97E	171866	35.4
CAP239 TF L278S	268758	39.3
CAP239 TF S481N	85293	29.9
CAP239 13-5G3	91438	22.8
CAP239 13-9B2	134942	37.1
CAP239 13-9C6	294575	44.2
CAP239 19-7B2	797150	75.7
CAP239 19-7C2	1520528	87.3
CAP239 19-7E4	399972	56.6
CAP239 19-7F2	447028	68.5
CAP239 19-7F4	861928	79.2
CAP255 2.00	78297	16.2
CAP256 2.00*	9223	8.41
CAP257 2.00	98344	15.3

*Env-IMCs did not infect CEM.NKR$_{CCR5}$ cells at levels high enough to use for ADCC assays.

Appendix A7. Standard buffers and solutions

A7.1. Luria Broth (LB)

10 g Tryptone, 5 g yeast extract, 10 g NaCl

Dissolved in 1 L distilled H_2O and sterilized by autoclaving.

A7.2. Luria Agar (LA)

10 g Tryptone, 5 g yeast extract, 10 g NaCl, 15 g Bacto agar

Dissolved in 1 L distilled H_2O and sterilized by autoclaving.

A7.3. Tris-Acetate-EDTA (TAE, 50X)

242 Tris base (Sigma) dissolved in 500 mL distilled H_2O, 57.1 mL glacial acetic added, 100 mL 0.5 M EDTA (pH 8.0) solution

Adjust volume to 1 L with distilled H_2O and sterilize by autoclaving.

A7.4. Carbenicillin

1 g Carbenicillin powder (Sigma) in 10 mL distilled H_2O.

Filter sterilized using a 0.22 µL filter.

Aliquoted into 500 µL aliquots and stored at room temperature.

A7.5. 1% agarose gel

100g SeaKem Agarose powder (Lonza) dissolved 1L 1x TAE

A7.6. pcDNA™3.1/V5-His-TOPO®

10 ng/µl plasmid DNA in: 50% glycerol, 50 mM Tris-HCl, pH 7.4 (at 25 °C),

1 mM EDTA, 2 mM DTT, 0.1% TritonR X-100, 100 µg/mL BSA,

30 µM phenol red

A7.7. Growth media

Complete growth media for adherent human tissue cell lines consisted of High glucose DMEM with L-glutamine and 25 mM HEPES (Lonza) supplemented with 10 % FCS (Biochrom) and 100 µg/mL Gentamicin (Lonza).

A7.8. R10 media

R10 growth media for suspension human tissue cell likes consisted of RPMI 1640 medium (Lonza) supplemented with 10% FCS (Biochrom) and 100 µg/mL Gentamicin (Lonza).

Appendix A8. Standard molecular biology techniques

A8.1. Plasmid Transformation

Top10 chemically competent cells were incubated on ice with 50 ng plasmid for 30 min to allow for equal distribution of DNA. The cells were heat shocked in a water bath for 30 s at 42 ºC to increase membrane permeability, and then incubated on ice for 2 min. 250 µL Luria Broth (LB) (Appendix A4) was added to the cells, which were then incubated for 60 min at 32 ºC to allow for expression of the ampicillin resistance gene of the vector. Subsequently, the cells were centrifuged at 7000 rpm for 3 min in a microcentrifuge, 150 µL media was removed and the cells were resuspended in the remaining 100 µL media. The resuspended cells were plated on Luria Agar (LA) (Appendix A7.2) containing 100 mg/mL Carbenicillin (an ampicillin analogue) (Sigma) (Appendix A7.4) and incubated at 37 ºC overnight.

A8.2. Viral RNA extraction

200 µL plasma was added to 800 µL prepared buffer AVL containing carrier RNA and mixed by pulse-vortexing for 15 s. The resulting solution was incubated at room temperature for 10 minutes to allow for complete viral particle lysis. 800 µL of 100% ethanol was added and mixed to the sample by pulse-vortexing for 15 s.

630 µL of the solution was applied to a QIAamp Mini column (Qiagen) and centrifuged at 8000 rpm for 1 min in a microcentrifuge. The column was placed in a clean 2 mL collection tube and the process was repeated until all the solution was applied to the column.

500 µL buffer AW1 was applied to the and the column was centrifuged at 8000 rpm for 1 min in a microcentrifuge. The filtrate was discarded and 500 µL buffer AW2 was applied to the column. The column was then centrifuged at 14000 rpm for 3 min in a microcentrifuge. The column was then placed in a clean 1.5 mL microcentrifuge tube. 50 µL buffer AVE was added to the column and allowed to incubate at room temperature for 1 min. The column was then centrifuged at 8000 rpm for 1 min in a microcentrifuge. The filtrate was collected and stored at -20 ºC till further required.

A8.3. Agarose gel electrophoresis

DNA fragments were visualised in 1-2% agarose gels. Agarose gel electrophoresis was performed using horizontal gel apparatus (Stratagene). The agarose gel was prepared by melting the appropriate weight per volume agarose (SeaKem Agarose, Lonza) poured into gel setting trays and allowed to cool to room temperature to set. Set gels were placed in a gel apparatus submerged in 1x TAE. Before loading, 3-5 µL PCR product mixed with 1 µL of 6x agarose gel electrophoresis loading dye. To determine the size of amplicons a DNA molecular weight marker, 1 kB plus O'GeneRuler (Thermofisher Scientific) was included in the first and last lanes of all gels. The gel was electrophoresed at 100 to 120 V according to gel size for 60 minutes or until sufficient separation of bands. The DNA fragments were visualized on a UVP transilluminator (UVP) at 256 nm wavelength and photographed with Kodak ds 1D Electrophoresis Documentation and Analysis System 120 V2.0.3 computerized gel imager.

A8.4. Gel Extraction

The gel was visualized under UV using a UviPro gel visualizer (Uvitec). DNA of the expected size was excised from the gel quickly using scalpel and transferred into a previously weighed 1.5 mL microcentrifuge tube. The gel and microcentrifuge tube were then weighed again to determine the mass of the gel excised. A Zymoclean Gel DNA Recovery Kit (Zymo Research) was then used as instructed by manufacturers. Briefly, 3 volumes of Agarose Dissolving Buffer (ADB) was added foe each volume of agarose excised from the gel (e.g. 300 µL of ADB for every 100 mg of agarose gel) and incubated at 50 °C for 15 min until the agarose had completely dissolved. The melted agarose solution was then transferred to a Zymo-Spin column in a collection tube and centrifuged for 60 s at 13200 rpm in a microcentrifuge. 200 µL DNA wash buffer was added to the column and centrifuged for 30 s at 13200 rpm in a microcentrifuge. This step was repeated. 10 µL PCR-grade water (Sigma) was added directly to the column matrix and this was centrifuged for 60 s at 13200 rpm in a microcentrifuge. The concentration, A_{260}/A_{280} and A_{260}/A_{230} of the excised DNA was then measured using a NanoDrop spectrophotometer (ThermoScientific).

Bibliography

1. **World Health Organization**. 2016. Global Aids Update.

2. **Cohen MS**, **Chen YQ**, **McCauley M**, **Gamble T**, **Hosseinipour MC**, **Kumarasamy N**, **Hakim JG**, **Kumwenda J**, **Grinsztejn B**, **Pilotto JHS**, **Godbole SV**, **Mehendale S**, **Chariyalertsak S**, **Santos BR**, **Mayer KH**, **Hoffman IF**, **Eshleman SH**, **Piwowar-Manning E**, **Wang L**, **Makhema J**, **Mills LA**, **de Bruyn G**, **Sanne I**, **Eron J**, **Gallant J**, **Havlir D**, **Swindells S**, **Ribaudo H**, **Elharrar V**, **Burns D**, **Taha TE**, **Nielsen-Saines K**, **Celentano D**, **Essex M**, **Fleming TR**. 2011. Prevention of HIV-1 Infection with Early Antiretroviral Therapy. N Engl J Med **365**:493–505.

3. **Fauci AS**, **Marston HD**. 2014. Ending AIDS - Is an HIV Vaccine Necessary? N Engl J Med **370**:495–498.

4. **Schouten J**, **Wit FW**, **Stolte IG**, **Kootstra NA**, **van der Valk M**, **Geerlings SE**, **Prins M**, **Reiss P**, **Wit FWNM**, **van der Valk M**, **Stolte IG**, **Martens M**, **Moll S**, **Berkel J**, **Moller L**, **Visser GR**, **Welling C**, **Zaheri S**, **Hillebregt MMJ**, **Gras LAJ**, **Ruijs YMC**, **Benschop DP**, **Reiss P**, **Kootstra NA**, **Harskamp-Holwerda AM**, **Maurer I**, **Mangas Ruiz MM**, **Girigorie AF**, **van Leeuwen E**, **Janssen FR**, **Heidenrijk M**, **Schrijver JHN**, **Zikkenheiner W**, **Wezel M**, **Jansen-Kok CSM**, **Geerlings SE**, **Godfried MH**, **Goorhuis A**, **van der Meer JTM**, **Nellen FJB**, **van der Poll T**, **Wiersinga WJ**, **Wit FWNM**, **van Eden J**, **Henderiks A**, **van Hes AMH**, **Mutschelknauss M**, **Nobel HE**, **Pijnappel FJJ**, **Westerman AM**, **de Jong J**, **Postema PG**, **Bisschop PHLT**, **Serlie MJM**, **Lips P**, **Dekker E**, **de Rooij SEJA**, **Willemsen JMR**, **Vogt L**, **Schouten J**, **Portegies P**, **Schmand BA**, **Geurtsen GJ**, **ter Stege JA**, **Klein Twennaar M**, **van Eck-Smit BLF**, **de Jong M**, **Richel DJ**, **Verbraak FD**, **Demirkaya N**, **Visser I**, **Ruhe HG**, **Nieuwkerk PT**, **van Steenwijk RP**, **Dijkers E**, **Majoie CBLM**, **Caan MWA**, **Su T**, **van Lunsen HW**, **Nievaard MAF**, **van den Born BJH**, **Stroes ESG**, **Mulder WMC**. 2014. Cross-sectional Comparison of the Prevalence of Age-Associated Comorbidities and Their Risk Factors Between HIV-Infected and Uninfected Individuals: The AGEhIV Cohort Study. Clin Infect Dis **59**:1787–1797.

5. **Friis-Møller N**, **Weber R**, **Reiss P**, **Thiébaut R**, **Kirk O**, **d'Arminio Monforte A**, **Pradier C**, **Morfeldt L**, **Mateu S**, **Law M**, **El-Sadr W**, **De Wit S**, **Sabin CA**, **Phillips AN**, **Lundgren JD**, **DAD study group**. 2003. Cardiovascular disease risk factors in HIV patients--association with antiretroviral therapy. Results from the DAD study. AIDS **17**:1179–93.

6. **Statistics South Africa**. 2015. Mid-year Population estimates: 2015 Statistical release P0302.

7. **Andre FE**, **Booy R**, **Bock HL**, **Clemens J**, **Datta SK**. 2014. Vaccination greatly reduces disease , disability , death and inequity worldwide. Bull World Health Organ.

8. **Haynes BF**, **Gilbert PB**, **McElrath MJ**, **Zolla-Pazner S**, **Tomaras GD**, **Alam SM**, **Evans DT**, **Montefiori DC**, **Karnasuta C**, **Sutthent R**, **Liao H-X**, **DeVico AL**, **Lewis GK**, **Williams Co**, **Pinter A**, **Fong Y**, **Janes H**, **DeCamp A**, **Huang Y**, **Rao M**, **Billings E**, **Karasavvas N**, **Robb ML**, **Ngauy V**, **de Souza MS**, **Paris R**, **Ferrari G**, **Bailer RT**, **Soderberg KA**, **Andrews C**, **Berman PW**, **Frahm N**, **De Rosa SC**, **Alpert MD**, **Yates NL**, **Shen X**, **Koup RA**, **Pitisuttithum P**, **Kaewkungwal J**, **Nitayaphan S**, **Rerks-Ngarm S**, **Michael NL**, **Kim JH**. 2012. Immune-Correlates Analysis of an HIV-1 Vaccine Efficacy Trial. N Engl J Med **14**:1275-1286.

9. **Haynes BF**, **McElrath MJ**. 2013. Progress in HIV-1 vaccine development. Curr Opin HIV AIDS **8**:326–32.

10. **Kim JH**, **Excler J-L**, **Michael NL**. 2014. Lessons from the RV144 Thai Phase III HIV-1 Vaccine Trial and the Search for Correlates of Protection. Annu Rev Med **66**:1–15.

11. **Sliva K**. 2014. Latest animal models for anti-HIV drug discovery. Expert Opin Drug Discov **10**:1–13.

12. **Burton DR**, **Mascola JR**. 2015. Antibody responses to envelope glycoproteins in HIV-1 infection. Nat Immunol **16**:571–576.

13. **Plotkin SA**. 2010. Correlates of protection induced by vaccination. Clin Vaccine Immunol **17**:1055-1065.

14. **Hemelaar J**, **Gouws E**, **Ghys PD**, **Osmanov S**. 2011. Global trends in molecular epidemiology of HIV-1 during 2000– 2007. AIDS **25**:679–689.

15. **Korber B**, **Gaschen B**, **Yusim K**, **Thakallapally R**, **Kesmir C**, **Detours V**. 2001. Evolutionary and immunological implications of contemporary HIV-1 variation. Br Med Bull **58**:19-42.

16. **Hirsch VM**, **Olmsted RA**, **Murphey-Corb M**, **Purcell RH**, **Johnson PR**. 1989. An African primate lentivirus (SIVsm) closely related to HIV-2. Nature **339**:389–92.

17. **Gao F**, **Yue L**, **White AT**, **Pappas PG**, **Barchue J**, **Hanson AP**, **Greene BM**, **Sharp PM**, **Shaw GM**, **Hahn BH**. 1992. Human infection by genetically diverse SIVSM-related HIV-2 in west Africa. Nature **358**:495–9.

18. **Gao F**, **Bailes E**, **Robertson DL**, **Chen Y**, **Rodenburg CM**, **Michael SF**, **Cummins LB**, **Arthur LO**, **Peeters M**, **Shaw GM**, **Sharp PM**, **Hahn BH**. 1999. Origin of HIV-1 in the chimpanzee Pan troglodytes troglodytes. Nature **397**:436–441.

19. **D'arc M**, **Ayouba A**, **Esteban A**, **Learn GH**, **Boué V**, **Liegeois F**, **Etienne L**, **Tagg N**, **Leendertz FH**, **Boesch C**, **Madinda NF**, **Robbins MM**, **Gray M**, **Cournil A**, **Ooms M**, **Letko M**, **Simon VA**, **Sharp PM**, **Hahn BH**, **Delaporte E**, **Mpoudi Ngole E**, **Peeters M**. 2015. Origin of the HIV-1 group O epidemic in western lowland gorillas. Proc Natl Acad Sci **112**:E1343-52.

20. **Clavel F**, **Guetard D**, **Brun-Vezinet F**, **Chamaret S**, **Rey M**, **Santos-Ferreira M**, **Laurent A**, **Dauguet C**, **Katlama C**, **Rouzioux C**, **Al. E**. 1986. Isolation of a new human retrovirus from West African patients with AIDS. Science **233**:343–346.

21. **Ariyoshi K**, **Schim van der Loeff M**, **Berry N**, **Jaffar S**, **Whittle H**. 1999. Plasma HIV viral load in relation to season and to Plasmodium falciparum parasitaemia. AIDS **13**:1145–6.

22. **Ariyoshi K**, **Jaffar S**, **Alabi AS**, **Berry N**, **Schim van der Loeff M**, **Sabally S**, **N'Gom PT**, **Corrah T**, **Tedder R**, **Whittle H**. 2000. Plasma RNA viral load predicts the rate of CD4 T cell decline and death in HIV-2-infected patients in West Africa. AIDS **14**:339–344.

23. **Wilkins A**, **Ricard D**, **Todd J**, **Whittle H**, **Dias F**, **Paulo Da Silva A**. 1993. The epidemiology of HIV infection in a rural area of Guinea-Bissau. AIDS **7**:1119–22.

24. **Burke DS**. 1997. Recombination in HIV: An Important Viral Evolutionary Strategy. Emerg Infect Dis **3**:253–259.

25. **Robertson DL**, **Anderson JP**, **Bradac JA**, **Carr JK**, **Foley B**, **Funkhouser RK**, **Gao F**, **Hahn BH**, **Kalish ML**, **Kuiken C**, **Learn GH**, **Leitner T**, **McCutchan F**, **Osmanov S**, **Peeters M**, **Pieniazek D**, **Salminen M**, **Sharp PM**, **Wolinsky S**, **Korber B**. 2000. HIV-1 nomenclature proposal. Science **288**:55–6.

26. **Sharp PM**, **Hahn BH**. 2011. Origins of HIV and the AIDS epidemic. Cold Spring Harb Perspect Med **1**:a006841.

27. **Vallari A**, **Holzmayer V**, **Harris B**, **Yamaguchi J**, **Ngansop C**, **Makamche F**, **Mbanya D**, **Kaptué L**, **Ndembi N**, **Gürtler L**, **Devare S**, **Brennan CA**. 2011. Confirmation of putative HIV-1 group P in Cameroon. J Virol **85**:1403–7.

28. **Sharp PM**. 2002. Origins of human virus diversity. Cell **108**:305–312.

29. **Hemelaar J**. 2012. The origin and diversity of the HIV-1 pandemic. Trends Mol Med **18**:182–192.

30. **Mushahwar IK**. 2006. Human Immunodeficiency Viruses: Molecular Virology, Pathogenesis, Diagnosis and Treatment. Perspect Med Virol **13**:75–87.

31. **Sundquist WI**, **Krausslich H-G**. 2012. HIV-1 Assembly, Budding, and Maturation. Cold Spring Harb Perspect Med **2**:a006924–a006924.

32. **Preston BD**, **Poiesz BJ**, **Loeb LA**. 1988. Fidelity of HIV-1 reverse transcriptase. Science **242**:1168–71.

33. **Holmes M**, **Zhang F**, **Bieniasz PD**. 2015. Single-Cell and Single-Cycle Analysis of HIV-1 Replication. PLOS Pathog **11**:e1004961.

34. **Perelson AS**, **Neumann AU**, **Markowitz M**, **Leonard JM**, **Ho DD**. 1996. HIV-1 dynamics in vivo: virion clearance rate, infected cell life-span, and viral generation time. Science **271**:1582–6.

35. **Holmes EC**, **Zhang LQ**, **Simmonds P**, **Ludlam CA**, **Brown AJ**. 1992. Convergent and divergent sequence evolution in the surface envelope glycoprotein of human immunodeficiency virus type 1 within a single infected patient. Proc Natl Acad Sci **89**:4835–9.

36. **Lemey P**, **Rambaut A**, **Pybus OG**. HIV evolutionary dynamics within and among hosts.

AIDS Rev **8**:125–40.

37. **Splettstoesser T**. 2014. HIV-1 Structure and Genome.

38. **Wyatt R**, **Sodroski J**. 1998. The HIV-1 envelope glycoproteins: fusogens, antigens, and immunogens. Science **280**:1884–1888.

39. **Willey RL**, **Rutledge RA**, **Dias S**, **Folks T**, **Theodore T**, **Buckler CE**, **Martin MA**. 1986. Identification of conserved and divergent domains within the envelope gene of the acquired immunodeficiency syndrome retrovirus. Proc Natl Acad Sci **83**:5038–5042.

40. **Starcich BR**, **Hahn BH**, **Shaw GM**, **McNeely PD**, **Modrow S**, **Wolf H**, **Parks ES**, **Parks WP**, **Josephs SF**, **Gallo RC**, **Wong-Staal F**. 1986. Identification and characterization of conserved and variable regions in the envelope gene of HTLV-III/LAV, the retrovirus of AIDS. Cell **45**:637–648.

41. **Leonard CK**, **Spellman MW**, **Riddle L**, **Harris RJ**, **Thomas JN**, **Gregory TJ**. 1990. Assignment of intrachain disulfide bonds and characterization of potential glycosylation sites of the type 1 recombinant human immunodeficiency virus envelope glycoprotein (gp120) expressed in Chinese hamster ovary cells. J Biol Chem **265**:10373–10382.

42. **Julien J-P**, **Cupo A**, **Sok D**, **Stanfield RL**, **Lyumkis D**, **Deller MC**, **Klasse P-J**, **Burton DR**, **Sanders RW**, **Moore JP**, **Ward AB**, **Wilson IA**. 2013. Crystal structure of a soluble cleaved HIV-1 envelope trimer. Science **342**:1477–83.

43. **Kwong PD**, **Wyatt R**, **Robinson J**, **Sweet RW**, **Sodroski J**, **Hendrickson WA**. 1998. Structure of an HIV gp120 envelope glycoprotein in complex with the CD4 receptor and a neutralizing human antibody. Nature **393**:648–659.

44. **Chen B**, **Vogan EM**, **Gong H**, **Skehel JJ**, **Wiley DC**, **Harrison SC**. 2005. Structure of an unliganded simian immunodeficiency virus gp120 core. Nature **433**:834–841.

45. **Trkola A**, **Dragic T**, **Arthos J**, **Binley JM**, **Olson WC**, **Allaway GP**, **Cheng-Mayer C**, **Robinson J**, **Maddon PJ**, **Moore JP**. 1996. CD4-dependent, antibody-sensitive interactions between HIV-1 and its co-receptor CCR-5. Nature **384**:184–187.

46. **Lapham CK**, **Zaitseva MB**, **Lee S**, **Romanstseva T**, **Golding H**. 1999. Fusion of monocytes and macrophages with HIV-1 correlates with biochemical properties of CXCR4

and CCR5. Nat Med **5**:303–308.

47. **Wu L**, **Gerard NP**, **Wyatt R**, **Choe H**, **Parolin C**, **Ruffing N**, **Borsetti A**, **Cardoso AA**, **Desjardin E**, **Newman W**, **Gerard C**, **Sodroski J**. 1996. CD4-induced interaction of primary HIV-1 gp120 glycoproteins with the chemokine receptor CCR-5. Nature **384**:179–183.

48. **Cormier EG**, **Tran DNH**, **Yukhayeva L**, **Olson WC**, **Dragic T**. 2001. Mapping the Determinants of the CCR5 Amino-Terminal Sulfopeptide Interaction with Soluble Human Immunodeficiency Virus Type 1 gp120-CD4 Complexes. J Virol **75**:5541–5549.

49. **Rizzuto CD**, **Wyatt R**, **Hernandez-Ramos N**, **Sun Y**, **Kwong PD**, **Hendrickson WA**, **Sodroski J**. 1998. A Conserved HIV gp120 Glycoprotein Structure Involved in Chemokine Receptor Binding. Science **280**:1949–1953.

50. **Rizzuto C**, **Sodroski J**. 2000. Fine Definition of a Conserved CCR5-Binding Region on the Human Immunodeficiency Virus Type 1 Glycoprotein 120. AIDS Res Hum Retroviruses **16**:741–749.

51. **Huang C-C**, **Tang M**, **Zhang M-Y**, **Majeed S**, **Montabana E**, **Stanfield RL**, **Dimitrov DS**, **Korber BTM**, **Sodroski J**, **Wilson IA**, **Wyatt RT**, **Kwong PD**. 2005. Structure of a V3-Containing HIV-1 gp120 Core. Science **310**:1025–1028.

52. **Hartley O**, **Klasse PJ**, **Sattentau QJ**, **Moore JP**. 2005. V3: HIV's switch-hitter. AIDS Res Hum Retroviruses **21**:171–189.

53. **Fouchier RA**, **Groenink M**, **Kootstra NA**, **Tersmette M**, **Huisman HG**, **Miedema F**, **Schuitemaker H**. 1992. Phenotype-associated sequence variation in the third variable domain of the human immunodeficiency virus type 1 gp120 molecule. J Virol **66**:3183–7.

54. **Nabatov AA**, **Pollakis G**, **Linnemann T**, **Kliphius A**, **Chalaby MIM**, **Paxton WA**. 2004. Intrapatient Alterations in the Human Immunodeficiency Virus Type 1 gp120 V1V2 and V3 Regions Differentially Modulate Coreceptor Usage, Virus Inhibition by CC/CXC Chemokines, Soluble CD4, and the b12 and 2G12 Monoclonal Antibodies. J Virol **78**:524–530.

55. **Checkley MA**, **Luttge BG**, **Freed EO**. 2011. HIV-1 Envelope Glycoprotein Biosynthesis, Trafficking, and Incorporation. J Mol Biol **410**:582–608.

56. **Sagar M**, **Wu X**, **Lee S**, **Overbaugh J**. 2006. Human immunodeficiency virus type 1 V1-V2 envelope loop sequences expand and add glycosylation sites over the course of infection, and these modifications affect antibody neutralization sensitivity. J Virol **80**:9586–98.

57. **Chohan B**, **Lang D**, **Sagar M**, **Korber B**, **Lavreys L**, **Richardson B**, **Overbaugh J**. 2005. Selection for human immunodeficiency virus type 1 envelope glycosylation variants with shorter V1-V2 loop sequences occurs during transmission of certain genetic subtypes and may impact viral RNA levels. J Virol **79**:6528–6531.

58. **Masciotra S**, **Owen SM**, **Rudolph D**, **Yang C**, **Wang B**, **Saksena N**, **Spira T**, **Dhawan S**, **Lal RB**. 2002. Temporal relationship between V1V2 variation, macrophage replication, and coreceptor adaptation during HIV-1 disease progression. Aids **16**:1887–1898.

59. **Kitrinos KM**, **Hoffman NG**, **Nelson JAE**, **Swanstrom R**. 2003. Turnover of env Variable Region 1 and 2 Genotypes in Subjects with Late-Stage Human Immunodeficiency Virus Type 1 Infection. J Virol **77**:6811–6822.

60. **Binley JM**, **Ban Y-EA**, **Crooks ET**, **Eggink D**, **Osawa K**, **Schief WR**, **Sanders RW**. 2010. Role of complex carbohydrates in human immunodeficiency virus type 1 infection and resistance to antibody neutralization. J Virol **84**:5637–5655.

61. **Wyatt R**, **Moore J**, **Accola M**, **Desjardin E**, **Robinson J**, **Sodroski J**. 1995. Involvement of the V1/V2 variable loop structure in the exposure of human immunodeficiency virus type 1 gp120 epitopes induced by receptor binding. J Virol **69**:5723–33.

62. **Pinter A**, **Honnen WJ**, **He Y**, **Gorny MK**, **Zolla-Pazner S**, **Kayman SC**. 2004. The V1/V2 domain of gp120 is a global regulator of the sensitivity of primary human immunodeficiency virus type 1 isolates to neutralization by antibodies commonly induced upon infection. J Virol **78**:5205–15.

63. **Allan JS**, **Coligan JE**, **Barin F**, **McLane MF**, **Sodroski JG**, **Rosen CA**, **Haseltine WA**, **Lee TH**, **Essex M**. 1985. Major glycoprotein antigens that induce antibodies in AIDS patients are encoded by HTLV-III. Science **228**:1091–1094.

64. **Montefiori DC**, **Robinson WE**, **Mitchell WM**. 1988. Role of protein N-glycosylation in pathogenesis of human immunodeficiency virus type 1. Proc Natl Acad Sci **85**:9248–9252.

65. **Lifson J**, **Coutré S**, **Huang E**, **Engleman E**. 1986. Role of envelope glycoprotein carbohydrate in human immunodeficiency virus (HIV) infectivity and virus-induced cell fusion. J Exp Med **164**:2101–2106.

66. **Li Y**, **Luo L**, **Rasool N**, **Kang CY**. 1993. Glycosylation is necessary for the correct folding of human immunodeficiency virus gp120 in CD4 binding. J Virol **67**:584–588.

67. **Fenouillet E**, **Jones IM**. 1995. The glycosylation of human immunodeficiency virus type 1 transmembrane glycoprotein (gp41) is important for the efficient intracellular transport of the envelope precursor gp160. J Gen Virol **76**:1509–1514.

68. **Freed EO**, **Myers DJ**, **Risser R**. 1990. Characterization of the fusion domain of the human immunodeficiency virus type 1 envelope glycoprotein gp41. Proc Natl Acad Sci **87**:4650–4654.

69. **Freed EO**, **Delwart EL**, **Buchschacher GL**, **Panganiban AT**. 1992. A mutation in the human immunodeficiency virus type 1 transmembrane glycoprotein gp41 dominantly interferes with fusion and infectivity. Proc Natl Acad Sci **89**:70–74.

70. **Dubay JW**, **Roberts SJ**, **Hahn BH**, **Hunter E**. 1992. Truncation of the human immunodeficiency virus type 1 transmembrane glycoprotein cytoplasmic domain blocks virus infectivity. J Virol **66**:6616–25.

71. **Chan DC**, **Fass D**, **Berger JM**, **Kim PS**. 1997. Core structure of gp41 from the HIV envelope glycoprotein. Cell **89**:263–273.

72. **Tan K**, **Liu J**, **Wang J**, **Shen S**, **Lu M**. 1997. Atomic structure of a thermostable subdomain of HIV-1 gp41. Proc Natl Acad Sci **94**:12303–12308.

73. **Weissenhorn W**, **Dessen A**, **Harrison SC**, **Skehel JJ**, **Wiley DC**. 1997. Atomic structure of the ectodomain from HIV-1 gp41. Nature **387**:426–430.

74. **Pancera M**, **Majeed S**, **Ban Y-EA**, **Chen L**, **Huang C**, **Kong L**, **Kwon YD**, **Stuckey J**, **Zhou T**, **Robinson JE**, **Schief WR**, **Sodroski J**, **Wyatt R**, **Kwong PD**. 2010. Structure of HIV-1 gp120 with gp41-interactive region reveals layered envelope architecture and basis of conformational mobility. Proc Natl Acad Sci **107**:1166–71.

75. **Muñoz-Barroso I**, **Salzwedel K**, **Hunter E**, **Blumenthal R**. 1999. Role of the membrane-

proximal domain in the initial stages of human immunodeficiency virus type 1 envelope glycoprotein-mediated membrane fusion. J Virol **73**:6089–6092.

76. **Salzwedel K**, **West JT**, **Hunter E**. 1999. A conserved tryptophan-rich motif in the membrane-proximal region of the human immunodeficiency virus type 1 gp41 ectodomain is important for Env-mediated fusion and virus infectivity. J Virol **73**:2469–2480.

77. **Dimitrov AS**, **Rawat SS**, **Jiang S**, **Blumenthal R**. 2003. Role of the Fusion Peptide and Membrane-Proximal Domain in HIV-1 Envelope Glycoprotein-Mediated Membrane Fusion. Biochemistry **42**:14150–14158.

78. **Noah E**, **Biron Z**, **Naider F**, **Arshava B**, **Anglister J**. 2008. The membrane proximal external region of the HIV-1 envelope glycoprotein gp41 contributes to the stabilization of the six-helix bundle formed with a matching N' peptide. Biochemistry **47**:6782–6792.

79. **Ingallinella P**, **Bianchi E**, **Ladwa NA**, **Wang Y-J**, **Hrin R**, **Veneziano M**, **Bonelli F**, **Ketas TJ**, **Moore JP**, **Miller MD**, **Pessi A**. 2009. Addition of a cholesterol group to an HIV-1 peptide fusion inhibitor dramatically increases its antiviral potency. Proc Natl Acad Sci **106**:5801–5806.

80. **Hollier MJ**, **Dimmock NJ**. 2005. The C-terminal tail of the gp41 transmembrane envelope glycoprotein of HIV-1 clades A, B, C, and D may exist in two conformations: an analysis of sequence, structure, and function. Virology **337**:284–296.

81. **Wild C**, **Shugars D**, **Greenwell TK**, **McDanal CB**, **Matthews TJ**. 1994. Peptides corresponding to a predictive alpha-helical domain of human immunodeficiency virus type 1 gp41 are potent inhibitors of virus infection. Proc Natl Acad Sci **91**:9770–9774.

82. **Piller SC**, **Dubay JW**, **Derdeyn CA**, **Hunter E**. 2000. Mutational Analysis of Conserved Domains within the Cytoplasmic Tail of gp41 from Human Immunodeficiency Virus Type 1: Effects on Glycoprotein Incorporation and Infectivity. J Virol **74**:11717–11723.

83. **Yu X**, **Yuan X**, **McLane M**, **Lee T**, **Essex M**. 1993. Mutations in the cytoplasmic domain of human immunodeficiency virus type 1 transmembrane protein impair the incorporation of Env proteins into mature virions. J Virol **19**:505–10.

84. **Dorfman T**, **Mammano F**, **Haseltine WA**, **Gottlinger HG**. 1994. Role of the matrix protein in the virion association of the human immunodeficiency virus type 1 envelope

glycoprotein. J Virol **68**:1689–1696.

85. **Freed EO**, **Martin MA**. 1996. Domains of the human immunodeficiency virus type 1 matrix and gp41 cytoplasmic tail required for envelope incorporation into virions. J Virol **70**:341–51.

86. **Murakami T**, **Freed EO**. 2000. Genetic Evidence for an Interaction between Human Immunodeficiency Virus Type 1 Matrix and alpha -Helix 2 of the gp41 Cytoplasmic Tail. J Virol **74**:3548–3554.

87. **Deschambeault J**, **Lalonde JP**, **Cervantes-Acosta G**, **Lodge R**, **Cohen EA**, **Lemay G**. 1999. Polarized human immunodeficiency virus budding in lymphocytes involves a tyrosine-based signal and favors cell-to-cell viral transmission. J Virol **73**:5010–7.

88. **Rousso I**, **Mixon MB**, **Chen BK**, **Kim PS**. 2000. Palmitoylation of the HIV-1 envelope glycoprotein is critical for viral infectivity. Proc Natl Acad Sci **97**:13523–5.

89. **Lodge R**, **Göttlinger H**, **Gabuzda D**, **Cohen EA**, **Lemay G**. 1994. The intracytoplasmic domain of gp41 mediates polarized budding of human immunodeficiency virus type 1 in MDCK cells. J Virol **68**:4857–61.

90. **Lyumkis D**, **Julien J-P**, **de Val N**, **Cupo A**, **Potter CS**, **Klasse P-J**, **Burton DR**, **Sanders RW**, **Moore JP**, **Carragher B**, **Wilson IA**, **Ward AB**. 2013. Cryo-EM structure of a fully glycosylated soluble cleaved HIV-1 envelope trimer. Science **342**:1484–90.

91. **Julien J-P**, **Lee JH**, **Cupo A**, **Murin CD**, **Derking R**, **Hoffenberg S**, **Caulfield MJ**, **King CR**, **Marozsan AJ**, **Klasse PJ**, **Sanders RW**, **Moore JP**, **Wilson IA.**, **Ward AB**. 2013. Asymmetric recognition of the HIV-1 trimer by broadly neutralizing antibody PG9. Proc Natl Acad Sci **110**:4351–6.

92. **Schrödinger L**. 2015. The {PyMOL} Molecular Graphics System, Version~1.8.

93. **Munro JB**, **Gorman J**, **Ma X**, **Zhou Z**, **Arthos J**, **Burton DR**, **Koff WC**, **Courter JR**, **Smith AB**, **Kwong PD**, **Blanchard SC**, **Mothes W**. 2014. Conformational dynamics of single HIV-1 envelope trimers on the surface of native virions. Science **346**:759–763.

94. **Guttman M**, **Cupo A**, **Julien J-P**, **Sanders RW**, **Wilson IA**, **Moore JP**, **Lee KK**. 2015. Antibody potency relates to the ability to recognize the closed, pre-fusion form of HIV Env.

Nature **6**:6144.

95. **Seaman MS**, **Janes H**, **Hawkins N**, **Grandpre LE**, **Devoy C**, **Giri A**, **Coffey RT**, **Harris L**, **Wood B**, **Daniels MG**, **Bhattacharya T**, **Lapedes A**, **Polonis VR**, **McCutchan FE**, **Gilbert PB**, **Self SG**, **Korber BT**, **Montefiori DC**, **Mascola JR**. 2010. Tiered categorization of a diverse panel of HIV-1 Env pseudoviruses for assessment of neutralizing antibodies. J Virol **84**:1439–1452.

96. **Rademeyer C**, **Korber B**, **Seaman MS**, **Giorgi EE**, **Thebus R**, **Robles A**, **Sheward DJ**, **Wagh K**, **Garrity J**, **Carey BR**, **Gao H**, **Greene KM**, **Tang H**, **Bandawe GP**, **Marais JC**, **Diphoko TE**, **Hraber P**, **Tumba N**, **Moore PL**, **Gray GE**, **Kublin J**, **McElrath MJ**, **Vermeulen M**, **Middelkoop K**, **Bekker LG**, **Hoelscher M**, **Maboko L**, **Makhema J**, **Robb ML**, **Abdool Karim SS**, **Abdool Karim Q**, **Kim JH**, **Hahn BH**, **Gao F**, **Swanstrom R**, **Morris L**, **Montefiori DC**, **Williamson C**. 2016. Features of Recently Transmitted HIV-1 Clade C Viruses that Impact Antibody Recognition: Implications for Active and Passive Immunization. PLoS Pathog **12**:1–29.

97. **Kwong PD**, **Doyle ML**, **Casper DJ**, **Cicala C**, **Leavitt SA**, **Majeed S**, **Steenbeke TD**, **Venturi M**, **Chaiken I**, **Fung M**, **Katinger H**, **Parren PWIH**, **Robinson J**, **Van Ryk D**, **Wang L**, **Burton DR**, **Freire E**, **Wyatt R**, **Sodroski J**, **Hendrickson WA**, **Arthos J**. 2002. HIV-1 evades antibody-mediated neutralization through conformational masking of receptor-binding sites. Nature **420**:678–682.

98. **Frey G**, **Peng H**, **Rits-Volloch S**, **Morelli M**, **Cheng Y**, **Chen B**. 2008. A fusion-intermediate state of HIV-1 gp41 targeted by broadly neutralizing antibodies. Proc Natl Acad Sci **105**:3739–3744.

99. **Poignard P**, **Moulard M**, **Golez E**, **Vivona V**, **Franti M**, **Venturini S**, **Wang M**, **Parren PWHI**, **Burton DR**. 2003. Heterogeneity of Envelope Molecules Expressed on Primary Human Immunodeficiency Virus Type 1 Particles as Probed by the Binding of Neutralizing and Nonneutralizing Antibodies. J Virol **77**:353–365.

100. **Moore PL**, **Crooks ET**, **Porter L**, **Zhu P**, **Cayanan CS**, **Grise H**, **Corcoran P**, **Zwick MB**, **Franti M**, **Morris L**, **Roux KH**, **Burton DR**, **Binley JM**. 2006. Nature of

nonfunctional envelope proteins on the surface of human immunodeficiency virus type 1. J Virol **80**:2515–2528.

101. **Zhu P**, **Liu J**, **Bess J**, **Chertova E**, **Lifson JD**, **Grisé H**, **Ofek GA**, **Taylor KA**, **Roux KH**. 2006. Distribution and three-dimensional structure of AIDS virus envelope spikes. Nature **441**:847–852.

102. **Klein JS**, **Gnanapragasam PNP**, **Galimidi RP**, **Foglesong CP**, **West AP**, **Bjorkman PJ**. 2009. Examination of the contributions of size and avidity to the neutralization mechanisms of the anti-HIV antibodies b12 and 4E10. Proc Natl Acad Sci **106**:7385–7390.

103. **Mouquet H**. 2014. Antibody B cell responses in HIV-1 infection. Trends Immunol **35**:549–561.

104. **Abrahams M-R**, **Anderson JA**, **Giorgi EE**, **Seoighe C**, **Mlisana K**, **Ping L-H**, **Athreya GS**, **Treurnicht FK**, **Keele BF**, **Wood N**, **Salazar-Gonzalez JF**, **Bhattacharya T**, **Chu H**, **Hoffman I**, **Galvin S**, **Mapanje C**, **Kazembe P**, **Thebus R**, **Fiscus S**, **Hide W**, **Cohen MS**, **Karim SA**, **Haynes BF**, **Shaw GM**, **Hahn BH**, **Korber BT**, **Swanstrom R**, **Williamson C**. 2009. Quantitating the Multiplicity of Infection with Human Immunodeficiency Virus Type 1 Subtype C Reveals a Non-Poisson Distribution of Transmitted Variants. J Virol **83**:3556–3567.

105. **Keele BF**, **Giorgi EE**, **Salazar-Gonzalez JF**, **Decker JM**, **Pham KT**, **Salazar MG**, **Sun C**, **Grayson T**, **Wang S**, **Li H**, **Wei X**, **Jiang C**, **Kirchherr JL**, **Gao F**, **Anderson JA**, **Ping L-H**, **Swanstrom R**, **Tomaras GD**, **Blattner WA**, **Goepfert PA**, **Kilby JM**, **Saag MS**, **Delwart EL**, **Busch MP**, **Cohen MS**, **Montefiori DC**, **Haynes BF**, **Gaschen B**, **Athreya GS**, **Lee HY**, **Wood N**, **Seoighe C**, **Perelson AS**, **Bhattacharya T**, **Korber BT**, **Hahn BH**, **Shaw GM**. 2008. Identification and characterization of transmitted and early founder virus envelopes in primary HIV-1 infection. Proc Natl Acad Sci **105**:7552–7557.

106. **Joseph SB**, **Swanstrom R**, **Kashuba ADM**, **Cohen MS**. 2015. Bottlenecks in HIV-1 transmission: insights from the study of founder viruses. Nat Rev Microbiol **13**:414–425.

107. **Anderson JA**, **Ping LH**, **Dibben O**, **Jabara CB**, **Arney L**, **Kincer L**, **Tang Y**, **Hobbs M**, **Hoffman I**, **Kazembe P**, **Jones CD**, **Borrow P**, **Fiscus S**, **Cohen MS**, **Swanstrom R**. 2010. HIV-1 populations in semen arise through multiple mechanisms. PLoS Pathog **6**:51–52.

108. **Boeras DI**, **Hraber PT**, **Hurlston M**, **Evans-Strickfaden T**, **Bhattacharya T**, **Giorgi EE**, **Mulenga J**, **Karita E**, **Korber BT**, **Allen S**, **Hart CE**, **Derdeyn CA**, **Hunter E**. 2011. Role of donor genital tract HIV-1 diversity in the transmission bottleneck. Proc Natl Acad Sci **108**:E1156-63.

109. **Bull ME**, **Heath LM**, **McKernan-Mullin JL**, **Kraft KM**, **Acevedo L**, **Hitti JE**, **Cohn SE**, **Tapia KA**, **Holte SE**, **Dragavon JA**, **Coombs RW**, **Mullins JI**, **Frenkel LM**. 2013. Human immunodeficiency viruses appear compartmentalized to the female genital tract in cross-sectional analyses but genital lineages do not persist over time. J Infect Dis **207**:1206–1215.

110. **Ping L-H**, **Joseph SB**, **Anderson J a**, **Abrahams M-R**, **Salazar-Gonzalez JF**, **Kincer LP**, **Treurnicht FK**, **Arney L**, **Ojeda S**, **Zhang M**, **Keys J**, **Potter EL**, **Chu H**, **Moore P**, **Salazar MG**, **Iyer S**, **Jabara C**, **Kirchherr J**, **Mapanje C**, **Ngandu N**, **Seoighe C**, **Hoffman I**, **Gao F**, **Tang Y**, **Labranche C**, **Lee B**, **Saville A**, **Vermeulen M**, **Fiscus S**, **Morris L**, **Abdool Karim SS**, **Haynes BF**, **Shaw GM**, **Korber BT**, **Hahn BH**, **Cohen MS**, **Montefiori D**, **Williamson C**, **Swanstrom R**. 2013. Comparison of viral Env proteins from acute and chronic infections with subtype C human immunodeficiency virus type 1 identifies differences in glycosylation and CCR5 utilization and suggests a new strategy for immunogen design. J Virol **87**:7218–33.

111. **Sagar M**, **Laeyendecker O**, **Lee S**, **Gamiel J**, **Wawer MJ**, **Gray RH**, **Serwadda D**, **Sewankambo NK**, **Shepherd JC**, **Toma J**, **Huang W**, **Quinn TC**. 2009. Selection of HIV Variants with Signature Genotypic Characteristics during Heterosexual Transmission. J Infect Dis **199**:580–589.

112. **Frost SDW**, **Liu Y**, **Pond SLK**, **Chappey C**, **Wrin T**, **Petropoulos CJ**, **Little SJ**, **Richman DD**. 2005. Characterization of human immunodeficiency virus type 1 (HIV-1) envelope variation and neutralizing antibody responses during transmission of HIV-1 subtype B. J Virol **79**:6523–6527.

113. **Liu Y**, **Curlin ME**, **Diem K**, **Zhao H**, **Ghosh AK**, **Zhu H**, **Woodward AS**, **Maenza J**, **Stevens CE**, **Stekler J**, **Collier AC**, **Genowati I**, **Deng W**, **Zioni R**, **Corey L**, **Zhu T**,

Mullins JI. 2008. Env length and N-linked glycosylation following transmission of human immunodeficiency virus Type 1 subtype B viruses. Virology **374**:229–233.

114. **Parrish NF**, **Gao F**, **Li H**, **Giorgi EE**, **Barbian HJ**, **Parrish EH**, **Zajic L**, **Iyer SS**, **Decker JM**, **Kumar A**, **Hora B**, **Berg A**, **Cai F**, **Hopper J**, **Denny TN**, **Ding H**, **Ochsenbauer C**, **Kappes JC**, **Galimidi RP**, **West AP**, **Bjorkman PJ**, **Wilen CB**, **Doms RW**, **O'Brien M**, **Bhardwaj N**, **Borrow P**, **Haynes BF**, **Muldoon M**, **Theiler JP**, **Korber B**, **Shaw GM**, **Hahn BH**. 2013. Phenotypic properties of transmitted founder HIV-1. Proc Natl Acad Sci **110**:6626–33.

115. **Banchereau J**, **Steinman RM**. 1998. Dendritic cells and the control of immunity. Nature **392**:245–252.

116. **Shen R**, **Kappes JC**, **Smythies LE**, **Richter HE**, **Novak L**, **Smith PD**. 2014. Vaginal myeloid dendritic cells transmit founder HIV-1. J Virol **88**:7683–8.

117. **Iyer SS**, **Bibollet-Ruche F**, **Sherrill-Mix S**, **Learn GH**, **Plenderleith L**, **Smith AG**, **Barbian HJ**, **Russell RM**, **Gondim MVP**, **Bahari CY**, **Shaw CM**, **Li Y**, **Decker T**, **Haynes BF**, **Shaw GM**, **Sharp PM**, **Borrow P**, **Hahn BH**. 2017. Resistance to type 1 interferons is a major determinant of HIV-1 transmission fitness. Proc Natl Acad Sci **114**:E590–E599.

118. **Stamatatos L**, **Morris L**, **Burton DR**, **Mascola JR**. 2009. Neutralizing antibodies generated during natural HIV-1 infection: good news for an HIV-1 vaccine? Nat Med **15**:866–870.

119. **Rowland-Jones SL**, **Dong T**, **Fowke KR**, **Kimani J**, **Krausa P**, **Newell H**, **Blanchard T**, **Ariyoshi K**, **Oyugi J**, **Ngugi E**, **Bwayo J**, **MacDonald KS**, **McMichael AJ**, **Plummer FA**. 1998. Cytotoxic T cell responses to multiple conserved HIV epitopes in HIV-resistant prostitutes in Nairobi. J Clin Invest **102**:1758–1765.

120. **Goonetilleke N**, **Liu MKP**, **Salazar-Gonzalez JF**, **Ferrari G**, **Giorgi E**, **Ganusov VV**, **Keele BF**, **Learn GH**, **Turnbull EL**, **Salazar MG**, **Weinhold KJ**, **Moore S**, **Letvin N**, **Haynes BF**, **Cohen MS**, **Hraber P**, **Bhattacharya T**, **Borrow P**, **Perelson AS**, **Hahn BH**, **Shaw GM**, **Korber BT**, **McMichael AJ**. 2009. The first T cell response to transmitted/founder virus contributes to the control of acute viremia in HIV-1 infection. J

Exp Med **206**:1253–1272.

121. **Lichterfeld M**, **Yu XG**, **Waring MT**, **Mui SK**, **Johnston MN**, **Cohen D**, **Addo MM**, **Zaunders J**, **Alter G**, **Pae E**, **Strick D**, **Allen TM**, **Rosenberg ES**, **Walker BD**, **Altfeld M**. 2004. HIV-1-specific cytotoxicity is preferentially mediated by a subset of CD8(+) T cells producing both interferon-gamma and tumor necrosis factor-alpha. Blood **104**:487–494.

122. **Mlotshwa M**, **Riou C**, **Chopera D**, **de Assis Rosa D**, **Ntale R**, **Treunicht F**, **Woodman Z**, **Werner L**, **van Loggerenberg F**, **Mlisana K**, **Abdool Karim SS**, **Williamson C**, **Gray CM**, **CAPRISA 002 Study Team**. 2010. Fluidity of HIV-1-specific T-cell responses during acute and early subtype C HIV-1 infection and associations with early disease progression. J Virol **84**:12018–29.

123. **Lamas JR**, **Brooks JM**, **Galocha B**, **Rickinson AB**, **López De Castro JA**. 1998. Relationship between peptide binding and T cell epitope selection: A study with subtypes of HLA-B27. Int Immunol **10**:259–266.

124. **Tomiyama H**, **Akari H**, **Adachi A**, **Takiguchi M**. 2002. Different effects of Nef-mediated HLA class I down-regulation on human immunodeficiency virus type 1-specific CD8(+) T-cell cytolytic activity and cytokine production. J Virol **76**:7535–43.

125. **Greenberg ME**, **Lafrate AJ**, **Skowronski J**. 1998. The SH3 domain-binding surface and an acidic motif in HIV-1 Nef regulate trafficking of class I MHC complexes. EMBO J **17**:2777–2789.

126. **Goulder PJR**, **Watkins DI**. 2004. HIV and SIV CTL escape: implications for vaccine design. Nat Rev Immunol **4**:630–640.

127. **Klenerman P**, **Rowland-Jones S**, **McAdam S**, **Edwards J**, **Daenke S**, **Lalloo D**, **Köppe B**, **Rosenberg W**, **Boyd D**, **Edwards A**. 1994. Cytotoxic T-cell activity antagonized by naturally occurring HIV-1 Gag variants. Nature **369**:403–7.

128. **Le Gall S**, **Stamegna P**, **Walker BD**. 2007. Portable flanking sequences modulate CTL epitope processing. J Clin Invest **117**:3563–75.

129. **Tenzer S**, **Wee E**, **Burgevin A**, **Stewart-Jones G**, **Friis L**, **Lamberth K**, **Chang C**, **Harndahl M**, **Weimershaus M**, **Gerstoft J**, **Akkad N**, **Klenerman P**, **Fugger L**, **Jones**

EY, **McMichael AJ**, **Buus S**, **Schild H**, **van Endert P**, **Iversen AKN**. 2009. Antigen processing influences HIV-specific cytotoxic T lymphocyte immunodominance. Nat Immunol **10**:636–46.

130. **Parham P**, **Adams EJ**, **Arnett KL**. 1995. The origins of HLA-A,B,C polymorphism. Immunol Rev **143**:141–80.

131. **Moore CB**, **John M**, **James IR**, **Christiansen FT**, **Witt CS**, **Mallal SA**. 2002. Evidence of HIV-1 adaptation to HLA-restricted immune responses at a population level. Science **296**:1439–43.

132. **Allen TM**, **Altfeld M**, **Geer SC**, **Kalife ET**, **Moore C**, **O'Sullivan KM**, **DeSouza I**, **Feeney ME**, **Eldridge RL**, **Maier EL**, **Kaufmann DE**, **Lahaie MP**, **Reyor L**, **Tanzi G**, **Johnston MN**, **Brander C**, **Draenert R**, **Rockstroh JK**, **Jessen H**, **Rosenberg ES**, **Mallal SA**, **Walker BD**. 2005. Selective Escape from CD8+ T-Cell Responses Represents a Major Driving Force of Human Immunodeficiency Virus Type 1 (HIV-1) Sequence Diversity and Reveals Constraints on HIV-1 Evolution. J Virol **79**:13239–13249.

133. **Brumme ZL**, **Brumme CJ**, **Heckerman D**, **Korber BT**, **Daniels M**, **Carlson J**, **Kadie C**, **Bhattacharya T**, **Chui C**, **Szinger J**, **Mo T**, **Hogg RS**, **Montaner JSG**, **Frahm N**, **Brander C**, **Walker BD**, **Harrigan PR**. 2007. Evidence of differential HLA class I-mediated viral evolution in functional and accessory/regulatory genes of HIV-1. PLoS Pathog **3**:0913–0927.

134. **Brumme ZL**, **John M**, **Carlson JM**, **Brumme CJ**, **Chan D**, **Brockman MA**, **Swenson LC**, **Tao I**, **Szeto S**, **Rosato P**, **Sela J**, **Kadie CM**, **Frahm N**, **Brander C**, **Haas DW**, **Riddler SA**, **Haubrich R**, **Walker BD**, **Harrigan PR**, **Heckerman D**, **Mallal S**. 2009. HLA-associated immune escape pathways in HIV-1 subtype B Gag, Pol and Nef proteins. PLoS One **4**:e6687.

135. **Kaslow RA**, **Carrington M**, **Apple R**, **Park L**, **Muñoz A**, **Saah AJ**, **Goedert JJ**, **Winkler C**, **O'Brien SJ**, **Rinaldo C**, **Detels R**, **Blattner W**, **Phair J**, **Erlich H**, **Mann DL**. 1996. Influence of combinations of human major histocompatibility complex genes on the course of HIV–1 infection. Nat Med **2**:405–411.

136. **Migueles SA**, **Sabbaghian MS**, **Shupert WL**, **Bettinotti MP**, **Marincola FM**, **Martino**

L, **Hallahan CW**, **Selig SM**, **Schwartz D**, **Sullivan J**, **Connors M**. 2000. HLA B*5701 is highly associated with restriction of virus replication in a subgroup of HIV-infected long term nonprogressors. Proc Natl Acad Sci **97**:2709–2714.

137. **Gao X**, **Nelson GW**, **Karacki P**, **Martin MP**, **Phair J**, **Kaslow R**, **Goedert JJ**, **Buchbinder S**, **Hoots K**, **Vlahov D**, **O'Brien SJ**, **Carrington M**. 2001. Effect of a Single Amino Acid Change in MHC Class I Molecules on the Rate of Progression to AIDS. N Engl J Med **344**:1668–1675.

138. **Kiepiela P**, **Leslie AJ**, **Honeyborne I**, **Ramduth D**, **Thobakgale C**, **Chetty S**, **Rathnavalu P**, **Moore C**, **Pfafferott KJ**, **Hilton L**, **Zimbwa P**, **Moore S**, **Allen T**, **Brander C**, **Addo MM**, **Altfeld M**, **James I**, **Mallal S**, **Bunce M**, **Barber LD**, **Szinger J**, **Day C**, **Klenerman P**, **Mullins J**, **Korber B**, **Coovadia HM**, **Walker BD**, **Goulder PJR**. 2004. Dominant influence of HLA-B in mediating the potential co-evolution of HIV and HLA. Nature **432**:769–775.

139. **Carrington M**, **Nelson GW**, **Martin MP**, **Kissner T**, **Vlahov D**, **Goedert JJ**, **Kaslow R**, **Buchbinder S**, **Hoots K**, **O'Brien SJ**. 1999. HLA and HIV-1: heterozygote advantage and B*35-Cw*04 disadvantage. Science **283**:1748–52.

140. **Ngumbela KC**, **Day CL**, **Mncube Z**, **Nair K**, **Ramduth D**, **Thobakgale C**, **Moodley E**, **Reddy S**, **de Pierres C**, **Mkhwanazi N**, **Bishop K**, **van der Stok M**, **Ismail N**, **Honeyborne I**, **Crawford H**, **Kavanagh DG**, **Rousseau C**, **Nickle D**, **Mullins J**, **Heckerman D**, **Korber B**, **Coovadia H**, **Kiepiela P**, **Goulder PJR**, **Walker BD**. 2008. Targeting of a CD8 T Cell Env Epitope Presented by HLA-B*5802 Is Associated with Markers of HIV Disease Progression and Lack of Selection Pressure. AIDS Res Hum Retroviruses **24**:72–82.

141. **Wei C-J**, **Boyington JC**, **McTamney PM**, **Kong W-P**, **Pearce MB**, **Xu L**, **Andersen H**, **Rao S**, **Tumpey TM**, **Yang Z-Y**, **Nabel GJ**. 2010. Induction of broadly neutralizing H1N1 influenza antibodies by vaccination. Science **329**:1060–1064.

142. **Patel M**, **Glass RI**, **Jiang B**, **Santosham M**, **Lopman B**, **Parashar U**. 2013. A systematic review of anti-rotavirus serum IgA antibody titer as a potential correlate of rotavirus vaccine

efficacy. J Infect Dis **208**:284-294.

143. **Pastrana D V**, **Vass WC**, **Lowy DR**, **Schiller JT**. 2001. NHPV16 VLP vaccine induces human antibodies that neutralize divergent variants of HPV16.Virology **279**:361-369.

144. **Joines RW**, **Blatter M**, **Abraham B**, **Xie F**, **De Clercq N**, **Baine Y**, **Reisinger KS**, **Kuhnen A**, **Parenti DL**. 2001. A prospective, randomized, comparative US trial of a combination hepatitis A and B vaccine (Twinrix®) with corresponding monovalent vaccines (Havrix® and Engerix-B®) in adults. Vaccine **19**:4710–4719.

145. **Alter G**, **Moody MA**. 2010. The humoral response to HIV-1: new insights, renewed focus. J Infect Dis **202 Suppl**:S315–S322.

146. **Tomaras GD**, **Yates NL**, **Liu P**, **Qin L**, **Fouda GG**, **Chavez LL**, **Decamp AC**, **Parks RJ**, **Ashley VC**, **Lucas JT**, **Cohen M**, **Eron J**, **Hicks CB**, **Liao H-X**, **Self SG**, **Landucci G**, **Forthal DN**, **Weinhold KJ**, **Keele BF**, **Hahn BH**, **Greenberg ML**, **Morris L**, **Karim SSA**, **Blattner WA**, **Montefiori DC**, **Shaw GM**, **Perelson AS**, **Haynes BF**. 2008. Initial B-cell responses to transmitted human immunodeficiency virus type 1: virion-binding immunoglobulin M (IgM) and IgG antibodies followed by plasma anti-gp41 antibodies with ineffective control of initial viremia. J Virol **82**:12449–12463.

147. **Cadogan M**, **Dalgleish AG**. 2008. HIV immunopathogenesis and strategies for intervention. Lancet Infect Dis **8**:675-684.

148. **Tyler DS**, **Stanley SD**, **Zolla-Pazner S**, **Gorny MK**, **Shadduck PP**, **Langlois AJ**, **Matthews TJ**, **Bolognesi DP**, **Palker TJ**, **Weinhold KJ**. 1990. Identification of sites within gp41 that serve as targets for antibody-dependent cellular cytotoxicity by using human monoclonal antibodies. J Immunol **145**:3276–3282.

149. **Rerks-Ngarm S**, **Pitisuttithum P**, **Nitayaphan S**, **Kaewkungwal J**, **Chiu J**, **Paris R**, **Premsri N**, **Namwat C**, **de Souza M**, **Adams E**, **Benenson M**, **Gurunathan S**, **Tartaglia J**, **McNeil JG**, **Francis DP**, **Stablein D**, **Birx DL**, **Chunsuttiwat S**, **Khamboonruang C**, **Thongcharoen P**, **Robb ML**, **Michael NL**, **Kunasol P**, **Kim JH**. 2009. Vaccination with ALVAC and AIDSVAX to prevent HIV-1 infection in Thailand. N Engl J Med **361**:2209–2220.

150. **Tomaras GD**, **Haynes BF**. 2010. Strategies for eliciting HIV-1 inhibitory antibodies. Curr

Opin HIV AIDS **5**:421–427.

151. **Aasa-Chapman MMI**, **Holuigue S**, **Aubin K**, **Wong M**, **Jones NA**, **Cornforth D**, **Pellegrino P**, **Newton P**, **Williams I**, **Borrow P**, **McKnight A**. 2005. Detection of antibody-dependent complement-mediated inactivation of both autologous and heterologous virus in primary human immunodeficiency virus type 1 infection. J Virol **79**:2823–2830.

152. **Kedzierska K**, **Mak J**, **Mijch A**, **Cooke I**, **Rainbird M**, **Roberts S**, **Paukovics G**, **Jolley D**, **Lopez A**, **Crowe SM**. 2000. Granulocyte-macrophage colony-stimulating factor augments phagocytosis of Mycobacterium avium complex by human immunodeficiency virus type 1-infected monocytes/macrophages in vitro and in vivo. J Infect Dis **181**:390-394.

153. **Kedzierska K**, **Mak J**, **Jaworowski A**, **Greenway A**, **Violo A**, **Chan HT**, **Hocking J**, **Purcell D**, **Sullivan JS**, **Mills J**, **Crowe S**. 2001. nef-deleted HIV-1 inhibits phagocytosis by monocyte-derived macrophages in vitro but not by peripheral blood monocytes in vivo. AIDS **15**:945–955.

154. **Bomsel M**, **Tudor D**, **Drillet AS**, **Alfsen A**, **Ganor Y**, **Roger MG**, **Mouz N**, **Amacker M**, **Chalifour A**, **Diomede L**, **Devillier G**, **Cong Z**, **Wei Q**, **Gao H**, **Qin C**, **Yang GB**, **Zurbriggen R**, **Lopalco L**, **Fleury S**. 2011. Immunization with HIV-1 gp41 Subunit Virosomes Induces Mucosal Antibodies Protecting Nonhuman Primates against Vaginal SHIV Challenges. Immunity **34**:269–280.

155. **Ackerman ME**, **Dugast A-S**, **Alter G**. 2012. Emerging Concepts on the Role of Innate Immunity in the Prevention and Control of HIV Infection. Annu Rev Med **63**:113-130.

156. **Huber M**, **Trkola A**. 2007. Humoral immunity to HIV-1: Neutralization and beyond. J Intern Med **262**:5-25.

157. **Overbaugh J**, **Morris L**. 2012. The antibody response against HIV-1. Cold Spring Harb Perspect Med **2**:1–17.

158. **Richman DD**, **Wrin T**, **Little SJ**, **Petropoulos CJ**. 2003. Rapid evolution of the neutralizing antibody response to HIV type 1 infection. Proc Natl Acad Sci **100**:4144–4149.

159. **Wei X**, **Decker JM**, **Wang S**, **Hui H**, **Kappes JC**, **Wu X**, **Salazar-Gonzalez JF**, **Salazar MG**, **Kilby JM**, **Saag MS**, **Komarova NL**, **Nowak MA**, **Hahn BH**, **Kwong PD**, **Shaw GM**. 2003. Antibody neutralization and escape by HIV-1. Nature **422**:307–312.

160. **Montefiori DC**, **Zhou IY**, **Barnes B**, **Lake D**, **Hersh EM**, **Masuho Y**, **Lefkowitz LB**. 1991. Homotypic antibody responses to fresh clinical isolates of human immunodeficiency virus. Virology **182**:635–643.

161. **Frost SDW**, **Wrin T**, **Smith DM**, **Kosakovsky Pond SL**, **Liu Y**, **Paxinos E**, **Chappey C**, **Galovich J**, **Beauchaine J**, **Petropoulos CJ**, **Little SJ**, **Richman DD**. 2005. Neutralizing antibody responses drive the evolution of human immunodeficiency virus type 1 envelope during recent HIV infection. Proc Natl Acad Sci **102**:18514–18519.

162. **Gray ES**, **Moore PL**, **Choge IA**, **Decker JM**, **Bibollet-Ruche F**, **Li H**, **Leseka N**, **Treurnicht F**, **Mlisana K**, **Shaw GM**, **Karim SSA**, **Williamson C**, **Morris L**. 2007. Neutralizing antibody responses in acute human immunodeficiency virus type 1 subtype C infection. J Virol **81**:6187–6196.

163. **Moore PL**, **Gray ES**, **Choge IA**, **Ranchobe N**, **Mlisana K**, **Abdool Karim SS**, **Williamson C**, **Morris L**. 2008. The c3-v4 region is a major target of autologous neutralizing antibodies in human immunodeficiency virus type 1 subtype C infection. J Virol **82**:1860–9.

164. **Moore PL**, **Ranchobe N**, **Lambson BE**, **Gray ES**, **Cave E**, **Abrahams M-R**, **Bandawe G**, **Mlisana K**, **Abdool Karim SS**, **Williamson C**, **Morris L**. 2009. Limited neutralizing antibody specificities drive neutralization escape in early HIV-1 subtype C infection. PLoS Pathog **5**:e1000598.

165. **Rong R**, **Bibollet-Ruche F**, **Mulenga J**, **Allen S**, **Blackwell JL**, **Derdeyn CA**. 2007. Role of V1V2 and other human immunodeficiency virus type 1 envelope domains in resistance to autologous neutralization during clade C infection. J Virol **81**:1350–9.

166. **Gray ES**, **Madiga MC**, **Hermanus T**, **Moore PL**, **Wibmer CK**, **Tumba NL**, **Werner L**, **Mlisana K**, **Sibeko S**, **Williamson C**, **Abdool Karim SS**, **Morris L**. 2011. The neutralization breadth of HIV-1 develops incrementally over four years and is associated with CD4+ T cell decline and high viral load during acute infection. J Virol **85**:4828–4840.

167. **Moore PL**, **Gray ES**, **Sheward D**, **Madiga M**, **Ranchobe N**, **Lai Z**, **Honnen WJ**, **Nonyane M**, **Tumba N**, **Hermanus T**, **Sibeko S**, **Mlisana K**, **Abdool Karim SS**, **Williamson C**, **Pinter A**, **Morris L**. 2011. Potent and broad neutralization of HIV-1 subtype C by plasma antibodies targeting a quaternary epitope including residues in the V2 loop. J Virol **85**:3128–3141.

168. **Mikell I**, **Sather DN**, **Kalams S a**, **Altfeld M**, **Alter G**, **Stamatatos L**. 2011. Characteristics of the earliest cross-neutralizing antibody response to HIV-1. PLoS Pathog **7**:e1001251.

169. **Doria-Rose N a**, **Klein RM**, **Daniels MG**, **O'Dell S**, **Nason M**, **Lapedes A**, **Bhattacharya T**, **Migueles SA**, **Wyatt RT**, **Korber BT**, **Mascola JR**, **Connors M**. 2010. Breadth of human immunodeficiency virus-specific neutralizing activity in sera: clustering analysis and association with clinical variables. J Virol **84**:1631–1636.

170. **Burton DR**, **Weiss RA**. 2010. AIDS/HIV. A boost for HIV vaccine design. Science **329**:770–773.

171. **Hraber P**, **Seaman MS**, **Bailer RT**, **Mascola JR**, **Montefiori DC**, **Korber BT**. 2014. Prevalence of broadly neutralizing antibody responses during chronic HIV-1 infection. AIDS **28**:163–9.

172. **Zhou T**, **Georgiev I**, **Wu X**, **Yang Z-Y**, **Dai K**, **Finzi A**, **Kwon Y Do**, **Scheid JF**, **Shi W**, **Xu L**, **Yang Y**, **Zhu J**, **Nussenzweig MC**, **Sodroski J**, **Shapiro L**, **Nabel GJ**, **Mascola JR**, **Kwong PD**. 2010. Structural basis for broad and potent neutralization of HIV-1 by antibody VRC01. Science **329**:811–817.

173. **Miller MD**, **Geleziunas R**, **Bianchi E**, **Lennard S**, **Hrin R**, **Zhang H**, **Lu M**, **An Z**, **Ingallinella P**, **Finotto M**, **Mattu M**, **Finnefrock AC**, **Bramhill D**, **Cook J**, **Eckert DM**, **Hampton R**, **Patel M**, **Jarantow S**, **Joyce J**, **Ciliberto G**, **Cortese R**, **Lu P**, **Strohl W**, **Schleif W**, **McElhaugh M**, **Lane S**, **Lloyd C**, **Lowe D**, **Osbourn J**, **Vaughan T**, **Emini E**, **Barbato G**, **Kim PS**, **Hazuda DJ**, **Shiver JW**, **Pessi A**. 2005. A human monoclonal antibody neutralizes diverse HIV-1 isolates by binding a critical gp41 epitope. Proc Natl Acad Sci **102**:14759–14764.

174. **Tomaras GD**, **Haynes BF**. 2009. HIV-1-specific antibody responses during acute and chronic HIV-1 infection. Curr Opin HIV AIDS **4**:373–379.

175. **Liu J**, **Bartesaghi A**, **Borgnia MJ**, **Sapiro G**, **Subramaniam S**. 2008. Molecular architecture of native HIV-1 gp120 trimers. Nature **455**:109–113.

176. **Pettersen EF**, **Goddard TD**, **Huang CC**, **Couch GS**, **Greenblatt DM**, **Meng EC**, **Ferrin TE**. 2004. UCSF Chimera: A visualization system for exploratory research and analysis. J Comput Chem **25**:1605–1612.

177. **McLellan JS**, **Pancera M**, **Carrico C**, **Gorman J**, **Julien J-P**, **Khayat R**, **Louder R**, **Pejchal R**, **Sastry M**, **Dai K**, **O'Dell S**, **Patel N**, **Shahzad-ul-Hussan S**, **Yang Y**, **Zhang B**, **Zhou T**, **Zhu J**, **Boyington JC**, **Chuang G-Y**, **Diwanji D**, **Georgiev I**, **Do Kwon Y**, **Lee D**, **Louder MK**, **Moquin S**, **Schmidt SD**, **Yang Z-Y**, **Bonsignori M**, **Crump JA**, **Kapiga SH**, **Sam NE**, **Haynes BF**, **Burton DR**, **Koff WC**, **Walker LM**, **Phogat S**, **Wyatt R**, **Orwenyo J**, **Wang L-X**, **Arthos J**, **Bewley CA**, **Mascola JR**, **Nabel GJ**, **Schief WR**, **Ward AB**, **Wilson IA**, **Kwong PD**. 2011. Structure of HIV-1 gp120 V1/V2 domain with broadly neutralizing antibody PG9. Nature **480**:336-343.

178. **Pejchal R**, **Doores KJ**, **Walker LM**, **Khayat R**, **Huang P-S**, **Wang S-K**, **Stanfield RL**, **Julien J-P**, **Ramos A**, **Crispin M**, **Depetris R**, **Katpally U**, **Marozsan A**, **Cupo A**, **Maloveste S**, **Liu Y**, **McBride R**, **Ito Y**, **Sanders RW**, **Ogohara C**, **Paulson JC**, **Feizi T**, **Scanlan CN**, **Wong C**, **Moore JP**, **Olson WC**, **Ward AB**, **Poignard P**, **Schief WR**, **Burton DR**, **Wilson IA**. 2011. A Potent and Broad Neutralizing Antibody Recognizes and Penetrates the HIV Glycan Shield. Science **334**:1097-1103.

179. **Scharf L**, **Scheid JF**, **Lee JH**, **West AP**, **Chen C**, **Gao H**, **Gnanapragasam PNP**, **Mares R**, **Seaman MS**, **Ward AB**, **Nussenzweig MC**, **Bjorkman PJ**. 2014. Antibody 8ANC195 Reveals a Site of Broad Vulnerability on the HIV-1 Envelope Spike. Cell Rep **7**:785–795.

180. **Blattner C**, **Lee JH**, **Sliepen K**, **Derking R**, **Falkowska E**, **de la Peña AT**, **Cupo A**, **Julien J-P**, **van Gils M**, **Lee PS**, **Peng W**, **Paulson JC**, **Poignard P**, **Burton DR**, **Moore JP**, **Sanders RW**, **Wilson IA**, **Ward AB**. 2014. Structural Delineation of a Quaternary, Cleavage-Dependent Epitope at the gp41-gp120 Interface on Intact HIV-1 Env Trimers. Immunity **40**:669–680.

181. **Takai T**. 2002. Roles of Fc receptors in autoimmunity. Nat Rev Immunol **2**:580–592.

182. **McCullough KC**, **Parkinson D**, **Crowther JR**. 1988. Opsonization-enhanced phagocytosis of foot-and-mouth disease virus. Immunology **65**:187–191.

183. **Baum LL**, **Cassutt KJ**, **Knigge K**, **Khattri R**, **Margolick J**, **Rinaldo C**, **Kleeberger CA**, **Nishanian P**, **Henrard DR**, **Phair J**. 1996. HIV-1 gp120-specific antibody-dependent cell-mediated cytotoxicity correlates with rate of disease progression. J Immunol **157**:2168–2173.

184. **Huber VC**, **Lynch JM**, **Bucher DJ**, **Le J**, **Metzger DW**. 2001. Fc receptor-mediated phagocytosis makes a significant contribution to clearance of influenza virus infections. J Immunol **166**:7381–7388.

185. **Chu C-F**, **Meador MG**, **Young CG**, **Strasser JE**, **Bourne N**, **Milligan GN**. 2008. Antibody-mediated protection against genital herpes simplex virus type 2 disease in mice by Fc gamma receptor-dependent and -independent mechanisms. J Reprod Immunol **78**:58–67.

186. **Lambotte O**, **Ferrari G**, **Moog C**, **Yates NL**, **Liao H-X**, **Parks RJ**, **Hicks CB**, **Owzar K**, **Tomaras GD**, **Montefiori DC**, **Haynes BF**, **Delfraissy J-F**. 2009. Heterogeneous neutralizing antibody and antibody-dependent cell cytotoxicity responses in HIV-1 elite controllers. AIDS **23**:897–906.

187. **Gessner JE**, **Heiken H**, **Tamm A**, **Schmidt RE**. 1998. The IgG Fc receptor family. Ann Hematol **76**:231-248.

188. **Nimmerjahn F**, **Ravetch J V**. 2005. Divergent immunoglobulin g subclass activity through selective Fc receptor binding. Science **310**:1510–1512.

189. **Asmal M**, **Sun Y**, **Lane S**, **Yeh W**, **Schmidt SD**, **Mascola JR**, **Letvin NL**. 2011. Antibody-dependent cell-mediated viral inhibition emerges after simian immunodeficiency virus SIVmac251 infection of rhesus monkeys coincident with gp140-binding antibodies and is effective against neutralization-resistant viruses. J Virol **85**:5465–5475.

190. **Ahmad A**, **Menezes J**. 1996. Antibody-dependent cellular cytotoxicity in HIV infections. FASEB J **10**:258–266.

191. **Bonsignori M**, **Pollara J**, **Moody MA**, **Alpert MD**, **Chen X**, **Hwang K-K**, **Gilbert PB**, **Huang Y**, **Gurley TC**, **Kozink DM**, **Marshall DJ**, **Whitesides JF**, **Tsao C-Y**, **Kaewkungwal J**, **Nitayaphan S**, **Pitisuttithum P**, **Rerks-Ngarm S**, **Kim JH**, **Michael NL**, **Tomaras GD**, **Montefiori DC**, **Lewis GK**, **DeVico A**, **Evans DT**, **Ferrari G**, **Liao H-X**, **Haynes BF**. 2012. Antibody-Dependent Cellular Cytotoxicity-Mediating Antibodies from an HIV-1 Vaccine Efficacy Trial Target Multiple Epitopes and Preferentially Use the VH1 Gene Family. J Virol **86**:11521-11532.

192. **Alter G**, **Teigen N**, **Ahern R**, **Streeck H**, **Meier A**, **Rosenberg ES**, **Altfeld M**. 2007. Evolution of innate and adaptive effector cell functions during acute HIV-1 infection. J Infect Dis **195**:1452–1460.

193. **Altfeld M**, **Fadda L**, **Frleta D**, **Bhardwaj N**. 2011. DCs and NK cells: critical effectors in the immune response to HIV-1. Nat Rev Immunol **11**:176–186.

194. **Alter G**, **Altfeld M**. 2009. NK cells in HIV-1 infection: Evidence for their role in the control of HIV-1 infection. J Intern Med **265**:29-42.

195. **Forthal DN**, **Moog C**. 2009. Fc receptor-mediated antiviral antibodies. Curr Opin HIV AIDS **4**:388–393.

196. **Holl V**, **Hemmerter S**, **Burrer R**, **Schmidt S**, **Bohbot A**, **Aubertin A-M**, **Moog C**. 2004. Involvement of Fc gamma RI (CD64) in the mechanism of HIV-1 inhibition by polyclonal IgG purified from infected patients in cultured monocyte-derived macrophages. J Immunol **173**:6274–6283.

197. **Holl V**, **Peressin M**, **Schmidt S**, **Decoville T**, **Zolla-Pazner S**, **Aubertin AM**, **Moog C**. 2006. Efficient inhibition of HIV-1 replication in human immature monocyte-derived dendritic cells by purified anti-HIV-1 IgG without induction of maturation. Blood **107**:4466–4474.

198. **Dugast A-S**, **Tonelli A**, **Berger CT**, **Ackerman ME**, **Sciaranghella G**, **Liu Q**, **Sips M**, **Toth I**, **Piechocka-Trocha A**, **Ghebremichael M**, **Alter G**. 2011. Decreased Fc receptor expression on innate immune cells is associated with impaired antibody-mediated cellular phagocytic activity in chronically HIV-1 infected individuals. Virology **415**:160–167.

199. **Holl V**, **Peressin M**, **Decoville T**, **Schmidt S**, **Zolla-Pazner S**, **Aubertin A-M**, **Moog C**. 2006. Nonneutralizing antibodies are able to inhibit human immunodeficiency virus type 1 replication in macrophages and immature dendritic cells. J Virol **80**:6177–6181.

200. **Brown BK**, **Wieczorek L**, **Kijak G**, **Lombardi K**, **Currier J**, **Wesberry M**, **Kappes JC**, **Ngauy V**, **Marovich M**, **Michael N**, **Ochsenbauer C**, **Montefiori DC**, **Polonis VR**. 2012. The role of natural killer (NK) cells and nk cell receptor polymorphisms in the assessment of HIV-1 neutralization. PLoS One **7**:e29454.

201. **Hessell AJ**, **Hangartner L**, **Hunter M**, **Havenith CEG**, **Beurskens FJ**, **Bakker JM**, **Lanigan CMS**, **Landucci G**, **Forthal DN**, **Parren PWHI**, **Marx PA**, **Burton DR**. 2007. Fc receptor but not complement binding is important in antibody protection against HIV. Nature **449**:101–104.

202. **Hessell AJ**, **Poignard P**, **Hunter M**, **Hangartner L**, **Tehrani DM**, **Bleeker WK**, **Parren PWHI**, **Marx P a**, **Burton DR**. 2009. Effective, low-titer antibody protection against low-dose repeated mucosal SHIV challenge in macaques. Nat Med **15**:951–954.

203. **Alsmadi O**, **Tilley SA**. 1998. Antibody-dependent cellular cytotoxicity directed against cells expressing human immunodeficiency virus type 1 envelope of primary or laboratory-adapted strains by human and chimpanzee monoclonal antibodies of different epitope specificities. J Virol **72**:286–293.

204. **Forthal DN**, **Landucci G**, **Phan TB**, **Becerra J**. 2005. Interactions between natural killer cells and antibody Fc result in enhanced antibody neutralization of human immunodeficiency virus type 1. J Virol **79**:2042–2049.

205. **Sun Y**, **Asmal M**, **Lane S**, **Permar SR**, **Schmidt SD**, **Mascola JR**, **Letvin NL**. 2011. Antibody-dependent cell-mediated cytotoxicity in simian immunodeficiency virus-infected rhesus monkeys. J Virol **85**:6906–6912.

206. **Hidajat R**, **Xiao P**, **Zhou Q**, **Venzon D**, **Summers LE**, **Kalyanaraman VS**, **Montefiori DC**, **Robert-Guroff M**. 2009. Correlation of vaccine-elicited systemic and mucosal nonneutralizing antibody activities with reduced acute viremia following intrarectal simian immunodeficiency virus SIVmac251 challenge of rhesus macaques. J Virol **83**:791–801.

207. **Chung AW**, **Navis M**, **Isitman G**, **Wren L**, **Silvers J**, **Amin J**, **Kent SJ**, **Stratov I**. 2011. Activation of NK Cells by ADCC Antibodies and HIV Disease Progression. J Acquir Immune Defic Syndr **58**:127–131.

208. **Forthal DN**, **Landucci G**, **Daar ES**. 2001. Antibody from patients with acute human immunodeficiency virus (HIV) infection inhibits primary strains of HIV type 1 in the presence of natural-killer effector cells. J Virol **75**:6953–6961.

209. **Forthal DN**, **Landucci G**, **Haubrich R**, **Keenan B**, **Kuppermann BD**, **Tilles JG**, **Kaplan J**. 1999. Antibody-dependent cellular cytotoxicity independently predicts survival in severely immunocompromised human immunodeficiency virus-infected patients. J Infect Dis **180**:1338–1341.

210. **Alpert MD**, **Harvey JD**, **Lauer WA**, **Reeves RK**, **Piatak M**, **Carville A**, **Mansfield KG**, **Lifson JD**, **Li W**, **Desrosiers RC**, **Johnson RP**, **Evans DT**. 2012. ADCC Develops Over Time during Persistent Infection with Live-Attenuated SIV and Is Associated with Complete Protection against SIVmac251 Challenge. PLoS Pathog **8**:e1002890.

211. **Banks ND**, **Kinsey N**, **Clements J**, **Hildreth JEK**. 2002. Sustained antibody-dependent cell-mediated cytotoxicity (ADCC) in SIV-infected macaques correlates with delayed progression to AIDS. AIDS Res Hum Retroviruses **18**:1197–1205.

212. **Gómez-Román VR**, **Patterson LJ**, **Venzon D**, **Liewehr D**, **Aldrich K**, **Florese R**, **Robert-Guroff M**. 2005. Vaccine-elicited antibodies mediate antibody-dependent cellular cytotoxicity correlated with significantly reduced acute viremia in rhesus macaques challenged with SIVmac251. J Immunol **174**:2185–2189.

213. **Florese RH**, **Demberg T**, **Xiao P**, **Kuller L**, **Larsen K**, **Summers LE**, **Venzon D**, **Cafaro A**, **Ensoli B**, **Robert-Guroff M**. 2009. Contribution of nonneutralizing vaccine-elicited antibody activities to improved protective efficacy in rhesus macaques immunized with Tat/Env compared with multigenic vaccines. J Immunol **182**:3718–3727.

214. **Xiao P**, **Zhao J**, **Patterson LJ**, **Brocca-Cofano E**, **Venzon D**, **Kozlowski PA**, **Hidajat R**, **Demberg T**, **Robert-Guroff M**. 2010. Multiple vaccine-elicited nonneutralizing antienvelope antibody activities contribute to protective efficacy by reducing both acute and chronic viremia following simian/human immunodeficiency virus SHIV89.6P challenge in

rhesus macaques. J Virol **84**:7161–7173.

215. **Broliden K**, **Sievers E**, **Tovo PA**, **Moschese V**, **Scarlatti G**, **Broliden PA**, **Fundaro C**, **Rossi P**. 1993. Antibody-dependent cellular cytotoxicity and neutralizing activity in sera of HIV-1-infected mothers and their children. Clin Exp Immunol **93**:56–64.

216. **Mabuka J**, **Nduati R**, **Odem-Davis K**, **Peterson D**, **Overbaugh J**. 2012. HIV-specific antibodies capable of ADCC are common in breastmilk and are associated with reduced risk of transmission in women with high viral loads. PLoS Pathog **8**:1–13.

217. **Tyler DS**, **Stanley SD**, **Nastala CA**, **Austin AA**, **Bartlett JA**, **Stine KC**, **Lyerly HK**, **Bolognesi DP**, **Weinhold KJ**. 1990. Alterations in antibody-dependent cellular cytotoxicity during the course of HIV-1 infection. J Immunol **144**:3375–3384.

218. **Ahmad R**, **Sindhu STAK**, **Toma E**, **Morisset R**, **Vincelette J**, **Menezes J**, **Ahmad A**. 2001. Evidence for a correlation between antibody-dependent cellular cytotoxicity-mediating anti-HIV-1 antibodies and prognostic predictors of HIV infection. J Clin Immunol **21**:227–233.

219. **Ljunggren K**, **Moschese V**, **Broliden PA**, **Giaquinto C**, **Quinti I**, **Fenyö EM**, **Wahren B**, **Rossi P**, **Jondal M**. 1990. Antibodies mediating cellular cytotoxicity and neutralization correlate with a better clinical stage in children born to human immunodeficiency virus-infected mothers. J Infect Dis **161**:198–202.

220. **Ahmad A**, **Morisset R**, **Thomas R**, **Menezes J**. 1994. Evidence for a defect of antibody-dependent cellular cytotoxic (ADCC) effector function and anti-HIV gp120/41-specific ADCC-mediating antibody titres in HIV-infected individuals. J Acquir Immune Defic Syndr **7**:428–437.

221. **Hirsch VM**, **Santra S**, **Goldstein S**, **Plishka R**, **Buckler-White A**, **Seth A**, **Ourmanov I**, **Brown CR**, **Engle R**, **Montefiori D**, **Glowczwskie J**, **Kunstman K**, **Wolinsky S**, **Letvin NL**. 2004. Immune failure in the absence of profound CD4+ T-lymphocyte depletion in simian immunodeficiency virus-infected rapid progressor macaques. J Virol **78**:275–284.

222. **Gottardo R**, **Bailer RT**, **Korber BT**, **Gnanakaran S**, **Phillips J**, **Shen X**, **Tomaras GD**, **Turk E**, **Imholte G**, **Eckler L**, **Wenschuh H**, **Zerweck J**, **Greene K**, **Gao H**, **Berman PW**, **Francis D**, **Sinangil F**, **Lee C**, **Nitayaphan S**, **Rerks-Ngarm S**, **Kaewkungwal J**,

Pitisuttithum P, **Tartaglia J**, **Robb ML**, **Michael NL**, **Kim JH**, **Zolla-Pazner S**, **Haynes BF**, **Mascola JR**, **Self S**, **Gilbert P**, **Montefiori DC**. 2013. Plasma IgG to Linear Epitopes in the V2 and V3 Regions of HIV-1 gp120 Correlate with a Reduced Risk of Infection in the RV144 Vaccine Efficacy Trial. PLoS One **8**:e75665.

223. **Burton DR**, **Hessell AJ**, **Keele BF**, **Klasse PJ**, **Ketas TA**, **Moldt B**, **Dunlop DC**, **Poignard P**, **Doyle LA**, **Cavacini L**, **Veazey RS**, **Moore JP**. 2011. Limited or no protection by weakly or nonneutralizing antibodies against vaginal SHIV challenge of macaques compared with a strongly neutralizing antibody. Proc Natl Acad Sci **108**:11181–11186.

224. **Barouch DH**, **Liu J**, **Li H**, **Maxfield LF**, **Abbink P**, **Lynch DM**, **Iampietro MJ**, **Sanmiguel A**, **Seaman MS**, **Ferrari G**, **Forthal DN**, **Ourmanov I**, **Hirsch VM**, **Carville A**, **Mansfield KG**, **Stablein D**, **Pau MG**, **Schuitemaker H**, **Sadoff JC**, **Billings EM**, **Rao M**, **Robb ML**, **Kim JH**, **Marovich MA**, **Goudsmit J**, **Michael NL**. 2012. Vaccine Protection Against Acquisition of Neutralization-Resistant SIV Challenges in Rhesus Monkeys. Nature **482**:3–8.

225. **Demberg T**, **Florese RH**, **Heath MJ**, **Larsen K**, **Kalisz I**, **Kalyanaraman VS**, **Lee EM**, **Pal R**, **Venzon D**, **Grant R**, **Patterson LJ**, **Korioth-Schmitz B**, **Buzby A**, **Dombagoda D**, **Montefiori DC**, **Letvin NL**, **Cafaro A**, **Ensoli B**, **Robert-Guroff M**. 2007. A replication-competent adenovirus-human immunodeficiency virus (Ad-HIV) *tat* and Ad-HIV *env* priming/Tat and Envelope protein boosting regimen elicits enhanced protective efficacy against simian/human immunodeficiency virus $SHIV_{89.6P}$ challenge in rhesus macaques. J Virol **81**:3414–3427.

226. **Alsmadi O**, **Herz R**, **Murphy E**, **Pinter A**, **Tilley SA**. 1997. A novel antibody-dependent cellular cytotoxicity epitope in gp120 is identified by two monoclonal antibodies isolated from a long-term survivor of human immunodeficiency virus type 1 infection. J Virol **71**:925–933.

227. **Koup RA**, **Sullivan JL**, **Levine PH**, **Brewster F**, **Mahr A**, **Mazzara G**, **McKenzie S**, **Panicali D**. 1989. Antigenic specificity of antibody-dependent cell-mediated cytotoxicity directed against human immunodeficiency virus in antibody-positive sera. J Virol **63**:584–590.

228. **Pollara J**, **Bonsignori M**, **Moody MA**, **Pazgier M**, **Haynes BF**, **Ferrari G**. 2013. Epitope specificity of human immunodeficiency virus-1 antibody dependent cellular cytotoxicity [ADCC] responses. Curr HIV Res **11**:378–87.

229. **Ferrari G**, **Pollara J**, **Kozink D**, **Harms T**, **Drinker M**, **Freel S**, **Moody MA**, **Alam SM**, **Tomaras GD**, **Ochsenbauer C**, **Kappes JC**, **Shaw GM**, **Hoxie JA**, **Robinson JE**, **Haynes BF**. 2011. An HIV-1 gp120 envelope human monoclonal antibody that recognizes a C1 conformational epitope mediates potent antibody-dependent cellular cytotoxicity (ADCC) activity and defines a common ADCC epitope in human HIV-1 serum. J Virol **85**:7029–7036.

230. **Hezareh M**, **Hessell AJ**, **Jensen RC**, **van de Winkel JG**, **Parren PW**. 2001. Effector function activities of a panel of mutants of a broadly neutralizing antibody against human immunodeficiency virus type 1. J Virol **75**:12161–12168.

231. **Liao HX**, **Bonsignori M**, **Alam SM**, **McLellan JS**, **Tomaras GD**, **Moody MA**, **Kozink DM**, **Hwang KK**, **Chen X**, **Tsao CY**, **Liu P**, **Lu X**, **Parks RJ**, **Montefiori DC**, **Ferrari G**, **Pollara J**, **Rao M**, **Peachman KK**, **Santra S**, **Letvin NL**, **Karasavvas N**, **Yang ZY**, **Dai K**, **Pancera M**, **Gorman J**, **Wiehe K**, **Nicely NI**, **Rerks-Ngarm S**, **Nitayaphan S**, **Kaewkungwal J**, **Pitisuttithum P**, **Tartaglia J**, **Sinangil F**, **Kim JH**, **Michael NL**, **Kepler TB**, **Kwong PD**, **Mascola JR**, **Nabel GJ**, **Pinter A**, **Zolla-Pazner S**, **Haynes BF**. 2013. Vaccine Induction of Antibodies against a Structurally Heterogeneous Site of Immune Pressure within HIV-1 Envelope Protein Variable Regions 1 and 2. Immunity **38**:176–186.

232. **Isitman G**, **Stratov I**, **Kent SJ**. 2012. Antibody-dependent cellular cytotoxicity and nk cell-driven immune escape in HIV infection: Implications for HIV vaccine development. Adv Virol.

233. **Chung AW**, **Isitman G**, **Navis M**, **Kramski M**, **Center RJ**, **Kent SJ**, **Stratov I**. 2011. Immune escape from HIV-specific antibody-dependent cellular cytotoxicity (ADCC) pressure. Proc Natl Acad Sci **108**:7505–7510.

234. **Moog C**, **Dereuddre-Bosquet N**, **Teillaud J-L**, **Biedma ME**, **Holl V**, **Van Ham G**, **Heyndrickx L**, **Van Dorsselaer A**, **Katinger D**, **Vcelar B**, **Zolla-Pazner S**, **Mangeot I**, **Kelly C**, **Shattock RJ**, **Le Grand R**. 2014. Protective effect of vaginal application of

neutralizing and nonneutralizing inhibitory antibodies against vaginal SHIV challenge in macaques. Mucosal Immunol **7**:46–56.

235. **Guan Y**, **Pazgier M**, **Sajadi MM**, **Kamin-Lewis R**, **Al-Darmarki S**, **Flinko R**, **Lovo E**, **Wu X**, **Robinson JE**, **Seaman MS**, **Fouts TR**, **Gallo RC**, **DeVico AL**, **Lewis GK**. 2013. Diverse specificity and effector function among human antibodies to HIV-1 envelope glycoprotein epitopes exposed by CD4 binding. Proc Natl Acad Sci **110**:E69-78.

236. **Trkola A**, **Purtscher M**, **Muster T**, **Ballaun C**, **Buchacher A**, **Sullivan N**, **Srinivasan K**, **Sodroski J**, **Moore JP**, **Katinger H**. 1996. Human monoclonal antibody 2G12 defines a distinctive neutralization epitope on the gp120 glycoprotein of human immunodeficiency virus type 1. J Virol **70**:1100–1108.

237. **Gómez-Román VR**, **Florese RH**, **Patterson LJ**, **Peng B**, **Venzon D**, **Aldrich K**, **Robert-Guroff M**. 2006. A simplified method for the rapid fluorometric assessment of antibody-dependent cell-mediated cytotoxicity. J Immunol Methods **308**:53–67.

238. **Stratov I**, **Chung A**, **Kent SJ**. 2008. Robust NK cell-mediated human immunodeficiency virus (HIV)-specific antibody-dependent responses in HIV-infected subjects. J Virol **82**:5450–5459.

239. **Pollara J**, **Hart L**, **Brewer F**, **Pickeral J**, **Packard BZ**, **Hoxie JA**, **Komoriya A**, **Ochsenbauer C**, **Kappes JC**, **Roederer M**, **Huang Y**, **Weinhold KJ**, **Tomaras GD**, **Haynes BF**, **Montefiori DC**, **Ferrari G**. 2011. High-throughput quantitative analysis of HIV-1 and SIV-specific ADCC-mediating antibody responses. Cytom Part A **79 A**:603–612.

240. **Pollara J**, **Bonsignori M**, **Moody MA**, **Liu P**, **Alam SM**, **Hwang K-K**, **Gurley TC**, **Kozink DM**, **Armand LC**, **Marshall DJ**, **Whitesides JF**, **Kaewkungwal J**, **Nitayaphan S**, **Pitisuttithum P**, **Rerks-Ngarm S**, **Robb ML**, **O'Connell RJ**, **Kim JH**, **Michael NL**, **Montefiori DC**, **Tomaras GD**, **Liao H-X**, **Haynes BF**, **Ferrari G**. 2014. HIV-1 Vaccine-Induced C1 and V2 Env-Specific Antibodies Synergize for Increased Antiviral Activities. J Virol **88**:7715–26.

241. **Bar KJ**, **Tsao C yen**, **Iyer SS**, **Decker JM**, **Yang Y**, **Bonsignori M**, **Chen X**, **Hwang KK**, **Montefiori DC**, **Liao HX**, **Hraber P**, **Fischer W**, **Li H**, **Wang S**, **Sterrett S**, **Keele BF**, **Ganusov V V**, **Perelson AS**, **Korber BT**, **Georgiev I**, **McLellan JS**, **Pavlicek JW**, **Gao F**, **Haynes BF**, **Hahn BH**, **Kwong PD**, **Shaw GM**. 2012. Early low-titer neutralizing antibodies impede HIV-1 replication and select for virus escape. PLoS Pathog **8**:e1002721.

242. **Abela IA**, **Berlinger L**, **Schanz M**, **Reynell L**, **Günthard HF**, **Rusert P**, **Trkola A**. 2012. Cell-cell transmission enables HIV-1 to evade inhibition by potent CD4bs directed antibodies. PLoS Pathog **8**:e1002634.

243. **Reh L**, **Magnus C**, **Schanz M**, **Weber J**, **Uhr T**, **Rusert P**, **Trkola A**. 2015. Capacity of Broadly Neutralizing Antibodies to Inhibit HIV-1 Cell-Cell Transmission Is Strain- and Epitope-Dependent. PLOS Pathog **11**:e1004966.

244. **Chen P**, **Hübner W**, **Spinelli MA**, **Chen BK**. 2007. Predominant mode of human immunodeficiency virus transfer between T cells is mediated by sustained Env-dependent neutralization-resistant virological synapses. J Virol **81**:12582–95.

245. **Durham ND**, **Yewdall AW**, **Chen P**, **Lee R**, **Zony C**, **Robinson JE**, **Chen BK**. 2012. Neutralization resistance of virological synapse-mediated HIV-1 Infection is regulated by the gp41 cytoplasmic tail. J Virol **86**:7484–95.

246. **Gombos RB**, **Kolodkin-Gal D**, **Eslamizar L**, **Owuor JO**, **Mazzola E**, **Gonzalez AM**, **Korioth-Schmitz B**, **Gelman RS**, **Montefiori DC**, **Haynes BF**, **Schmitz JE**. 2015. Inhibitory Effect of Individual or Combinations of Broadly Neutralizing Antibodies and Antiviral Reagents against Cell-Free and Cell-to-Cell HIV-1 Transmission. J Virol **89**:7813–28.

247. **Malbec M**, **Porrot F**, **Rua R**, **Horwitz J**, **Klein F**, **Halper-Stromberg A**, **Scheid JF**, **Eden C**, **Mouquet H**, **Nussenzweig MC**, **Schwartz O**. 2013. Broadly neutralizing antibodies that inhibit HIV-1 cell to cell transmission. J Exp Med **210**:2813–2821.

248. **Li H**, **Zony C**, **Chen P**, **Chen BK**. 2017. Reduced Potency and Incomplete Neutralization of Broadly Neutralizing Antibodies against Cell-to-Cell Transmission of HIV-1 with Transmitted Founder Envs. J Virol **91**:JVI.02425-16.

249. **Sattentau Q**. 2008. Avoiding the void: cell-to-cell spread of human viruses. Nat Rev

Microbiol **6**:815–826.

250. **Jolly C**, **Kashefi K**, **Hollinshead M**, **Sattentau QJ**. 2004. HIV-1 Cell to Cell Transfer across an Env-induced, Actin-dependent Synapse. J Exp Med **199**:283–293.

251. **Jolly C**, **Sattentau QJ**. 2004. Retroviral Spread by Induction of Virological Synapses. Traffic **5**:643–650.

252. **Sato H**, **Orenstein J**, **Dimitrov D**, **Martin M**. 1992. Cell-to-cell spread of HIV-1 occurs within minutes and may not involve the participation of virus particles. Virology **186**:712–24.

253. **Dimitrov DS**, **Willey RL**, **Sato H**, **Chang LJ**, **Blumenthal R**, **Martin MA**. 1993. Quantitation of human immunodeficiency virus type 1 infection kinetics. J Virol **67**:2182–90.

254. **Mazurov D**, **Ilinskaya A**, **Heidecker G**, **Lloyd P**, **Derse D**. 2010. Quantitative Comparison of HTLV-1 and HIV-1 Cell-to-Cell Infection with New Replication Dependent Vectors. PLoS Pathog **6**:e1000788.

255. **van Loggerenberg F**, **Mlisana K**, **Williamson C**, **Auld SC**, **Morris L**, **Gray CM**, **Karim QA**, **Grobler A**, **Barnabas N**, **Iriogbe I**, **Abdool Karim SS**. 2008. Establishing a cohort at high risk of HIV infection in South Africa: Challenges and experiences of the CAPRISA 002 acute infection study. PLoS One **3**:e1954.

256. **Jabara CB**, **Jones CD**, **Roach J**, **Anderson JA**, **Swanstrom R**. 2011. Accurate sampling and deep sequencing of the HIV-1 protease gene using a Primer ID. Proc Natl Acad Sci **108**:20166-20171.

257. **Wibmer CK**, **Gorman J**, **Anthony CS**, **Mkhize NN**, **Druz A**, **York T**, **Schmidt SD**, **Labuschagne P**, **Louder MK**, **Bailer RT**, **Abdool Karim SS**, **Mascola JR**, **Williamson C**, **Moore PL**, **Kwong PD**, **Morris L**. 2016. Structure of an N276-dependent HIV-1 Neutralizing Antibody Targeting a Rare V5 Glycan Hole adjacent to the CD4 Binding Site. J Virol **105**:JVI.01357-16.

258. **Blankenberg D**, **Gordon A**, **Von Kuster G**, **Coraor N**, **Taylor J**, **Nekrutenko A**, **Team G**. 2010. Manipulation of FASTQ data with galaxy. Bioinformatics **26**:1783–1785.

259. **Blankenberg D**, **Kuster G Von**, **Coraor N**, **Ananda G**, **Lazarus R**, **Mangan M**, **Nekrutenko A**, **Taylor J**. 2010. Galaxy: A web-based genome analysis tool for experimentalists. Curr Protoc Mol Biol **Chapter 19**:Unit 19.10.1-21.

260. **Giardine B**, **Riemer C**, **Hardison RC**, **Burhans R**, **Elnitski L**, **Shah P**, **Zhang Y**, **Blankenberg D**, **Albert I**, **Taylor J**, **Miller W**, **Kent WJ**, **Nekrutenko A**. 2005. Galaxy: A platform for interactive large-scale genome analysis. Genome Res **15**:1451–1455.

261. **Zhang J**, **Kobert K**, **Flouri T**, **Stamatakis A**. 2014. PEAR: A fast and accurate Illumina Paired-End reAd mergeR. Bioinformatics **30**:614–620.

262. **Katoh K**, **Standley DM**. 2013. MAFFT multiple sequence alignment software version 7: Improvements in performance and usability. Mol Biol Evol **30**:772–780.

263. **Ranwez V**, **Harispe S**, **Delsuc F**, **Douzery EJP**. 2011. MACSE: Multiple alignment of coding SEquences accounting for frameshifts and stop codons. PLoS One **6**:e22594.

264. **Hall TA**. 1999. BioEdit: a user-friendly biological sequence alignment editor and analysis program for Windows 95/98/NT. Nucleic acids Symposium Series No. 41.

265. **Murrell B**, **Moola S**, **Mabona A**, **Weighill T**, **Sheward D**, **Kosakovsky Pond SL**, **Scheffler K**. 2013. FUBAR: A Fast, Unconstrained Bayesian AppRoximation for inferring selection. Mol Biol Evol **30**:1196–1205.

266. **Kosakovsky Pond SL**, **Frost SDW**, **Muse S V.** 2005. HyPhy: Hypothesis testing using phylogenies. Bioinformatics **21**:676–679.

267. **Lin J**. 1991. Divergence measures based on the Shannon entropy. IEEE Trans Inf Theory **37**:145–151.

268. **Salazar-Gonzalez JF**, **Bailes E**, **Pham KT**, **Salazar MG**, **Guffey MB**, **Keele BF**, **Derdeyn CA**, **Farmer P**, **Hunter E**, **Allen S**, **Manigart O**, **Mulenga J**, **Anderson JA**, **Swanstrom R**, **Haynes BF**, **Athreya GS**, **Korber BTM**, **Sharp PM**, **Shaw GM**, **Hahn BH**. 2008. Deciphering human immunodeficiency virus type 1 transmission and early envelope diversification by single-genome amplification and sequencing. J Virol **82**:3952–3970.

269. **Li M**, **Gao F**, **Mascola JR**, **Stamatatos L**, **Polonis VR**, **Koutsoukos M**, **Voss G**, **Goepfert P**, **Gilbert P**, **Greene KM**, **Bilska M**, **Kothe DL**, **Salazar-gonzalez JF**, **Wei X**, **Decker JM**, **Hahn BH**, **Montefiori DC**. 2005. Human Immunodeficiency Virus Type 1 env Clones from Acute and Early Subtype B Infections for Standardized Assessments of Vaccine-Elicited Neutralizing Antibodies **79**:10108–10125.

270. **Edmonds TG**, **Ding H**, **Yuan X**, **Wei Q**, **Smith KS**, **Conway JA**, **Wieczorek L**, **Brown B**, **Polonis V**, **West JT**, **Montefiori DC**, **Kappes JC**, **Ochsenbauer C**. 2010. Replication competent molecular clones of HIV-1 expressing Renilla luciferase facilitate the analysis of antibody inhibition in PBMC. Virology **408**:1–13.

271. **Bhiman JN**. 2012. Autologous neutralizing antibody specificities in HIV-1 subtype C: Characterising the C3V4 region and defining mechanisms of escape. University of Witswatersrand.

272. **Giorgi EE**, **Funkhouser B**, **Athreya G**, **Perelson AS**, **Korber BT**, **Bhattacharya T**. 2010. Estimating time since infection in early homogeneous HIV-1 samples using a poisson model. BMC Bioinformatics **11**:532.

273. **Anthony C**, **York T**, **Bekker V**, **Matten D**, **Selhorst P**, **Ferreria R-C**, **Garrett NJ**, **Abdool Karim SS**, **Morris L**, **Wood NT**, **Moore PL**, **Williamson C**. 2017. Co-operation between strain-specific and broadly neutralizing responses limited viral escape, and prolonged exposure of the broadly neutralizing epitope. J Virol. JVI.00828-17.

274. **Bhiman JN**, **Anthony C**, **Doria-Rose NA**, **Karimanzira O**, **Schramm CA**, **Khoza T**, **Kitchin D**, **Botha G**, **Gorman J**, **Garrett NJ**, **Abdool Karim SS**, **Shapiro L**, **Williamson C**, **Kwong PD**, **Mascola JR**, **Morris L**, **Moore PL**. 2015. Viral variants that initiate and drive maturation of V1V2-directed HIV-1 broadly neutralizing antibodies. Nat Med **21**:1332–6.

275. **Domingo E**, **Sheldon J**, **Perales C**. 2012. Viral quasispecies evolution. Microbiol Mol Biol Rev **76**:159–216.

276. **Mascola JR**, **Lewis MG**, **Stiegler G**, **Harris D**, **VanCott TC**, **Hayes D**, **Louder MK**, **Brown CR**, **Sapan C V**, **Frankel SS**, **Lu Y**, **Robb ML**, **Katinger H**, **Birx DL**. 1999. Protection of Macaques against pathogenic simian/human immunodeficiency virus 89.6PD

by passive transfer of neutralizing antibodies. J Virol **73**:4009–4018.

277. **Nishimura Y**, **Igarashi T**, **Haigwood N**, **Sadjadpour R**, **Plishka RJ**, **Buckler-White A**, **Shibata R**, **Martin MA**. 2002. Determination of a statistically valid neutralization titer in plasma that confers protection against simian-human immunodeficiency virus challenge following passive transfer of high-titered neutralizing antibodies. J Virol **76**:2123–2130.

278. **Parren PW**, **Marx PA**, **Hessell AJ**, **Luckay A**, **Harouse J**, **Cheng-Mayer C**, **Moore JP**, **Burton DR**. 2001. Antibody protects macaques against vaginal challenge with a pathogenic R5 simian/human immunodeficiency virus at serum levels giving complete neutralization in vitro. J Virol **75**:8340–8347.

279. **Chakraborty H**, **Sen PK**, **Helms RW**, **Vernazza PL**, **Fiscus S a**, **Eron JJ**, **Patterson BK**, **Coombs RW**, **Krieger JN**, **Cohen MS**. 2001. Viral burden in genital secretions determines male-to-female sexual transmission of HIV-1: a probabilistic empiric model. AIDS **15**:621–627.

280. **Pilcher CD**, **Tien HC**, **Eron JJJ**, **Vernazza PL**, **Leu S-Y**, **Stewart PW**, **Goh L-E**, **Cohen MS**. 2004. Brief but efficient: acute HIV infection and the sexual transmission of HIV. J Infect Dis **189**:1785–1792.

281. **Hessell AJ**, **Jaworski JP**, **Epson E**, **Matsuda K**, **Pandey S**, **Kahl C**, **Reed J**, **Sutton WF**, **Hammond KB**, **Cheever TA**, **Barnette PT**, **Legasse AW**, **Planer S**, **Stanton JJ**, **Pegu A**, **Chen X**, **Wang K**, **Siess D**, **Burke D**, **Park BS**, **Axthelm MK**, **Lewis A**, **Hirsch VM**, **Graham BS**, **Mascola JR**, **Sacha JB**, **Haigwood NL**. 2016. Early short-term treatment with neutralizing human monoclonal antibodies halts SHIV infection in infant macaques. Nat Med **22**:362–8.

282. **Liu J**, **Ghneim K**, **Sok D**, **Bosche WJ**, **Li Y**, **Chipriano E**, **Berkemeier B**, **Oswald K**, **Borducchi E**, **Cabral C**, **Peter L**, **Brinkman A**, **Shetty M**, **Jimenez J**, **Mondesir J**, **Lee B**, **Giglio P**, **Chandrashekar A**, **Abbink P**, **Colantonio A**, **Gittens C**, **Baker C**, **Wagner W**, **Lewis MG**, **Li W**, **Sekaly R-P**, **Lifson JD**, **Burton DR**, **Barouch DH**. 2016. Antibody-mediated protection against SHIV challenge includes systemic clearance of distal virus. Science **353**:1045–1049.

283. **Chung AW**, **Ghebremichael M**, **Robinson H**, **Brown E**, **Choi I**, **Lane S**, **Dugast A-S**, **Schoen MK**, **Rolland M**, **Suscovich TJ**, **Mahan AE**, **Liao L**, **Streeck H**, **Andrews C**, **Rerks-Ngarm S**, **Nitayaphan S**, **de Souza MS**, **Kaewkungwal J**, **Pitisuttithum P**, **Francis D**, **Michael NL**, **Kim JH**, **Bailey-Kellogg C**, **Ackerman ME**, **Alter G**. 2014. Polyfunctional Fc-effector profiles mediated by IgG subclass selection distinguish RV144 and VAX003 vaccines. Sci Transl Med **6**:228–238.

284. **Voss JE**, **Macauley MS**, **Rogers KA**, **Villinger F**, **Duan L**, **Shang L**, **Fink EA**, **Andrabi R**, **Colantonio AD**, **Robinson JE**, **Johnson RP**, **Burton DR**, **Haase AT**. 2016. Reproducing SIVΔnef vaccine correlates of protection: trimeric gp41 antibody concentrated at mucosal front lines. AIDS **30**:2427–2438.

285. **Rolland M**, **Edlefsen PT**, **Larsen BB**, **Tovanabutra S**, **Sanders-Buell E**, **Hertz T**, **DeCamp AC**, **Carrico C**, **Menis S**, **Magaret CA**, **Ahmed H**, **Juraska M**, **Chen L**, **Konopa P**, **Nariya S**, **Stoddard JN**, **Wong K**, **Zhao H**, **Deng W**, **Maust BS**, **Bose M**, **Howell S**, **Bates A**, **Lazzaro M**, **O'Sullivan A**, **Lei E**, **Bradfield A**, **Ibitamuno G**, **Assawadarachai V**, **O'Connell RJ**, **DeSouza MS**, **Nitayaphan S**, **Rerks-Ngarm S**, **Robb ML**, **McLellan JS**, **Georgiev I**, **Kwong PD**, **Carlson JM**, **Michael NL**, **Schief WR**, **Gilbert PB**, **Mullins JI**, **Kim JH**. 2012. Increased HIV-1 vaccine efficacy against viruses with genetic signatures in Env V2. Nature **490**:417-420.

286. **Pollara J**, **Bonsignori M**, **Moody MA**, **Pazgier M**, **Haynes BF**, **Ferrari G**. 2013. Epitope specificity of human immunodeficiency virus-1 antibody dependent cellular cytotoxicity [ADCC] responses. Curr HIV Res **11**:378–87.

287. **Niwa R**, **Sakurada M**, **Kobayashi Y**, **Uehara A**, **Matsushima K**, **Ueda R**, **Nakamura K**, **Shitara K**. 2005. Enhanced natural killer cell binding and activation by low-fucose IgG1 antibody results in potent antibody-dependent cellular cytotoxicity induction at lower antigen density. Clin Cancer Res **11**:2327–36.

288. **Niwa R**, **Hatanaka S**, **Shoji-Hosaka E**, **Sakurada M**, **Kobayashi Y**, **Uehara A**, **Yokoi H**, **Nakamura K**, **Shitara K**. 2004. Enhancement of the antibody-dependent cellular cytotoxicity of low-fucose IgG1 is independent of FcgammaRIIIa functional polymorphism. Clin Cancer Res **10**:6248–55.

289. **Webb B**, **Sali A**. 2014. Comparative Protein Structure Modeling Using MODELLER. Current Protoc Bioinformatics **Chapter 2**:Unit 2.9.

290. **Bohne-Lang A**, **von der Lieth C-W**. 2005. GlyProt: in silico glycosylation of proteins. Nucleic Acids Res **33**:W214–W219.

291. **Forthal DN**, **Landucci G**, **Keenan B**. 2001. Relationship between antibody-dependent cellular cytotoxicity, plasma HIV type 1 RNA, and CD4+ lymphocyte count. AIDS Res Hum Retroviruses **17**:553–561.

292. **Forthal DN**, **Landucci G**, **Gorny MK**, **Zolla-Pazner S**, **Robinson WE**. 1995. Functional Activities of 20 Human Immunodeficiency Virus Type 1 (HIV-1)-Specific Human Monoclonal Antibodies. AIDS Res Hum Retroviruses **11**:1095–1099.

293. **Freund NT**, **Wang H**, **Scharf L**, **Nogueira L**, **Horwitz JA**, **Bar-On Y**, **Golijanin J**, **Sievers SA**, **Sok D**, **Cai H**, **Cesar Lorenzi JC**, **Halper-Stromberg A**, **Toth I**, **Piechocka-Trocha A**, **Gristick HB**, **van Gils MJ**, **Sanders RW**, **Wang L-X**, **Seaman MS**, **Burton DR**, **Gazumyan A**, **Walker BD**, **West AP**, **Bjorkman PJ**, **Nussenzweig MC**. 2017. Coexistence of potent HIV-1 broadly neutralizing antibodies and antibody-sensitive viruses in a viremic controller. Sci Transl Med **9**:eaal2144.

294. **West AP**, **Scharf L**, **Horwitz J**, **Klein F**, **Nussenzweig MC**, **Bjorkman PJ**. 2013. Computational analysis of anti-HIV-1 antibody neutralization panel data to identify potential functional epitope residues. Proc Natl Acad Sci **110**:10598–10603.

295. **Shingai M**, **Donau OK**, **Plishka RJ**, **Buckler-White A**, **Mascola JR**, **Nabel GJ**, **Nason MC**, **Montefiori D**, **Moldt B**, **Poignard P**, **Diskin R**, **Bjorkman PJ**, **Eckhaus MA**, **Klein F**, **Mouquet H**, **Cetrulo Lorenzi JC**, **Gazumyan A**, **Burton DR**, **Nussenzweig MC**, **Martin MA**, **Nishimura Y**. 2014. Passive transfer of modest titers of potent and broadly neutralizing anti-HIV monoclonal antibodies block SHIV infection in macaques. J Exp Med **211**:2061–2074.

296. **Moldt B**, **Rakasz EG**, **Schultz N**, **Chan-Hui P-Y**, **Swiderek K**, **Weisgrau KL**, **Piaskowski SM**, **Bergman Z**, **Watkins DI**, **Poignard P**, **Burton DR**. 2012. Highly potent HIV-specific antibody neutralization in vitro translates into effective protection against mucosal SHIV challenge in vivo. Proc Natl Acad Sci **109**:18921-18925.

297. **Klein F**, **Halper-Stromberg A**, **Horwitz JA**, **Gruell H**, **Scheid JF**, **Bournazos S**, **Mouquet H**, **Spatz LA**, **Diskin R**, **Abadir A**, **Zang T**, **Dorner M**, **Billerbeck E**, **Labitt RN**, **Gaebler C**, **Marcovecchio PM**, **Incesu R-B**, **Eisenreich TR**, **Bieniasz PD**, **Seaman MS**, **Bjorkman PJ**, **Ravetch J V.**, **Ploss A**, **Nussenzweig MC**. 2012. HIV therapy by a combination of broadly neutralizing antibodies in humanized mice. Nature **492**:118–122.

298. **Horwitz JA**, **Halper-Stromberg A**, **Mouquet H**, **Gitlin AD**, **Tretiakova A**, **Eisenreich TR**, **Malbec M**, **Gravemann S**, **Billerbeck E**, **Dorner M**, **Buning H**, **Schwartz O**, **Knops E**, **Kaiser R**, **Seaman MS**, **Wilson JM**, **Rice CM**, **Ploss A**, **Bjorkman PJ**, **Klein F**, **Nussenzweig MC**. 2013. HIV-1 suppression and durable control by combining single broadly neutralizing antibodies and antiretroviral drugs in humanized mice. Proc Natl Acad Sci **110**:16538–16543.

299. **Gautam R**, **Nishimura Y**, **Pegu A**, **Nason MC**, **Klein F**, **Gazumyan A**, **Golijanin J**, **Buckler-White A**, **Sadjadpour R**, **Wang K**, **Mankoff Z**, **Schmidt SD**, **Lifson JD**, **Mascola JR**, **Nussenzweig MC**, **Martin MA**. 2016. A single injection of anti-HIV-1 antibodies protects against repeated SHIV challenges. Nature **533**:105–109.

300. **Barouch DH**, **Whitney JB**, **Moldt B**, **Klein F**, **Oliveira TY**, **Liu J**, **Stephenson KE**, **Chang H-W**, **Shekhar K**, **Gupta S**, **Nkolola JP**, **Seaman MS**, **Smith KM**, **Borducchi EN**, **Cabral C**, **Smith JY**, **Blackmore S**, **Sanisetty S**, **Perry JR**, **Beck M**, **Lewis MG**, **Rinaldi W**, **Chakraborty AK**, **Poignard P**, **Nussenzweig MC**, **Burton DR**. 2013. Therapeutic efficacy of potent neutralizing HIV-1-specific monoclonal antibodies in SHIV-infected rhesus monkeys. Nature **503**:224–228.

301. **Caskey M**, **Klein F**, **Lorenzi JCC**, **Seaman MS**, **West AP**, **Buckley N**, **Kremer G**, **Nogueira L**, **Braunschweig M**, **Scheid JF**, **Horwitz J a.**, **Shimeliovich I**, **Ben-Avraham S**, **Witmer-Pack M**, **Platten M**, **Lehmann C**, **Burke L a.**, **Hawthorne T**, **Gorelick RJ**, **Walker BD**, **Keler T**, **Gulick RM**, **Fätkenheuer G**, **Schlesinger SJ**, **Nussenzweig MC**. 2015. Viraemia suppressed in HIV-1-infected humans by broadly neutralizing antibody 3BNC117. Nature **522**:487-491.

302. **Caskey M**, **Schoofs T**, **Gruell H**, **Settler A**, **Karagounis T**, **Kreider EF**, **Murrell B**, **Pfeifer N**, **Nogueira L**, **Oliveira TY**, **Learn GH**, **Cohen YZ**, **Lehmann C**, **Gillor D**, **Shimeliovich I**, **Unson-O'Brien C**, **Weiland D**, **Robles A**, **Kümmerle T**, **Wyen C**, **Levin**

R, **Witmer-Pack M**, **Eren K**, **Ignacio C**, **Kiss S**, **West AP**, **Mouquet H**, **Zingman BS**, **Gulick RM**, **Keler T**, **Bjorkman PJ**, **Seaman MS**, **Hahn BH**, **Fätkenheuer G**, **Schlesinger SJ**, **Nussenzweig MC**, **Klein F**. 2017. Antibody 10-1074 suppresses viremia in HIV-1-infected individuals. Nat Med **23**:185–191.

303. **Lynch RM**, **Boritz E**, **Coates EE**, **DeZure A**, **Madden P**, **Costner P**, **Enama ME**, **Plummer S**, **Holman L**, **Hendel CS**, **Gordon I**, **Casazza J**, **Conan-Cibotti M**, **Migueles SA**, **Tressler R**, **Bailer RT**, **McDermott A**, **Narpala S**, **ODell S**, **Wolf G**, **Lifson JD**, **Freemire BA**, **Gorelick RJ**, **Pandey JP**, **Mohan S**, **Chomont N**, **Fromentin R**, **Chun T-W**, **Fauci AS**, **Schwartz RM**, **Koup RA**, **Douek DC**, **Hu Z**, **Capparelli E**, **Graham BS**, **Mascola JR**, **Ledgerwood JE**. 2015. Virologic effects of broadly neutralizing antibody VRC01 administration during chronic HIV-1 infection. Sci Transl Med **7**:319ra206.

304. **Pham TNQ**, **Lukhele S**, **Dallaire F**, **Perron G**, C**ohen ÉA.** 2016. Enhancing Virion Tethering by BST2 Sensitizes Productively and Latently HIV-infected T cells to ADCC Mediated by Broadly Neutralizing Antibodies. Sci Rep **6**:37225.

305. **von Bredow B**, **Arias JF**, **Heyer LN**, **Moldt B**, **Le K**, **Robinson JE**, **Zolla-Pazner S**, **Burton DR**, **Evans DT**. 2016. Comparison of Antibody-Dependent Cell-Mediated Cytotoxicity and Virus Neutralization by HIV-1 Env-Specific Monoclonal Antibodies. J Virol **90**:6127–6139.

306. **Bruel T**, **Guivel-Benhassine F**, **Amraoui S**, **Malbec M**, **Richard L**, **Bourdic K**, **Donahue DA**, **Lorin V**, **Casartelli N**, **Noël N**, **Lambotte O**, **Mouquet H**, **Schwartz O**. 2016. Elimination of HIV-1-infected cells by broadly neutralizing antibodies. Nat Commun **7**:10844.

307. **Moldt B**, **Schultz N**, **Dunlop DC**, **Alpert MD**, **Harvey JD**, **Evans DT**, **Poignard P**, **Hessell AJ**, **Burton DR**. 2011. A Panel of IgG1 b12 Variants with Selectively Diminished or Enhanced Affinity for Fc Receptors To Define the Role of Effector Functions in Protection against HIV. J Virol **85**:10572-10581.

308. **Halper-Stromberg A**, **Lu C-L**, **Klein F**, **Horwitz JA**, **Bournazos S**, **Nogueira L**, **Eisenreich TR**, **Liu C**, **Gazumyan A**, **Schaefer U**, **Furze RC**, **Seaman MS**, **Prinjha R**, **Tarakhovsky A**, **Ravetch JV**, **Nussenzweig MC**. 2014. Broadly Neutralizing Antibodies

and Viral Inducers Decrease Rebound from HIV-1 Latent Reservoirs in Humanized Mice. Cell **158**:989–999.

309. **Bournazos S**, **Klein F**, **Pietzsch J**, **Seaman M**, **Nussenzweig M**, **Ravetch J**. 2014. Broadly Neutralizing Anti-HIV-1 Antibodies Require Fc Effector Functions for In Vivo Activity. Cell **158**:1243–1253.

310. **Lu C-L**, **Murakowski DK**, **Bournazos S**, **Schoofs T**, **Sarkar D**, **Halper-Stromberg A**, **Horwitz JA**, **Nogueira L**, **Golijanin J**, **Gazumyan A**, **Ravetch J V.**, **Caskey M**, **Chakraborty AK**, **Nussenzweig MC**. 2016. Enhanced clearance of HIV-1-infected cells by broadly neutralizing antibodies against HIV-1 in vivo. Science **352**:1001–1004.

311. **Lewis G**, **Finzi A**, **DeVico A**, **Pazgier M**. 2015. Conformational Masking and Receptor-Dependent Unmasking of Highly Conserved Env Epitopes Recognized by Non-Neutralizing Antibodies That Mediate Potent ADCC against HIV-1. Viruses **7**:5115–5132.

312. **Santra S**, **Tomaras GD**, **Warrier R**, **Nicely NI**, **Liao H-X**, **Pollara J**, **Liu P**, **Alam SM**, **Zhang R**, **Cocklin SL**, **Shen X**, **Duffy R**, **Xia S-M**, **Schutte RJ**, **Pemble IV CW**, **Dennison SM**, **Li H**, **Chao A**, **Vidnovic K**, **Evans A**, **Klein K**, **Kumar A**, **Robinson J**, **Landucci G**, **Forthal DN**, **Montefiori DC**, **Kaewkungwal J**, **Nitayaphan S**, **Pitisuttithum P**, **Rerks-Ngarm S**, **Robb ML**, **Michael NL**, **Kim JH**, **Soderberg KA**, **Giorgi EE**, **Blair L**, **Korber BT**, **Moog C**, **Shattock RJ**, **Letvin NL**, **Schmitz JE**, **Moody MA**, **Gao F**, **Ferrari G**, **Shaw GM**, **Haynes BF**. 2015. Human Non-neutralizing HIV-1 Envelope Monoclonal Antibodies Limit the Number of Founder Viruses during SHIV Mucosal Infection in Rhesus Macaques. PLOS Pathog **11**:e1005042.

313. **Veillette M**, **Desormeaux A**, **Medjahed H**, **Gharsallah N-E**, **Coutu M**, **Baalwa J**, **Guan Y**, **Lewis G**, **Ferrari G**, **Hahn BH**, **Haynes BF**, **Robinson JE**, **Kaufmann DE**, **Bonsignori M**, **Sodroski J**, **Finzi A**, **Silvestri G**. 2014. Interaction with Cellular CD4 Exposes HIV-1 Envelope Epitopes Targeted by Antibody-Dependent Cell-Mediated Cytotoxicity. J Virol **88**:2633–2644.

314. **Veillette M**, **Coutu M**, **Richard J**, **Batraville L-A**, **Dagher O**, **Bernard N**, **Tremblay C**, **Kaufmann DE**, **Roger M**, **Finzi A**. 2015. The HIV-1 gp120 CD4-Bound Conformation Is Preferentially Targeted by Antibody-Dependent Cellular Cytotoxicity-Mediating

Antibodies in Sera from HIV-1-Infected Individuals. J Virol **89**:545–551.

315. **Tamura K**, **Dudley J**, **Nei M**, **Kumar S**. 2007. MEGA4: Molecular Evolutionary Genetics Analysis (MEGA) software version 4.0. Mol Biol Evol **24**:1596–9.

316. **Price MN**, **Dehal PS**, **Arkin AP**. 2009. FastTree: Computing Large Minimum Evolution Trees with Profiles instead of a Distance Matrix. Mol Biol Evol **26**:1641–1650.

317. **Acharya P**, **Tolbert WD**, **Gohain N**, **Wu X**, **Yu L**, **Liu T**, **Huang W**, **Huang C -c.**, **Kwon Y Do**, **Louder RK**, **Luongo TS**, **McLellan JS**, **Pancera M**, **Yang Y**, **Zhang B**, **Flinko R**, **Foulke JS**, **Sajadi MM**, **Kamin-Lewis R**, **Robinson JE**, **Martin L**, **Kwong PD**, **Guan Y**, **DeVico AL**, **Lewis GK**, **Pazgier M**. 2014. Structural Definition of an Antibody-Dependent Cellular Cytotoxicity Response Implicated in Reduced Risk for HIV-1 Infection. J Virol **88**:12895–12906.

318. **Wagh K**, **Bhattacharya T**, **Williamson C**, **Robles A**, **Bayne M**, **Garrity J**, **Rist M**, **Rademeyer C**, **Yoon H**, **Lapedes A**, **Gao H**, **Greene K**, **Louder MK**, **Kong R**, **Karim SA**, **Burton DR**, **Barouch DH**, **Nussenzweig MC**, **Mascola JR**, **Morris L**, **Montefiori DC**, **Korber B**, **Seaman MS**. 2016. Optimal Combinations of Broadly Neutralizing Antibodies for Prevention and Treatment of HIV-1 Clade C Infection. PLOS Pathog **12**:e1005520.

319. **Moore JP**, **Willey RL**, **Lewis GK**, **Robinson J**, **Sodroski J**. 1994. Immunological evidence for interactions between the first, second, and fifth conserved domains of the gp120 surface glycoprotein of human immunodeficiency virus type 1. J Virol **68**:6836–47.

320. **Finzi A**, **Xiang S-H**, **Pacheco B**, **Wang L**, **Haight J**, **Kassa A**, **Danek B**, **Pancera M**, **Kwong PD**, **Sodroski J**. 2010. Topological Layers in the HIV-1 gp120 Inner Domain Regulate gp41 Interaction and CD4-Triggered Conformational Transitions. Mol Cell **37**:656–667.

321. **Ding S**, **Veillette M**, **Coutu M**, **Prévost J**, **Scharf L**, **Bjorkman PJ**, **Ferrari G**, **Robinson JE**, **Stürzel C**, **Hahn BH**, **Sauter D**, **Kirchhoff F**, **Lewis GK**, **Pazgier M**, **Finzi A**. 2016. A Highly Conserved Residue of the HIV-1 gp120 Inner Domain Is Important for Antibody-Dependent Cellular Cytotoxicity Responses Mediated by Anti-cluster A Antibodies. J Virol **90**:2127–2134.

322. **Bruel T**, **Guivel-Benhassine F**, **Lorin V**, **Lortat-Jacob H**, **Baleux F**, **Bourdic K**, **Noël N**, **Lambotte O**, **Mouquet H**, **Schwartz O**. 2017. Lack of ADCC Breadth of Human Nonneutralizing Anti-HIV-1 Antibodies. J Virol **91**:e02440-16.

323. **Mellor JD**, **Brown MP**, **Irving HR**, **Zalcberg JR**, **Dobrovic A**. 2013. A critical review of the role of Fc gamma receptor polymorphisms in the response to monoclonal antibodies in cancer. J Hematol Oncol **6**:1.

324. **Sondermann P**, **Huber R**, **Oosthuizen V**, **Jacob U**. 2000. The 3.2-A crystal structure of the human IgG1 Fc fragment-Fc gammaRIII complex. Nature **406**:267–273.

325. **Radaev S**, **Motyka S**, **Fridman WH**, **Sautes-Fridman C**, **Sun PD**. 2001. The structure of a human type III Fcgamma receptor in complex with Fc. J Biol Chem **276**:16469–16477.

326. **Biedma M**, **Decoville T**, **Su B**, **Schmidt S**, **Laumond G**, **Moog C**. 2014. Antibodies Induced Lysis of Primary Infected Cells by ADCC Is HIV-1 Strain Specific. AIDS Res Hum Retroviruses **30**:A153.

327. **Falkowska E**, **Le KM**, **Ramos A**, **Doores KJ**, **Lee JH**, **Blattner C**, **Ramirez A**, **Derking R**, **van Gils MJ**, **Liang C-H**, **Mcbride R**, **von Bredow B**, **Shivatare SS**, **Wu C-Y**, **Chan-Hui P-Y**, **Liu Y**, **Feizi T**, **Zwick MB**, **Koff WC**, **Seaman MS**, **Swiderek K**, **Moore JP**, **Evans D**, **Paulson JC**, **Wong C-H**, **Ward AB**, **Wilson IA**, **Sanders RW**, **Poignard P**, **Burton DR**. 2014. Broadly Neutralizing HIV Antibodies Define a Glycan-Dependent Epitope on the Prefusion Conformation of gp41 on Cleaved Envelope Trimers. Immunity **40**:657–668.

328. **Forthal DN, Moog C**. 2009. Fc receptor-mediated antiviral antibodies. Curr Opin HIV AIDS **4**:388-393.